Chapter 5 Mass Uptake of Penetrants

5.1 Introduction

This chapter contains a discussion of the transport of two series of linear penetrants- *n*-alkanes and esters, through the R/flex polymeric adhesive. Dynamic solvent uptake measurements were undertaken to evaluate equilibrium and kinetic properties, which in turn were utilized to investigate the effects of *molecular size*, *shape*, and *chemical nature* on the transport process.

5.2 Dynamic Solvent Uptake of Linear Alkanes

Diffusion of a low molecular weight species into a polymer matrix is a complex theoretical problem with diverse applications. Several experimental techniques have been used to study the solvent transport properties of a polymeric matrix[1,2,3,4]. Of these, the gravimetric method, although simple, has been shown by many to yield reliable data.[5,6,7,8]

In this study, the sorption of linear n-alkanes ranging from hexane to heptadecane (Tables 3-1) into free-standing polymer films was investigated. The films were exposed directly in a scintillation vial containing pure solvent, and their mass increase at several test temperatures was measured using an analytical balance. Prior to the experiment, all samples and solvents were equilibrated at the test temperatures for 20 minutes.

Typical raw data for each aliphatic penetrant at 23°C, in terms of fractional mass uptake (M_t/M_∞), are given in Figure 5-1. M_t and M_∞ are defined as the experimental mass uptakes at time t and ∞, respectively, and are given by the expressions:

(1) $M_t = W_t - W_{t0}$

(2) $M_\infty = W_{t\infty} - W_{t0}$

where M_t = mass uptake at time *t*,
M_∞ = mass uptake at equilibrium
W_{to} = initial weight of sample
W_t = weight at time *t*
W_∞ = weight at equilibrium.

Plots of M_t/M_∞ versus the square root of time (normalized by the film thickness) are known as reduced sorption plots. These normalizations for the *n*-alkanes at 23°, 45°, 55°, 65° and 85°C are shown in Figure 5-2 through Figure 5-6, respectively. All the

curves are similar in shape and possess the Fickian characteristic of linearity up to 60% fractional weight uptake (M_t/M_∞=0.60). They are concave toward the abscissa, and smoothly approach equilibrium sorption values, where equilibrium is defined by the plateau of the curve.

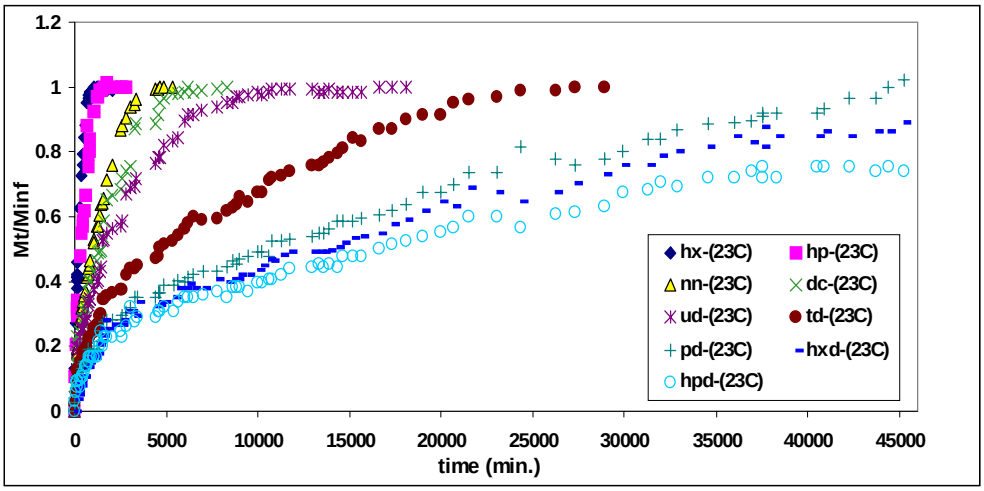

Figure 5-1. Fractional Mass Uptake for *n*-alkanes at 23°C as a Function of *Linear* Time (M_t/M_∞ is designated as M_t/M_{inf} above)

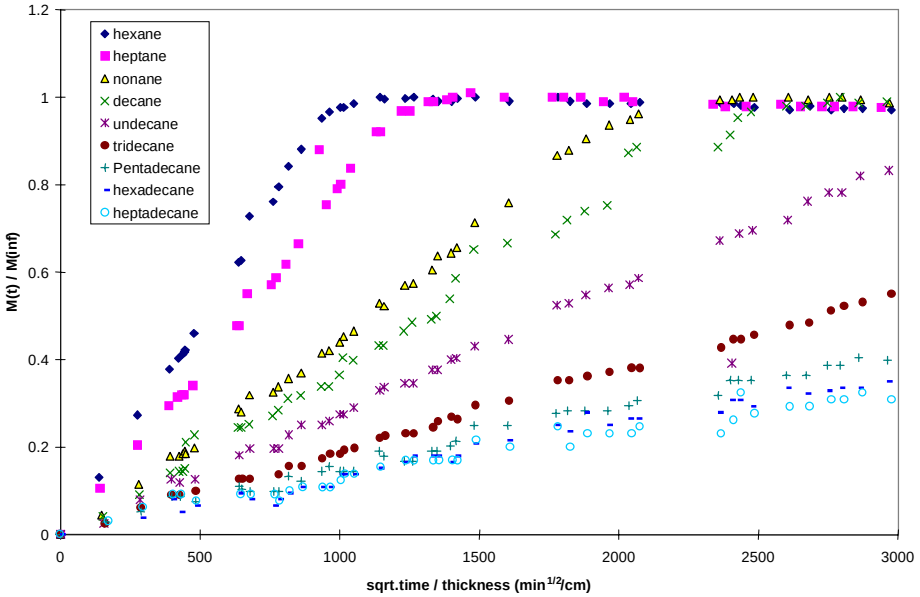

Figure 5-2. Fractional Mass Uptake for *n*-alkanes at 23°C as a Function of *Normalized* Time (M_t/M_∞ is designated as M_t/M_{inf} above)

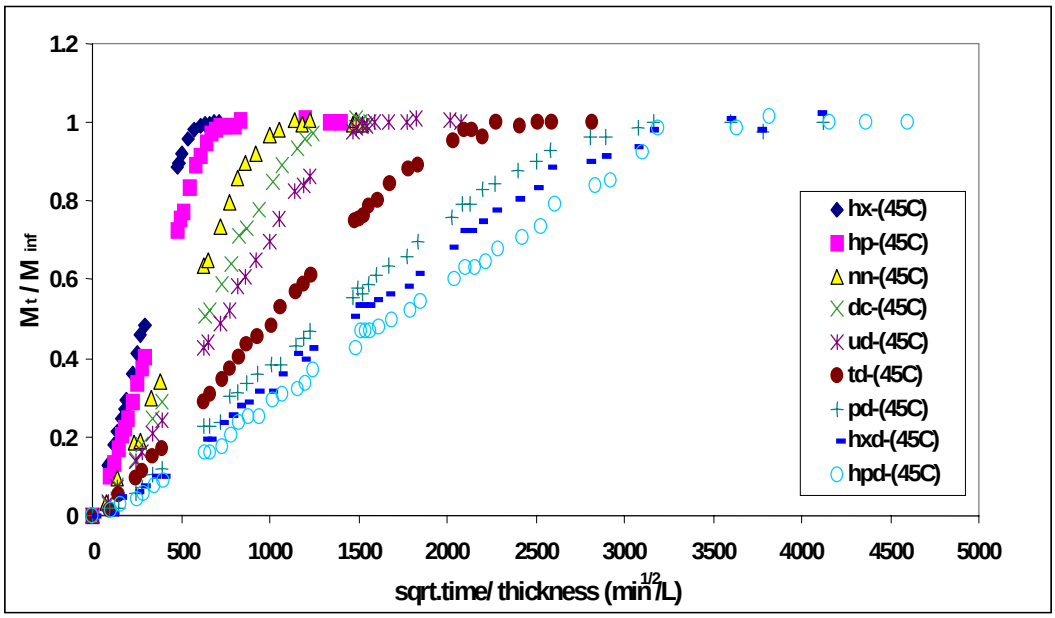

Figure 5-3. Fractional Mass Uptake for *n*-alkanes at 45°C as a Function of *Normalized* Time (M_t/M_∞ is designated as M_t/M_{inf} above)

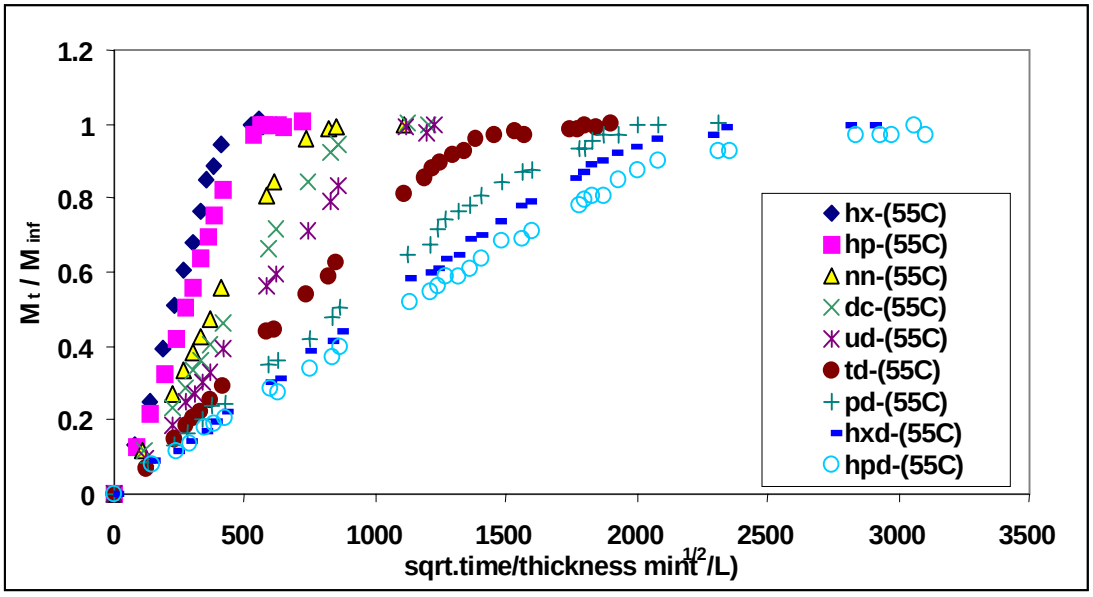

Figure 5-4. Fractional Mass Uptake for *n*-alkanes at 55°C as a Function of *Normalized* Time (M_t/M_∞ is designated as M_t/M_{inf} above)

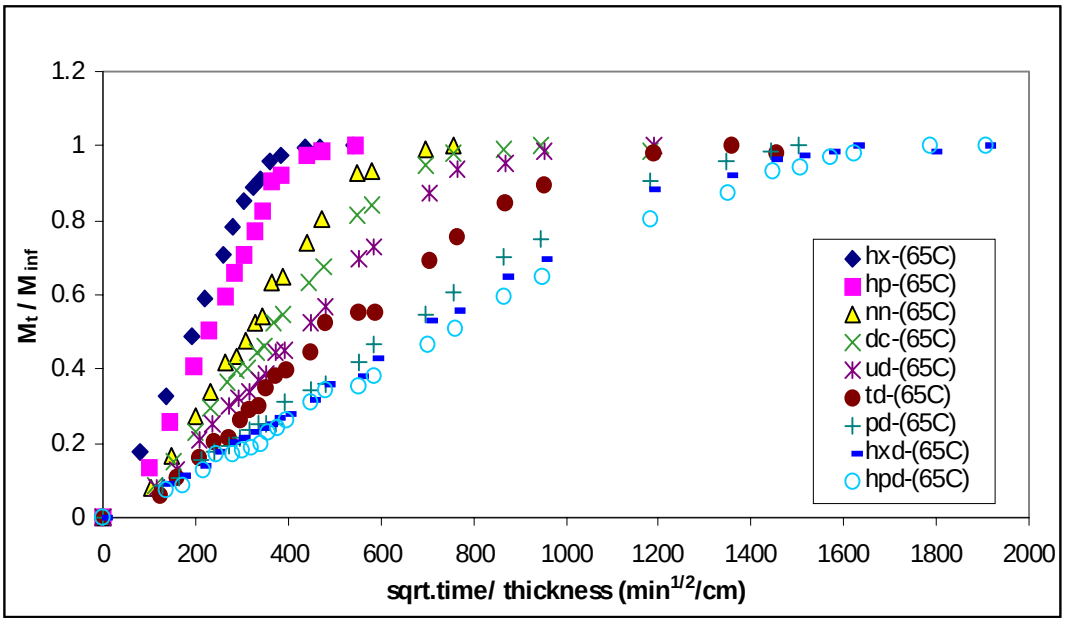

Figure 5-5. Fractional Mass Uptake for *n*-alkanes at 65°C as a Function of *Normalized* Time (M_t/M_∞ is designated as M_t/M_{inf} above)

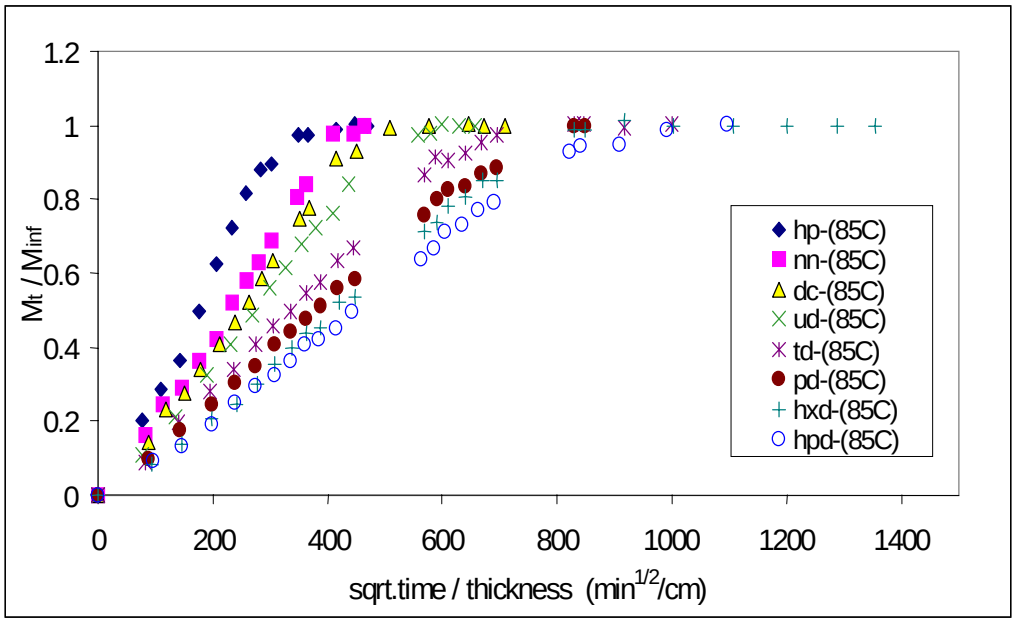

Figure 5-6. Fractional Mass Uptake for *n*-alkanes at 85°C as a Function of *Normalized* Time (M_t/M_∞ is designated as M_t/M_{inf} above)

It is necessary to select an appropriate model in order to examine the sorption data. A Fickian model is the most common and the easiest means of analysis, but is not valid in some cases. To investigate its applicability to this study, the results have been compared to a time power law equation[9,10],

$$\frac{M_t}{M_\infty} = Kt^n \tag{3}$$

where K is a constant that depends upon the structural characteristics of the polymer, in addition to its interaction with the solvent. The value of the exponent, *n*, indicates the nature of the transport mechanism as:[6,9,10,11,12]

$n = 0.5 \Rightarrow$ Fickian transport
$n = 1.0 \Rightarrow$ Case II transport
$0.5 < n < 1.0 \Rightarrow$ anomalous transport.

Nonlinear curve fitting of the data up to 97% of the fractional uptake value has been performed using a Leveberg-Marquardt algorithm. The results for heptadecane (HPD) at 23°C are shown in Figure 5-7. The values of *n* and K for each penetrant and temperature have been evaluated, and are listed in Table 5-1 through Table 5-5.

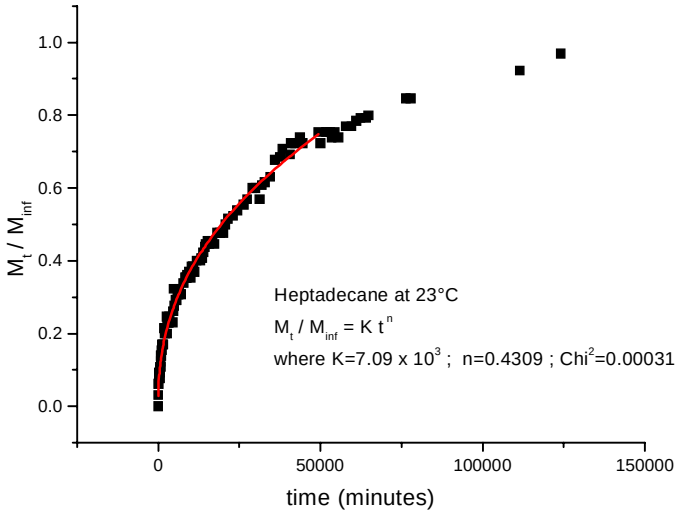

Figure 5-7. Nonlinear Curve Fit of equation (3) to experimental data of Heptadecane at 23°C (M_t/M_∞ is designated as M_t/M_{inf} above)

All the values of *n* are approximately 0.5, representative of a Fickian-type diffusion. This behavior is due to the fact that low T_g (elastomeric) materials have sufficiently rapid segmental motions, so that relaxation effects are absent and Fickian

kinetics are induced[11]. The constant K exhibited a systematic decrease with increasing number of carbon atoms and decreasing temperature (Figure 5-8). However, no such trend was observed for *n*. Aminabhavi *et al*.[12] have suggested that such a behavior is due to increased polymer segmental interactions with the penetrant. This idea is addressed in greater detail in a later section.

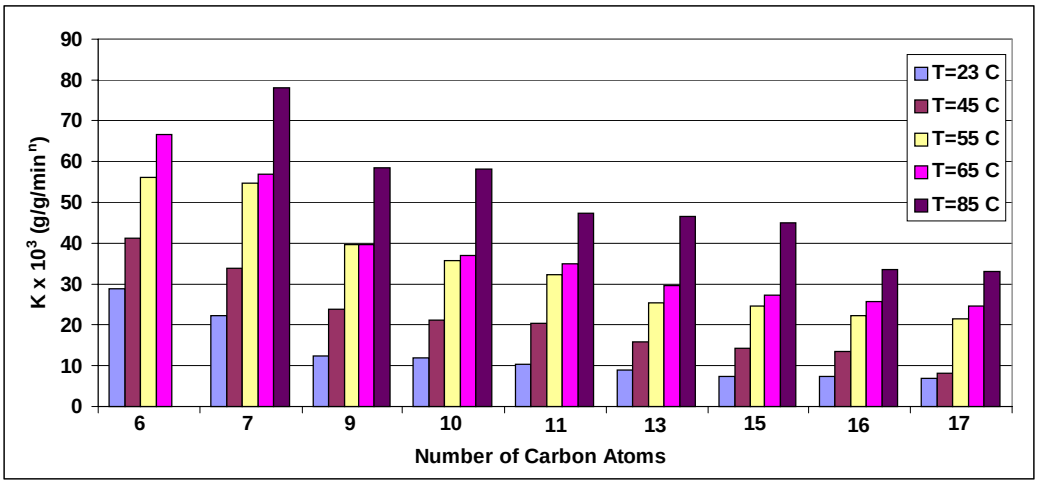

Figure 5-8. Structural and temperature dependence of the parameter K for the *n*-alkanes

The equilibrium *percent weight uptake* (solubility) of the penetrant-polymer systems is plotted as a function of number of carbon atoms in Figure 5-9 where,

$$\% \text{ Weight Uptake} = \frac{\text{Final Mass} - \text{Initial Mass}}{\text{Initial Mass}} \times 100 \tag{4}$$

An inverse dependence between solubility and molecular size of the penetrant is seen in this figure.

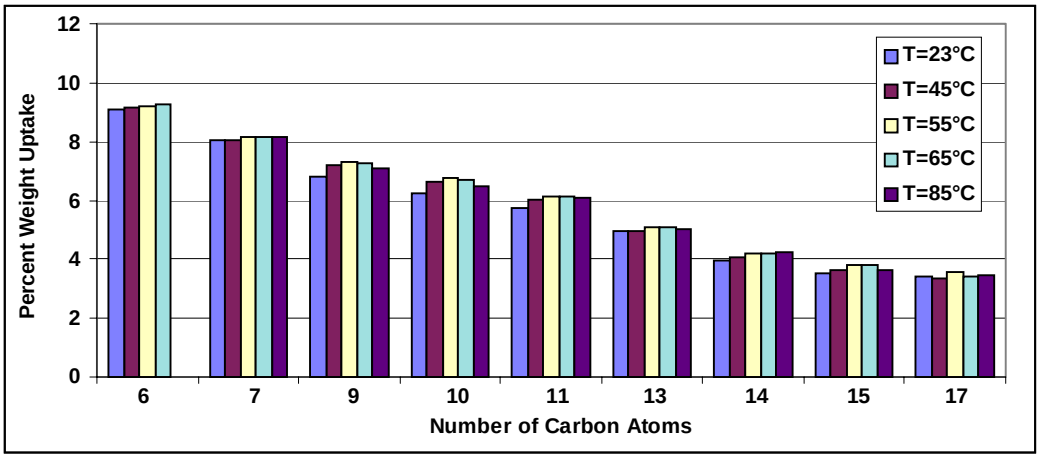

Figure 5-9. Equilibrium sorption for *n*-alkanes and its dependence upon temperature

Another convenient means of comparing the sorption of penetrants is via an equilibrium *mole percent weight gain*[11,12] defined as:

$$\text{Mole Weight \%} = \frac{\text{Final mass - Initial Mass}}{\text{Initial Mass}} \times \frac{1}{\text{Mass}} \times 100 \quad (5)$$

This quantity is plotted as a function of solubility parameters (δ) of the penetrants at room temperature in Figure 5-10.

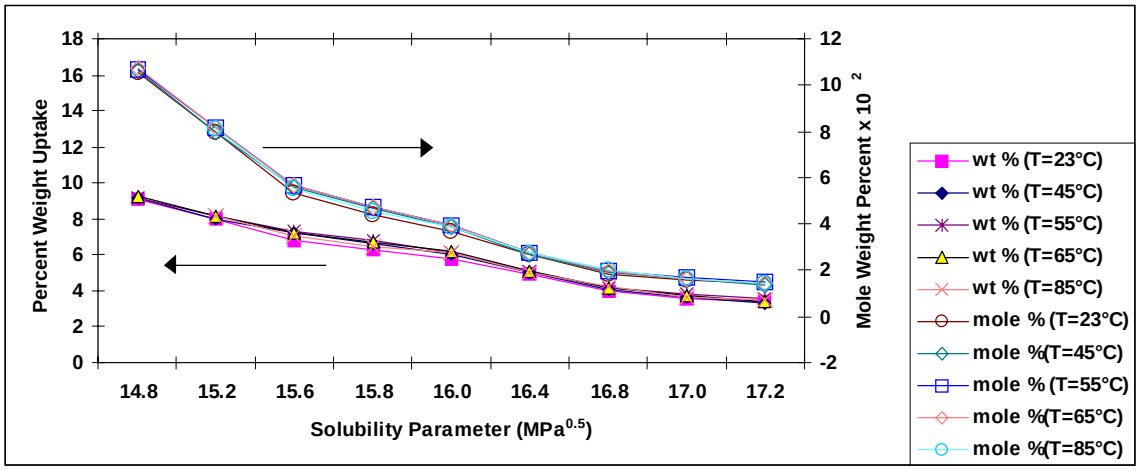

Figure 5-10. Equilibrium sorption as a function of solubility parameter for *n*-alkanes

It can be seen that equilibrium uptake exhibits the same dependence on δ as that found for molecular weight. This implies a systematic decrease in solubility with increasing number of penetrant carbon atoms[13] and is attributed to the fact that alkane sorption is an entropically driven process. The aliphatic nature of these penetrants only involves van der Waals and dispersion forces in the system, thereby rendering any enthalpic contributions negligible. For example, these ideas are reflected in the greater extent of sorption of hexane (C_6) when compared to heptadecane (C_{17}).

The temperature dependence of the equilibrium sorption values of Figure 5-9 and Figure 5-10 is not very significant, indicative of a low heat of solution. This is due to the elastomeric behavior of the material. For an elastomer, swelling theory[14] states that equilibrium is achieved when the free energy change of mixing (ΔG_{mix}) equals that due to elastic swelling (ΔG_{el}). For UCST behavior, as temperature increases, ΔG_{mix} decreases, favoring solubility of the penetrant. This in turn yields greater swelling and extension of the polymer chains and lower configurational entropy. These changes are countered by the retraction of the polymer chains due to the increased thermal energy, resulting in the small temperature dependence.

A "thin-film" solution for a Fickian model of transport was utilized in the analysis. The boundary conditions for a film of thickness h are listed below.

at t = 0	0 < x < h	C = 0
at t > 0	x = 0 , x = h	C = C_∞

where C is the penetrant concentration in the polymer matrix at a time t and a distance x. In this case, the relationship between fractional mass uptake and diffusivity is given by:

(6) $$\frac{M_t}{M_\infty} = 1 - \sum_{n=0}^{\infty} \frac{8}{(2n+1)^2 \pi^2} \exp\left[\frac{-D(2n+1)^2 n^2 t}{4L^2}\right]$$

Isothermal sorption curves are reduced by their corresponding film thicknesses and equation (6) is approximated to:

(7) $$\frac{M_t}{M_\infty} = \frac{2}{L}\left(\frac{D}{\pi}\right)^{1/2} t^{1/2} \qquad \text{(for short times)}$$

Hence, the initial linear slope of a reduced curve is directly proportional to the diffusion coefficient, D, as:

(8) $$D = \frac{\pi}{4} \times (\text{Slope})^2$$

Utilization of (equation
(7)) has been shown[15] to yield diffusion coefficients whose relative error is only 0.15% from those calculated with equation (6). This justifies the adoption of the short time approximation in the current study. An example of a linear fit to the initial slope (up to 55% M_t/M_∞) for an *undecane* sorption curve is shown in Figure 5-11. For all alkane experiments, the statistical R^2 values were between 0.990 and 1.000, indicating excellent correlation.

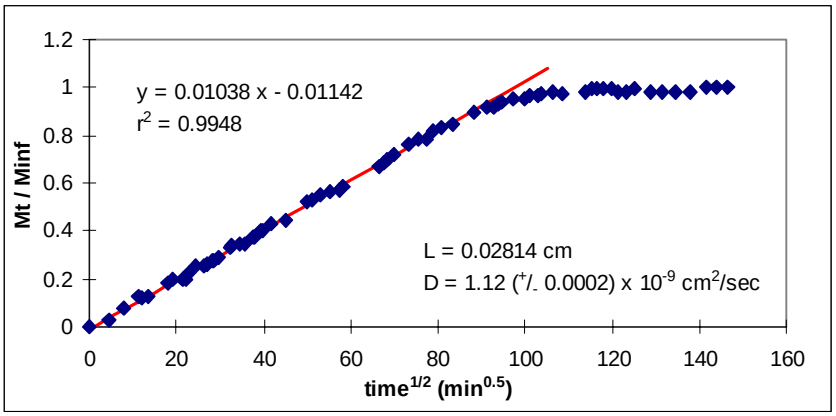

Figure 5-11. Evaluation of diffusion coefficient for *undecane* penetrant at 23°C is shown above. The initial slope of the fractional mass uptake (M_t/M_∞ is designated as M_t/M_{inf}

above) versus the square root of time is proportional to the diffusivity. Red line shows the result of a linear fit.

Values of D for the alkanes (at various temperatures) calculated from sorption data are given in Table 5-8. The two main sources of error in these experiments were from the measurements of thickness, L, and mass. However, the thicknesses of all the films used were the same, and an average of five measurements was employed to yield a single L. Thus, the error due to L was kept at a minimum. Due to the subjectivity involved in the weighing procedure, the method for estimating error was based upon meticulously duplicating a single experiment 11 times to yield an average error percentage. This was done by repeatedly exposing 11 different polymer films to decane at a temperature of 55°C and evaluating D for each trial. The diffusivities and their range are shown in Figure 5-12. The error calculated was applied to all other experiments.

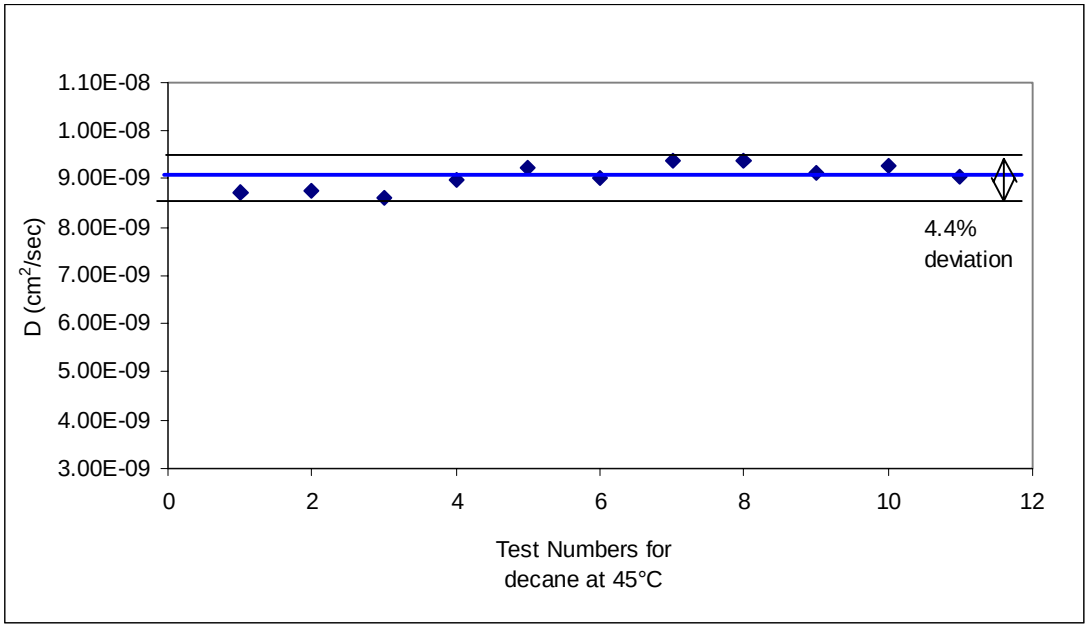

Figure 5-12. Error analysis involving decane at 45°C. The average value for D was 9.05 (±0.4) x10^{-9} cm^2/sec. A deviation of 4.4% is given for all 11 experiments.

Table 5-1

K and n parameters for *n*-alkanes at 23°C from non-linear fit to equation (3) $\frac{M_t}{M_\infty} = Kt^n$.

Penetrant	K x 10^3 (g/g/min^n)	n	χ^2
Hexane	29.0	0.535	0.00031
Heptane	22.2	0.534	0.00022
Nonane	12.2	0.541	0.00016
Decane	12.1	0.519	0.00086
Undecane	10.6	0.494	0.00026
Tridecane	8.76	0.464	0.00009
Pentadecane	7.38	0.452	0.00027
Hexadecane	7.18	0.440	0.00041
Heptadecane	7.09	0.431	0.00031

Table 5-2.

K and n Parameters for *n*-alkanes at 45°C from non-linear fit to equation (3) $\frac{M_t}{M_\infty} = Kt^n$

Penetrant	K x 10^3 (g/g/min^n)	n	χ^2
Hexane	41.2	0.583	0.0001
Heptane	34.0	0.580	0.00024
Nonane	23.7	0.564	0.00106
Decane	21.3	0.548	0.00058
Undecane	20.4	0.527	0.00047
Tridecane	15.7	0.514	0.00033
Pentadecane	14.1	0.490	0.00051
Hexadecane	13.5	0.483	0.00056
Heptadecane	8.26	0.529	0.00021

Table 5-3.

K and n Parameters for *n*-alkanes at 55°C for non-linear fit to equation (3) $\frac{M_t}{M_\infty} = Kt^n$

Penetrant	K x 10^3 (g/g/min^n)	n	χ^2
Hexane	56.0	0.578	0.0003
Heptane	54.6	0.539	0.00086
Nonane	39.7	0.528	0.00041
Decane	35.7	0.516	0.00018
Undecane	32.5	0.501	0.00062
Tridecane	25.2	0.497	0.00028
Pentadecane	24.8	0.470	0.00028
Hexadecane	22.5	0.464	0.00018
Heptadecane	21.7	0.456	0.00023

Table 5-4.

K and n Parameters for *n*-alkanes at 65°C from non-linear fit to equation (3) $\frac{M_t}{M_\infty} = Kt^n$

Penetrant	K x 10^3 (g/g/min^n)	n	χ^2
Hexane	66.4	0.590	0.00045
Heptane	56.9	0.577	0.00161
Nonane	39.6	0.576	0.00100
Decane	37.0	0.554	0.00087
Undecane	34.9	0.531	0.00124
Tridecane	29.6	0.524	0.00099
Pentadecane	27.2	0.497	0.00061
Hexadecane	25.8	0.498	0.00031
Heptadecane	24.5	0.490	0.00045

Table 5-5.

K and n Parameters for *n*-alkanes at 85°C from non-linear fit to equation (3) $\frac{M_t}{M_\infty} = Kt^n$

Penetrant	K x 10^3 (g/g/min^n)	n	χ^2
Hexane	*a*	*a*	*a*
Heptane	78.2	0.576	0.00078
Nonane	58.7	0.568	0.00015
Decane	58.2	0.549	0.00026
Undecane	47.2	0.569	0.00012
Tridecane	46.4	0.526	0.00017
Pentadecane	44.8	0.506	0.00022
Hexadecane	33.3	0.546	0.00048
Heptadecane	33.0	0.531	0.0002

a Data not obtained due to its low boiling point

Table 5-6
Equilibrium sorption values for *n*-alkanes expressed in terms of percent weight uptake

	Temperature (°C)				
Penetrant	23°C	45°C	55°C	65°C	85°C
Hexane	9.09	9.13	9.20	9.28	a
Heptane	8.02	8.01	8.16	8.16	8.12
Nonane	6.81	7.20	7.29	7.26	7.06
Decane	6.27	6.62	6.75	6.70	6.46
Undecane	5.77	6.01	6.15	6.17	6.09
Tridecane	4.94	4.97	5.07	5.10	5.04
Pentadecane	3.95	4.07	4.19	4.20	4.26
Hexadecane	3.53	3.63	3.81	3.77	3.65
Heptadecane	3.38	3.35	3.59	3.43	3.45

a-*Data not obtained due to its low boiling point*

Table 5-7
Equilibrium sorption values for *n*-alkanes expressed in terms of mole weight percent uptake * 10^2

	Temperature (°C)				
Penetrant	23°C	45°C	55°C	65°C	85°C
Hexane	10.6	10.6	10.7	10.8	a
Heptane	8.00	8.00	8.14	8.15	8.11
Nonane	5.31	5.61	5.69	5.66	5.51
Decane	4.41	4.65	4.75	4.71	4.54
Undecane	3.69	3.85	3.93	3.95	3.90
Tridecane	2.68	2.70	2.75	2.77	2.73
Pentadecane	1.86	1.91	1.97	1.98	2.00
Hexadecane	1.56	1.60	1.68	1.66	1.61
Heptadecane	1.41	1.39	1.49	1.43	1.43

a-*Data not obtained due to its low boiling point*

Table 5-8.
Diffusion coefficients (D x 10^9 cm^2/sec) for *n*-alkanes as a function of temperature

	Temperature (°C)				
Penetrant	23°C	45°C	55°C	65°C	85°C
Hexane	12.3	37.1	67.9	92.2	a
Heptane	7.84	25.5	48.9	71.2	115
Nonane	2.79	10.8	23.9	37.7	61.1
Decane	1.69	9.05	16.2	28.6	52.4
Undecane	1.12	6.55	12.3	19.9	46.7
Tridecane	0.427	3.44	7.59	16.7	31.2
Pentadecane	0.211	2.13	4.27	8.32	23.9
Hexadecane	0.157	1.69	3.78	7.29	20.7
Heptadecane	0.111	1.29	2.58	6.21	17.1

a-*Data not obtained due to its low boiling point*

Many efforts have been made in the past to correlate diffusion coefficients to physical properties such as molecular weight and molar volumes of the penetrants[16,17,18,19]. An inverse dependence of D on the molecular weight of the alkanes was obtained in the current study and is shown in Table 5-8. This is due to the geometric size requirements of the molecule in diffusing and the kinetic energy it may possess at a selected temperature. The behavior is consistent with the predictions of Fujita *et al.*[20,21] using free volume arguments. Furthermore, D was found to increase with decreasing temperature (T) as a result of the greater molecular mobility and free volume of the polymer.

Diffusion coefficients for the alkanes are plotted as a function of molar mass in Figure 5-13, where a logarithmic behavior is observed. This strong decrease in diffusivity with molecular size is in accordance with other results for linear aliphatic penetrants[13,22] and is generally[4,23] described by a power law expression,

(9) $$D = bM^{a}$$

where D = diffusivity (cm^2/sec)
M = molecular weight (g/mole)
b and *a* are material parameters. The front factor *b* is influenced by the polymer and polymer-penetrant attractions.

Experimental diffusion coefficients obtained at different temperatures were fit to the power law expression of equation (9) using a Levenberg-Marquardt algorithm, as shown in Figure 5-13. The corresponding *b* and *a* parameters are listed in Table 5-9. The values obtained for the exponent *a* are typical of aliphatic materials and exhibit a decreasing molecular weight dependence with increasing temperature. Equation (9) assumes that molecular mass is the major factor in governing transport behavior. Any arguments regarding penetrant shape, isomerism and mechanism of the diffusion process are ignored. Despite these limitations, an excellent agreement with the results for this series of linear alkanes is seen. Figure 5-13 also shows the extensive range of molecular weights over which this relationship holds. Such a range is possible since the species studied are all of the same homologous linear series with negligible attractions to the polymer matrix.

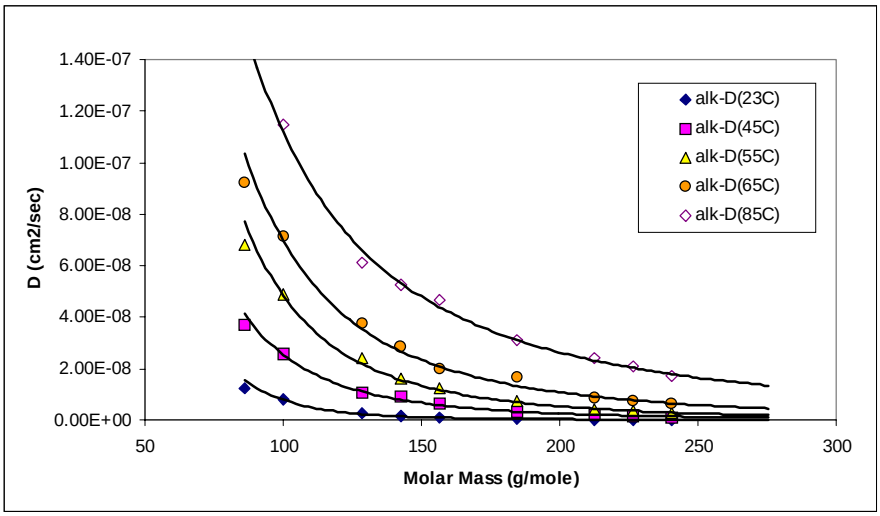

Figure 5-13. Molecular weight dependence of diffusivity for alkanes- equation (9)

Table 5-9. Power law coefficients for molecular weight dependence for alkanes as described by equation (9)

Temperature (ºC)	b($cm^2/sec.g^{-n}$)	a	R^2
23	20.1	-4.71	0.9937
45	0.0918	-3.28	0.9954
55	0.103	-3.17	0.9942
65	0.0165	-2.69	0.9885
85	0.00160	-2.09	0.9945

Molecular size of a penetrant is also expressed in terms of molar volume, V_m, which is described as an *average* value due to changing bond angles, rotations and chain conformations. During the transport process, a net jump of a penetrant occurs when an adjacent "hole" large enough to accommodate it exists[13]. Based on these considerations, V_m has been used to describe the diffusion behavior in the current study. Diffusivities (D) for the *n*-alkanes are plotted as a function of molar volume in Figure 5-14 where a linear dependence is observed. Variations in physical size of the penetrant do not cause any abrupt changes in the diffusion mechanism over the range of molecular weights studied. This may be due to the high degree of flexibility of the alkanes. The effects of molar volume on D are interpreted in terms of the free volume between polymer chains. The slopes of the lines decrease with increasing temperature, indicating that the increase in volume of the polymer (with temperature) is greater than that of the penetrants, thus enabling easier transport.

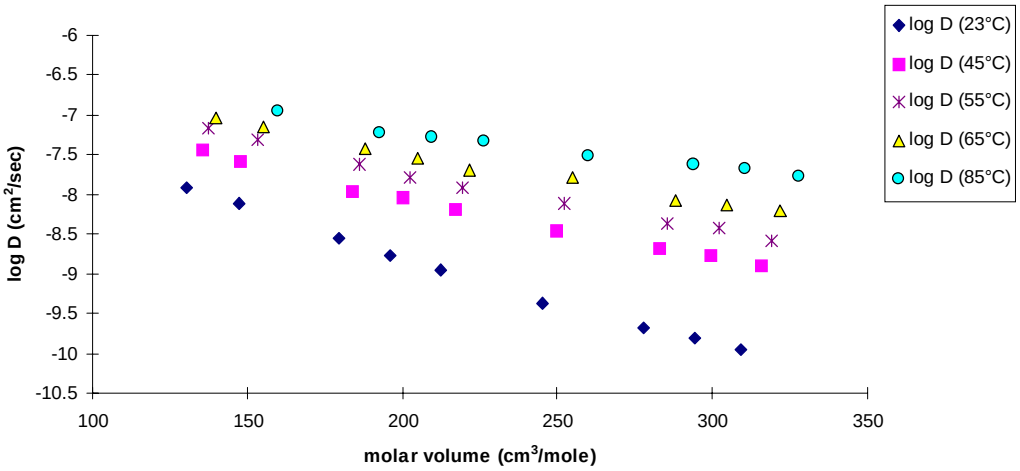

Figure 5-14. Plot of Log D (cm^2/sec) as a function of molar volume for the *n*-alkanes

5.2.1 Temperature Effects and Activation Parameters

Significant advances made in the understanding of the transport phenomenon at a microscopic level have elucidated major differences between the properties of glassy polymers and low T_g (rubbery) polymers[24]. The Arrhenius relationship has been experimentally shown[25] to be valid for $T > T_g$. In the current study, temperature dependence of the diffusion coefficients are assumed to be constant over the range investigated, obeying an Arrhenius model of kinetics,

(10) $$D = D_0 \exp \frac{-E_d}{RT}$$

where E_d = activation energy of diffusion (kJ/mole), and
D_o = Arrhenius front factor.

The activation energy, E_d, is defined as the amount of energy required to complete the unit transport of one mole of a diffusing molecule by creating an opening between polymer chains large enough to permit passage of the penetrant. Thus, it is a function of the inter- and intra-chain forces that must be overcome to create this space. It follows that

the E_d value will be greater, the larger the diffusant, the stronger the polymer cohesive energy, or the more rigid the polymer chains.

Slopes of linearized plots of log D versus 1/Temperature (Figure 5-15) are proportional to E_d. Each of the curves represents an alkane, designated in the legend by the number of carbon atoms. Results from this analysis including log D_o values are listed in Table 5-10. Although the values of R^2 deviate from 1, the fact that no major inflections are observed in Figure 5-15 indicates that there is no drastic change in the material or the mechanism of diffusion due to temperature. This observation, in addition to fact only qualitative comparisons are being made between penetrants, justifies the assumption of a constant activation energy that is utilized.

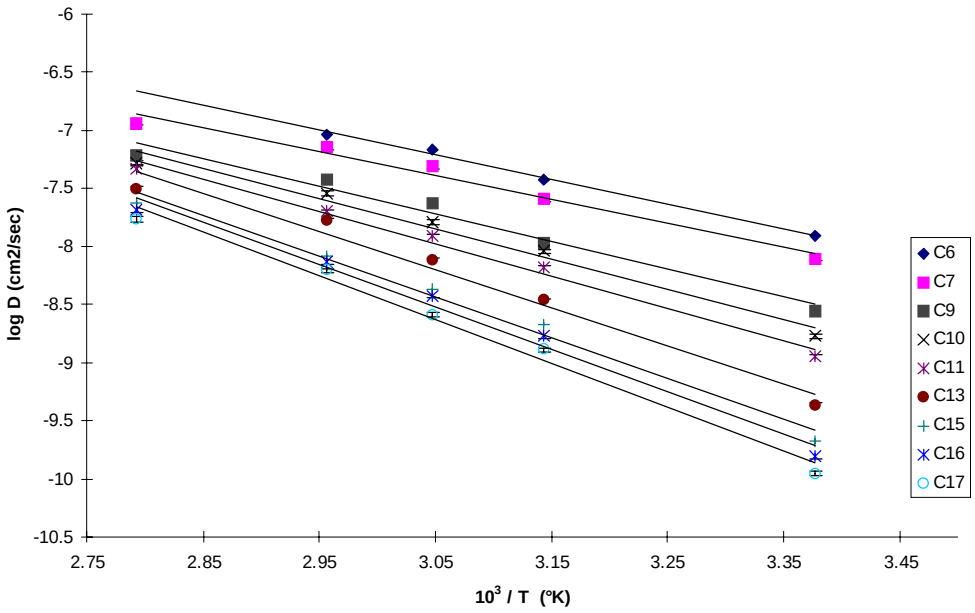

Figure 5-15. Arrhenius analysis for *n*-alkanes. Plot shows log D (cm^2/sec) as a function of 1/T. (number of carbon atoms designated in legend)

Table 5-10
Arrhenius parameters from evaluation of activation energy of diffusion for alkanes

Penetrant	Number of Carbon Atoms	E_d (kJ/mole)	Log D_o	R^2
Hexane	6	40.9	-0.704	0.9948
Heptane	7	39.4	-1.12	0.9798
Nonane	9	45.6	-0.464	0.9732
Decane	10	49.7	0.0662	0.9809
Undecane	11	53.2	0.503	0.9893
Tridecane	13	62.8	1.80	0.9744
Pentadecane	15	67.4	2.29	0.9876
Hexadecane	16	69.8	2.61	0.9856
Heptadecane	17	72.2	2.88	0.9870

The values of E_d obtained are higher than those of typical glassy polymers and are indicative of diffusion in the rubbery state[26]. This is due to the increased mobility of the polymer chains that allow more segments to become involved in the transport process. Furthermore, increasing values of E_d with increasing penetrant size imply that more complex segmental motions are necessary for the diffusion of larger molecules[6,27]. The activation energies of alkanes from Table 5-10 are plotted against molar volume in Figure 5-16, wherein a linear relationship is observed with the exception of hexane. The behavior of hexane may be indicative of a *critical volume* above which additional energy is required to overcome the forces necessary to accommodate a penetrant, thereby resulting in a change in mechanism at the elemental activation step. Similar observations were made by Koszinowski[28] on the diffusion of linear alkanes in polyolefins.

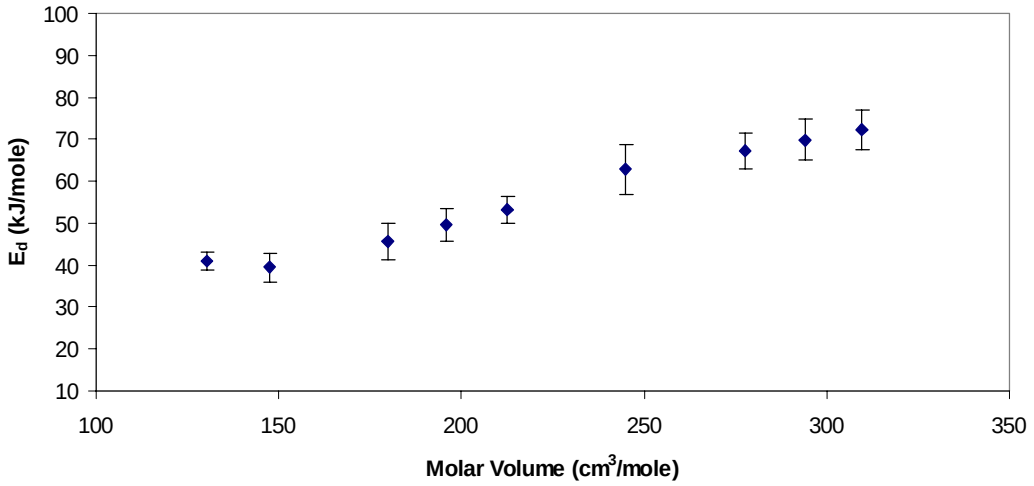

Figure 5-16. Molar volume dependence of the activation energy of diffusion, E_d, for *n*-alkanes (error bars represent standard error)

It has been shown[28,29,30] that the front factor, D_o, may be defined by Eyring's activated state theory as:

$$D_0 = e\lambda^2\left(\frac{kT}{h}\right)\exp\left(\frac{\Delta S_d}{R}\right) \quad (11)$$

where k = the Boltzmann constant
h = Planck's constant
R = the gas constant
λ = the jump distance of a molecule after the activation step, and
ΔS_d = the entropy change involved in the process.

Due to the fact that the activation energy of diffusion is also defined as a free energy, it is rewritten in terms of an enthalpic (ΔH_d) and entropic contributions (ΔS_d). Chen and Edin[16] have shown that this entropy of diffusion, ΔS_d, increases linearly with E_d. This is reasonable since the entropy term is a measure of local segmental "disturbance" for the activation process in diffusion. Intuitively, this "disturbance" becomes larger as the penetrant size increases. Since the diffusion front factor, D_o, contains the entropy term, it also reflects this increase in E_d. Therefore, a correlation exists between D_o and ΔH_d, which in turn results in a correlation between D_o and E_d (same as ΔE) since $\Delta H_d = \Delta E - RT$. This has been demonstrated for a number of polymers[4,31,25]. Figure 5-17 depicts the linear dependence of log D_o on E_d for the polymer-alkane systems in this study.

From the above discussion, it is possible to predict diffusion coefficients for penetrant molecules of the same type using the general form of the Arrhenius equation (equation (10)). The activation energy, E_d, may be extrapolated from knowledge of the molecular size (Figure 5-16). The corresponding D_o was determined from its dependence on E_d (Figure 5-17). Such calculations have been carried out by van Krevelen[32] and Meares[27].

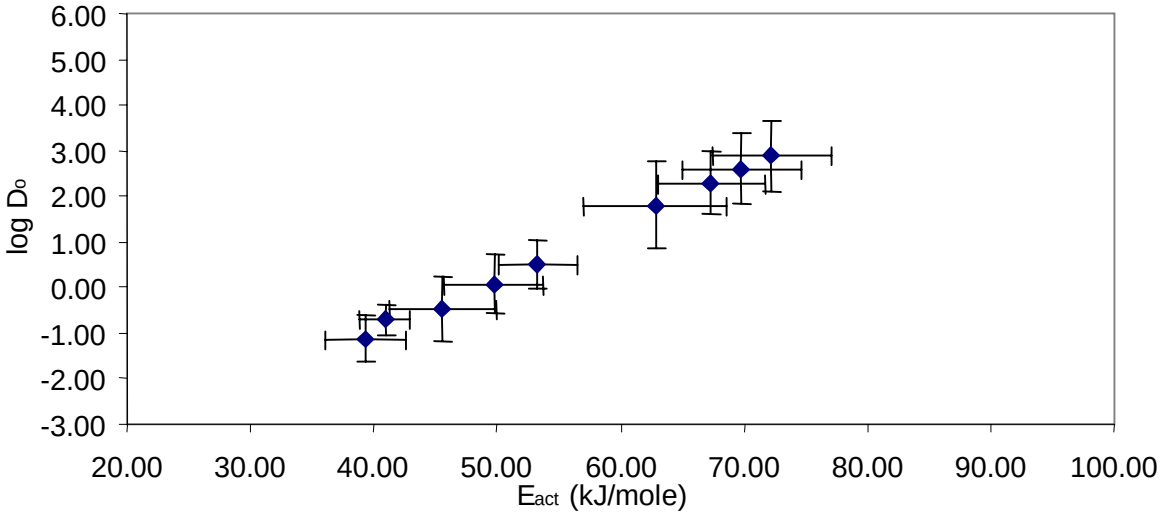

Figure 5-17. Relationship between the Arrhenius diffusion front factor (D_o) and the activation energy of diffusion (E_d) for the *n*-alkane

The permeation of a low molecular weight species through a rubbery or glassy polymer has been investigated by a number of researchers[33,34]. Since this is a solution-diffusion process, permeability (P) is a useful concept.

$$P \equiv D^{*}S$$

where S = solubility (grams of solvent per gram of the polymer ($g^{*}g^{-1}$))
D = diffusion coefficient.
Values of permeability coefficients for the *n*-alkanes studied are listed in Table 5-11.

The solubility coefficient (S) is expressed in terms of the van't Hoff relationship over a reasonable temperature range as[11,13,23]:

(12) $$S = S_0 \exp\left(\frac{-\Delta H_s}{RT}\right)$$

where S_o = a pre-exponential factor, and
ΔH_s = the heat of sorption.

ΔH_s is a composite parameter that contains information regarding the type of sorption mechanism involved - Henry's law or Langmuir (hole-filling) type of sorption. Henry's law mechanism involves the formation of a vacant site requiring motions of polymer segments (an endothermic process) followed by filling of this site with the solvent. The Langmuir mode of sorption assumes that vacancies pre-exist in the polymer matrix, thereby resulting in an exothermic process of solution.

Similar to the diffusion coefficient (D), the permeability (P) is also expressed in an Arrhenius form as:

(13) $$P = P_0 \exp\left(\frac{-E_p}{RT}\right)$$

where E_p = the activation energy of permeation
P_o = permeability front factor.

Plots of log P versus 1/Temperature for the alkanes are shown in Figure 5-18, where a decrease in P with increasing number of carbon atoms is observed, with hexane (C6) being the most permeable. Slopes of these lines are proportional to E_p and are listed in Table 5-12 along with the corresponding values of E_d. It can be seen that both E_p and E_d possess the same type of dependence on penetrant size. The decrease in P with decreasing temperature is expected since the equilibrium uptake exhibits very little temperature dependence, thereby allowing diffusivity to dominate the process.

An expression for E_p is obtained by substituting equations (10) and (12) into equation (13) using the definition P = D * S. Values for ΔH_s are evaluated from the

difference between E_p and E_d ($\Delta H_s = E_p - E_d$) and are given in Table 5-12. No clear trend relating ΔH_s to the number of carbon atoms is observed, contrary to expectations. However, for all linear alkanes the *positive* ΔH_s suggests that the endothermic Henry's law dissolution process governs the permeation mechanism.

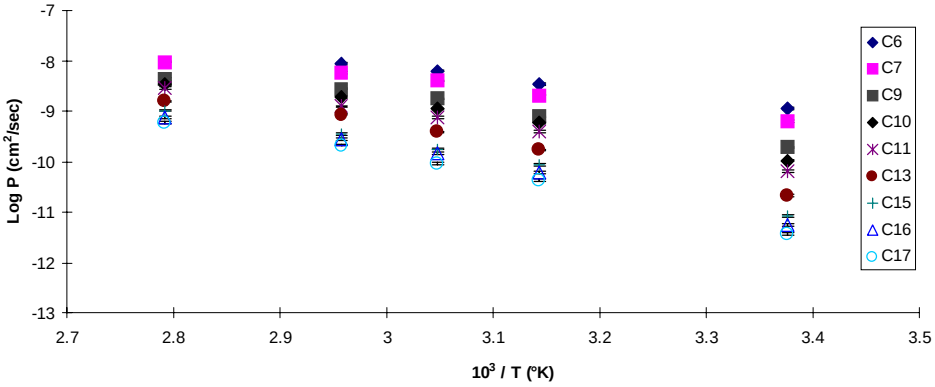

Figure 5-18. Arrhenius analysis of *n*-alkane permeability (cm^2/sec)

Table 5-11
Permeability coefficients (P x 10^9 cm^2/sec) for *n*-alkanes.

	Temperature				
Penetrant	23°C	45°C	55°C	65°C	85°C
Hexane	1.12	3.39	6.25	8.56	a
Heptane	0.629	2.04	3.99	5.81	9.34
Nonane	0.190	0.777	1.74	2.74	4.32
Decane	0.106	0.599	1.09	1.92	3.39
Undecane	0.0646	0.394	0.756	1.23	2.84
Tridecane	0.0211	0.171	0.385	0.852	1.57
Pentadecane	0.00833	0.0866	0.179	0.350	1.02
Hexadecane	0.00554	0.0614	0.144	0.275	0.755
Heptadecane	0.00375	0.0433	0.0926	0.213	0.590

Table 5-12
Activation parameters (E_d , E_p , and ΔH_s all in kJ/mole) for *n*-alkanes

Penetrant	E_p (kJ/mole)	E_d (kJ/mole)	$\Delta H_s=E_p-E_d$ (kJ/mole)
Hexane	41.3	40.9	0.387
Heptane	39.6	39.4	0.249
Nonane	46.2	45.6	0.584
Decane	50.2	49.7	0.536
Undecane	54.1	53.2	0.850
Tridecane	63.2	62.8	0.379
Pentadecane	68.5	67.4	1.12
Hexadecane	70.5	69.8	0.644
Heptadecane	72.6	72.2	0.373

According to Harogoppad *et al.*[35] and Southern and Thomas[36,37], when a polymer film is immersed in a liquid, its surface layer initially swells; but, the lateral expansion is constrained by the underlying unswollen material. Thus, a two-dimensional compressive force develops on the surface that reduces its equilibrium swelling. As the process progresses, the stresses are reduced since the swelling of the layer approaches that of the free, unconstrained state. Therefore, the first-order kinetic equation is used to study the sorption kinetics for low swelling ratios:

$$\frac{dC}{dt} = k\left(C_\infty - C_t\right) \tag{14}$$

where k = the first-order rate constant
C_t = concentration at time t
C_∞ = concentration at infinity.

Integration of equation (14) gives:

$$k't = \ln\left(\frac{C_\infty}{C_\infty - C_t}\right) \tag{15}$$

Since C_∞ and C_t are analogous to the corresponding terms of mass[33], equation (15) is rewritten as:

$$k't = \ln\left(\frac{M_\infty}{M_\infty - M_t}\right) \tag{16}$$

Graphs of ln $[M_\infty/(M_\infty-M_t)]$ versus time for all the alkanes were made, and the first-order rate constants k′ were determined from a least-squares analysis of these plots. A representative plot for tridecane is shown in Figure 5-19. The k′ for all the penetrants at the various test temperatures are listed in Table 5-13.

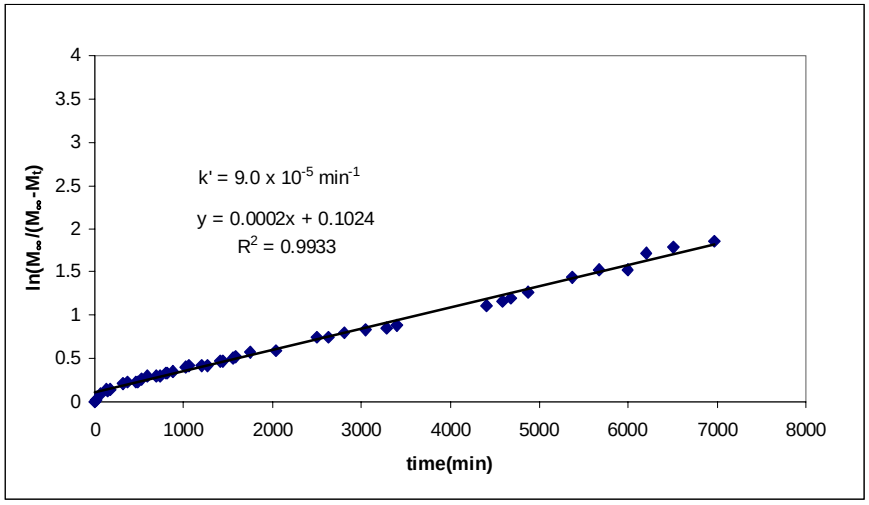

Figure 5-19. Kinetic plot of tridecane sorption at 23°C

It can be seen that the rate constants increase with temperature and decrease with molecular size, similar to the behavior of linear alcohols in a variety of elastomers[13]. The same dependence is exhibited by the diffusion coefficients, D and is explained by the fact that the kinetic equation (16) is equivalent to the reduced form of the diffusion equation (6) by neglecting the terms $n \geq 1$ for long sorption times.

(17) $$\ln\left(\frac{M_\infty}{M_\infty - M_t}\right) \cong \frac{\pi^2 Dt}{L^2}$$ where

(18) $$k' = \pi^2 \frac{D}{L^2}$$

Further support for the use of first-order kinetics is derived from other studies on low T_g materials such as those by Poinescu *et al.*[38] and Smith and Fisher[39]. Solvent uptake data was related to diffusivity, and it was suggested that the sorption behavior followed first-order kinetics.

Additional information on sorption kinetics of the aliphatic penetrants were obtained from the entropy of sorption, $\Delta S_{o.}$ The equilibrium sorption (S) values determined experimentally were regarded as thermodynamic equilibrium sorption constants designated by the symbol K_s. A plot of log S versus 1/T for the alkanes is shown in Figure 5-20. Using the van't Hoff equation,

(19) $$LogK_s = \frac{\Delta S_0}{2.303R} - \frac{\Delta H_0}{2.303RT}$$

the standard enthalpy, ΔH_o and the entropy, ΔS_o of sorption for each alkane have been evaluated from the slope and intercept, respectively and are listed in Table 5-14. These ΔH_o values correspond to the ΔH_s evaluated from the difference E_p-E_d, further implying that transport in *n*-alkanes is an endothermic process. The values of ΔS_o become increasingly negative as the size of the penetrant increases. This is due to the fact that the neighboring polymer chains "squeeze" together to a greater extent in order to accommodate a larger penetrant, thereby increasing the overall order of the polymer matrix[35,40] and resulting in a more negative ΔS_o.

Table 5-13
First-order sorption kinetic parameters ($k' \times 10^3$ min^{-1}) for the *n*-alkanes at 23°, 45°, 55°, 65°, and 85°C

	Temperature									
	23°C		45°C		55°C		65°C		85°C	
Penetrant	k′	R^2	k′	R^2	k′	R^2	k′	R^2	k′	R^2
HX	3.30	0.9802	8.20	0.9963	14.9	0.9962	23.6	0.9893	a	a
HP	2.00	0.9811	6.70	0.9984	11.5	0.9928	16.3	0.9984	31.1	0.9876
NN	0.60	0.9917	3.30	0.9897	5.70	0.9980	8.80	0.9947	15.6	0.9923
DC	0.40	0.9816	2.20	0.9948	3.60	0.9974	6.50	0.9933	12.8	0.9946
UD	0.20	0.9933	1.40	0.9966	2.60	0.9980	4.50	0.9934	10.1	0.9968
TD	0.09	0.9923	0.70	0.9977	1.40	0.9934	3.80	0.9892	6.10	0.9983
PD	0.04	0.9788	0.40	0.9932	0.90	0.9945	1.80	0.9966	5.30	0.9960
HXD	0.03	0.9816	0.30	0.9939	0.70	0.9962	1.50	0.9951	4.70	0.9965
HPD	0.01	0.9863	0.20	0.9919	0.50	0.9969	1.30	0.9965	3.70	0.9969

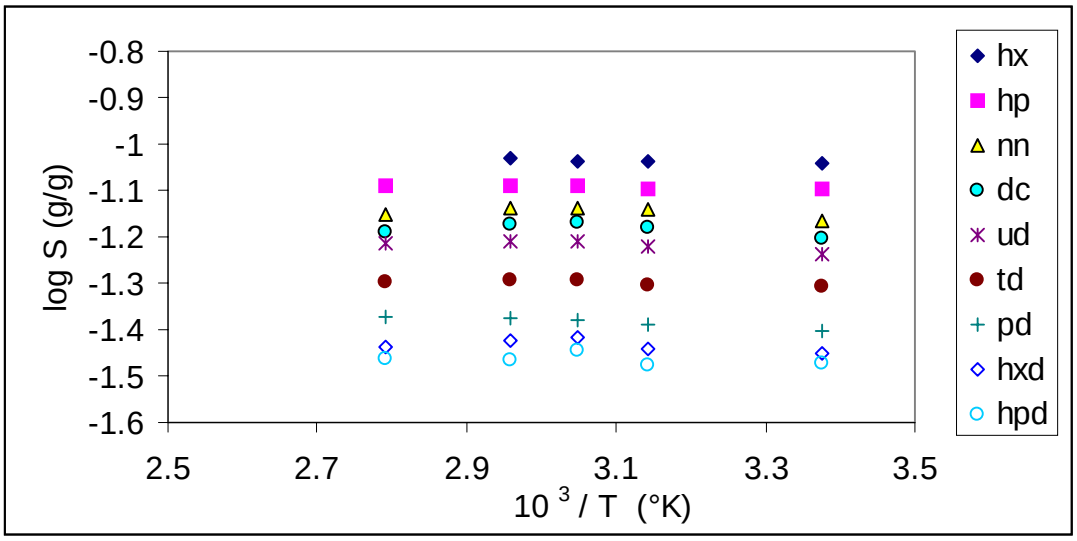

Figure 5-20. Van't Hoff analysis of *n*-alkane solubility as a function of temperature

	penetrants								
	HX	HP	NN	DC	UD	TD	PD	HXD	HPD
ΔH_o	0.3870	0.2488	0.5838	0.5363	0.8504	0.3786	1.1150	0.6442	0.3727
ΔS_s	-1.87	-2.01	-2.02	-2.10	-2.07	-2.37	-2.31	-2.55	-2.69

Table 5-14. Standard enthalpy (ΔH_o kJ/mole) and entropy of sorption (ΔS_o x 10^2 kJ/mole/°K)

5.3 Dynamic Solvent Uptake of Esters

Parallel to the sorption study of linear *n*-alkanes discussed in the previous section, a linear ester series ranging from methyl acetate (C5) to isopropyl myristate (C17) (Tables 3-2) was also investigated. In addition, another ester, isodecyl pelargonate (same molecular weight as isopropyl myristate) was studied in order to view the effects of position of the ester moiety on its transport.

Solvent uptake of esters was studied using the procedure as described earlier, for the *n*-alkanes (section 5-2). Reduced plots of fractional mass (M_t/ M_∞) at all the test temperatures are shown in Figure 5-21 through Figure 5-25. These curves exhibit linearity up to at least 60% fractional uptake. They are concave down and smoothly approach equilibrium sorption values, typical of Fickian diffusion.

As in the alkane series, the validity of a Fickian model for this sorption had to be tested. This was done using the power law equation[9,10] for fractional mass uptake equation (9). Nonlinear curve fitting was utilized to fit the isothermal (ester) curves (up to 97% fractional uptake) was performed. The resulting *K* and *n* values at the different temperatures are listed in Table 5-15 through Table 5-19.

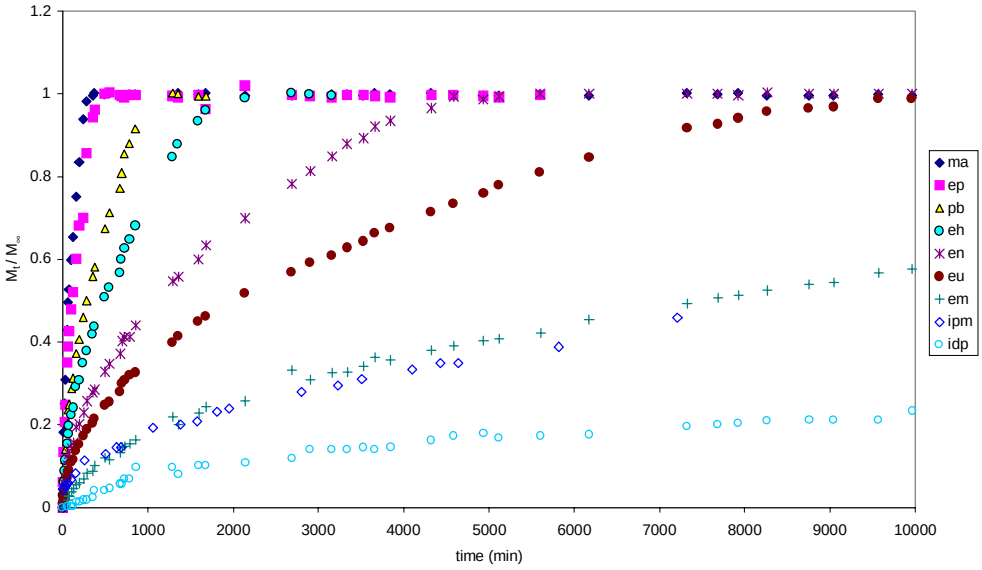

Figure 5-21. Fractional mass uptake for ester penetrants at 23°C

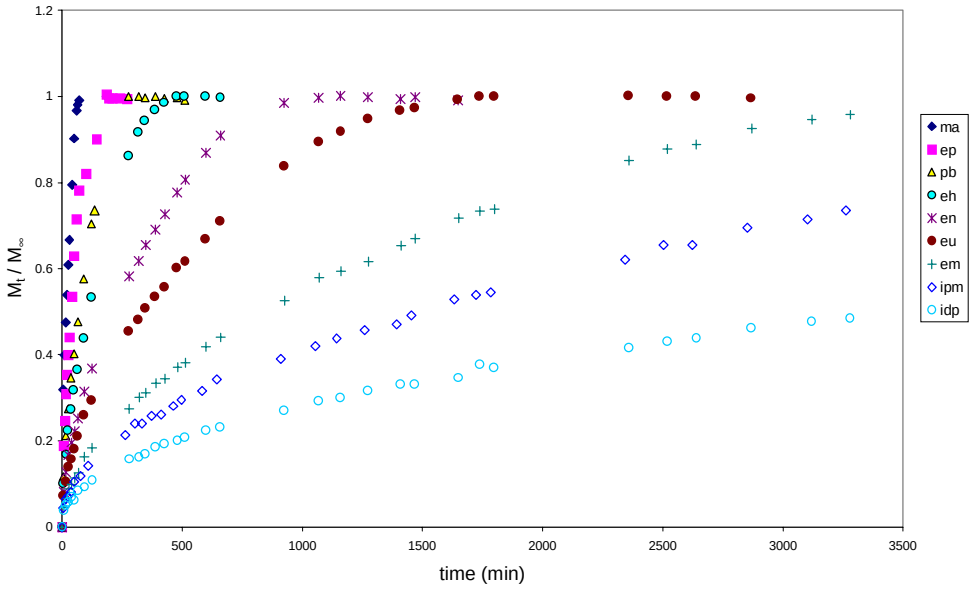

Figure 5-22. Fractional mass uptake for ester penetrants at 45°C

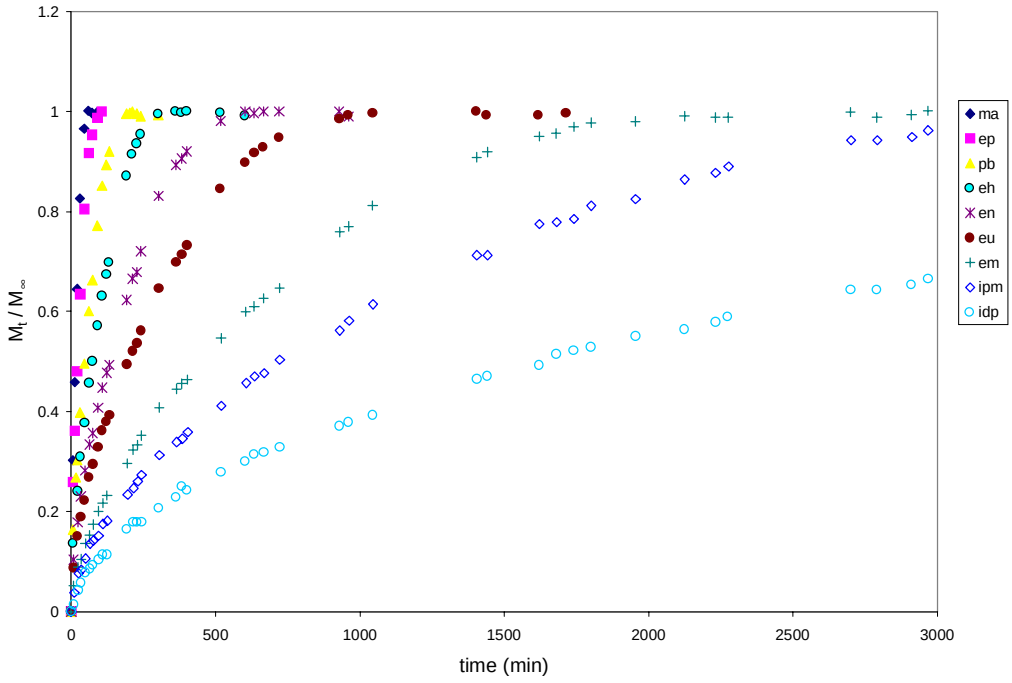

Figure 5-23. Fractional mass uptake for ester penetrants at 55°C

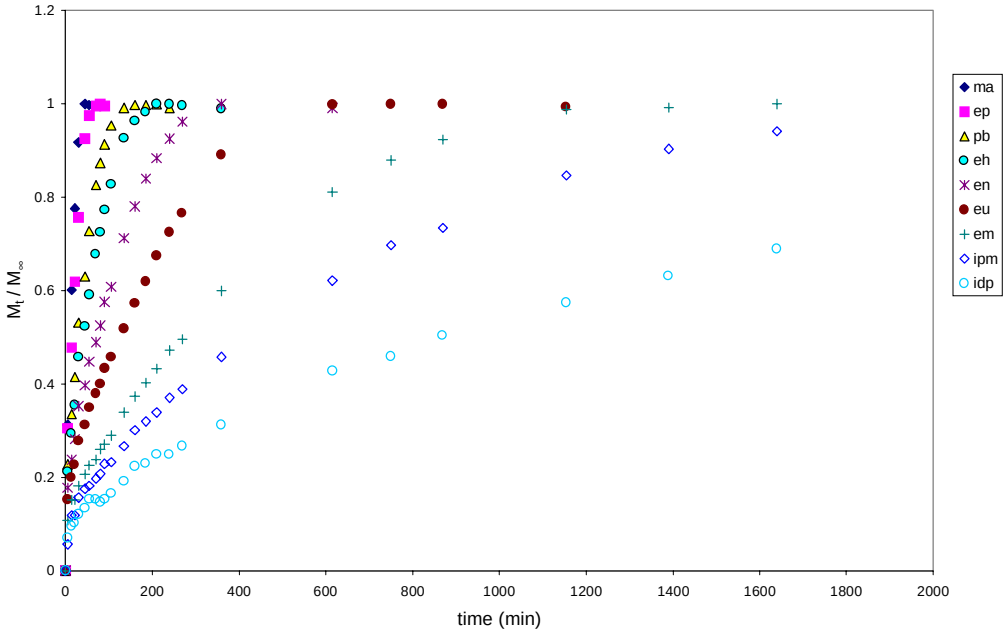

Figure 5-24. Fractional mass uptake for ester penetrants at 65°C

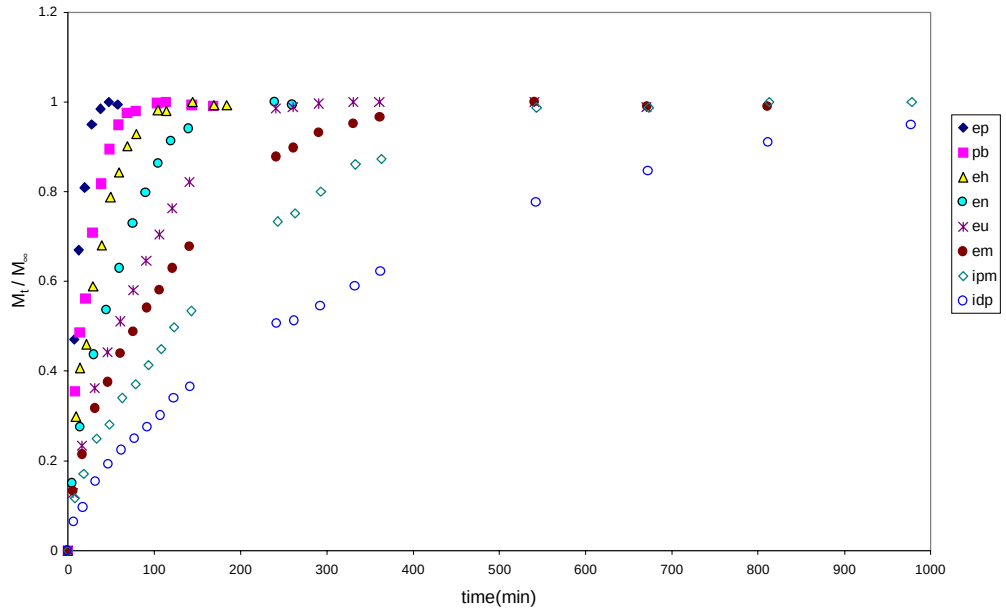

Figure 5-25. Fractional mass uptake for ester penetrants at 85°C

Table 5-15

K and *n* parameters for sorption of ester penetrants at 23°C using equation (3) $\frac{M_t}{M_\infty} = Kt^n$

Penetrant	**K x 10^3 (g/g/min^n)**	***n***	χ^2
Methyl Acetate	56.1	0.515	0.00021
Ethyl Propionate	41.0	0.533	0.00050
Propyl Butyrate	22.7	0.548	0.00014
Ethyl Heptanoate	18.9	0.530	0.00010
Ethyl Nonanoate	14.2	0.508	0.00010
Ethyl Undecanoate	12.2	0.485	0.00010
Ethyl Myristate	5.21	0.511	0.00020
Isopropyl Myristate	11.1	0.407	0.00015
Isodecyl Pelargonate	3.09	0.467	0.00020

Table 5-16

K and *n* parameters for sorption of ester penetrants at 45°C using equation (3) $\frac{M_t}{M_\infty} = Kt^n$

Penetrant	**K x 10^3 (g/g/min^n)**	***n***	χ^2
Methyl Acetate	125	0.497	0.00043
Ethyl Propionate	54.5	0.623	0.00023
Propyl Butyrate	41.9	0.585	0.00005
Ethyl Heptanoate	34.5	0.568	0.00008
Ethyl Nonanoate	27.3	0.542	0.00004
Ethyl Undecanoate	25.3	0.512	0.00004
Ethyl Myristate	16.4	0.507	0.00012
Isopropyl Myristate	15.6	0.474	0.00010
Isodecyl Pelargonate	12.5	0.451	0.00007

Table 5-17

K and *n* parameters for ester penetrants at 55°C using equation ((3) $\frac{M_t}{M_\infty} = Kt^n$

Penetrant	**K x 10^3 (g/g/min^n)**	***n***	χ^2
Methyl Acetate	127	0.539	0.00075
Ethyl Propionate	97.7	0.540	0.00085
Propyl Butyrate	51.0	0.598	0.00018
Ethyl Heptanoate	44.7	0.562	0.00011
Ethyl Nonanoate	31.9	0.565	0.00012
Ethyl Undecanoate	29.4	0.535	0.00010
Ethyl Myristate	16.2	0.560	0.00016
Isopropyl Myristate	14.1	0.539	0.00010
Isodecyl Pelargonate	12.8	0.493	0.00016

Table 5-18

K and *n* parameters for sorption of esters at 65°C using equation (3) $\frac{M_t}{M_\infty} = Kt^n$

Penetrant	**K x 10^3 (g/g/min^n)**	***n***	χ^2
Methyl Acetate	126	0.587	0.00041
Ethyl Propionate	124	0.528	0.00027
Propyl Butyrate	93.8	0.505	0.00043
Ethyl Heptanoate	82.9	0.493	0.00022
Ethyl Nonanoate	65.4	0.484	0.00031
Ethyl Undecanoate	49.1	0.489	0.00035
Ethyl Myristate	27.0	0.524	0.00044
Isopropyl Myristate	23.2	0.509	0.00021
Isodecyl Pelargonate	19.5	0.479	0.00025

Table 5-19

K and *n* values for sorption of esters at 85°C using equation (3) $\frac{M_t}{M_\infty} = Kt^n$

Penetrant	**K x 10^3 (g/g/min^n)**	***n***	**χ^2**
Methyl Acetate	*a*	*a*	*a*
Ethyl Propionate	177	0.511	0.00071
Propyl Butyrate	134	0.488	0.00057
Ethyl Heptanoate	103	0.513	0.00057
Ethyl Nonanoate	70.4	0.534	0.00051
Ethyl Undecanoate	56.7	0.538	0.00022
Ethyl Myristate	52.3	0.516	0.00004
Isopropyl Myristate	34.1	0.554	0.00020
Isodecyl Pelargonate	24.0	0.548	0.00012

a—Data not obtained due to its low boiling point

All the *n* values are approximately 0.5, typical of ideal Fickian diffusion[13]. This behavior results from the rapid segmental motions in the polymeric material that minimize any relaxation effects. The constant K exhibited a systematic decrease with increasing number of carbon atoms and decreasing temperature (Figure 5-26). No such trend was observed for *n*. The temperature dependence of K may be attributed to the increase in mobility of the penetrant and increase in volume within the polymer, with temperature.

The solubility *(equilibrium weight percent uptake*) of the esters shown in Figure 5-27 bears a similar dependence upon molecular weight as those of the alkanes (section 5-2). However, the esters possess greater solubilities and yield an apparent maximum for ethyl propionate. According to Cowie[41], such a maximum for an elastomeric system occurs when the difference in solubility parameters (δ) between the polymer and solvent are at a minimum. Equilibrium sorption of the esters is plotted as a function of δ of each penetrant in Figure 5-28. The maximum appears at ~18 $MPa^{0.5}$ and may be taken as the δ of the polymeric adhesive. This value is consistent with solubility parameters of typical polyamide-type materials[42].

All the ester penetrants posses a single polar ester functionality. The polarity of a low molecular weight species is relatively high due to the fact that the ester group comprises the majority of the molecule. This increases its potential for specific interactions with the polymer. However, with an increase in the number of carbon atoms, the polarity is "diluted" by the presence of a long hydrophobic tail, whose flexibility enables the molecule to "fold" back on itself, thereby shielding the ester functionality. This results in lower δ's for the esters approaching those of the alkanes. Similar effects have been reported by Koszinowski[43] with phenoxy alcohols in LDPE.

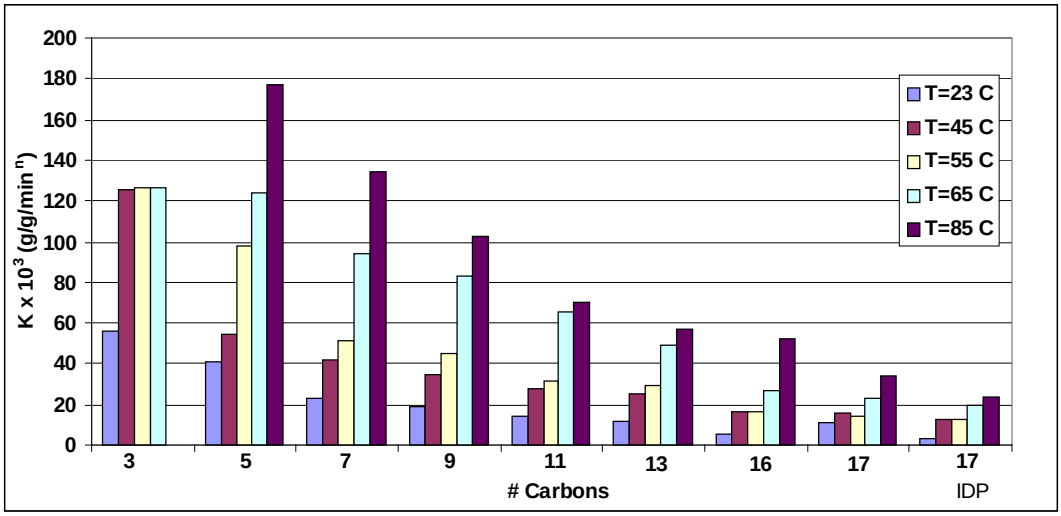

Figure 5-26. *K* versus the number of carbon atoms in the ester penetrants for temperature isotherms.

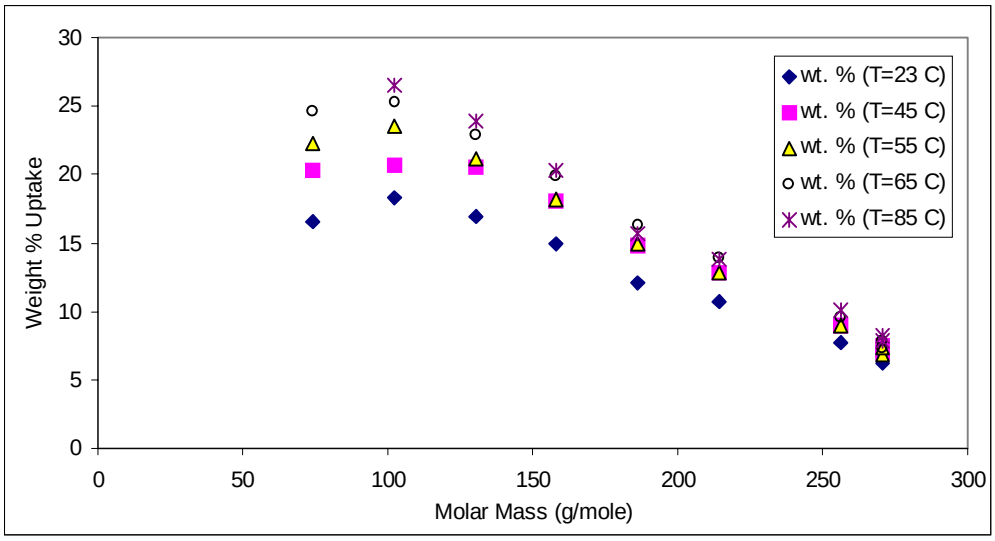

Figure 5-27. Equilibrium weight uptake versus molar mass of the esters

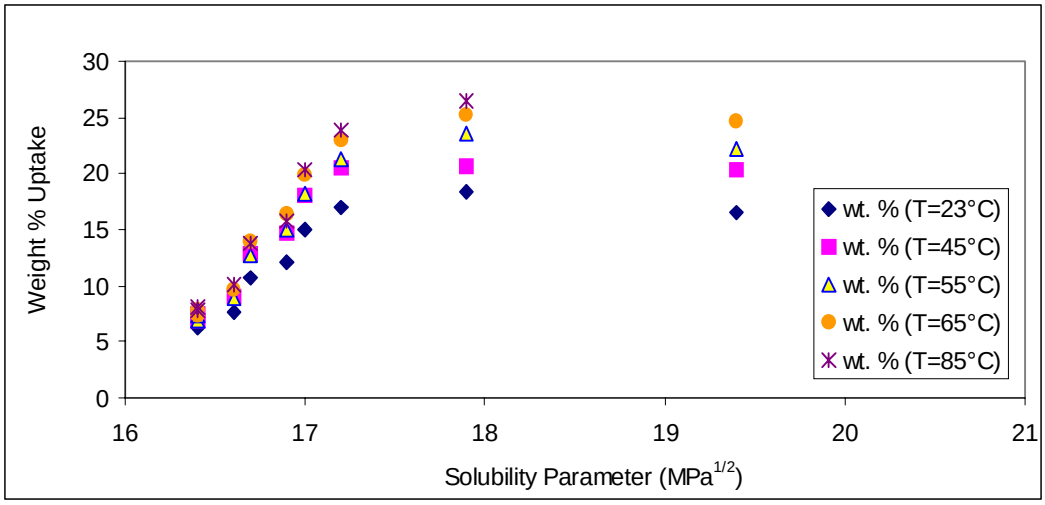

Figure 5-28. Equilibrium weight percent uptake for esters as a function of their solubility parameters.

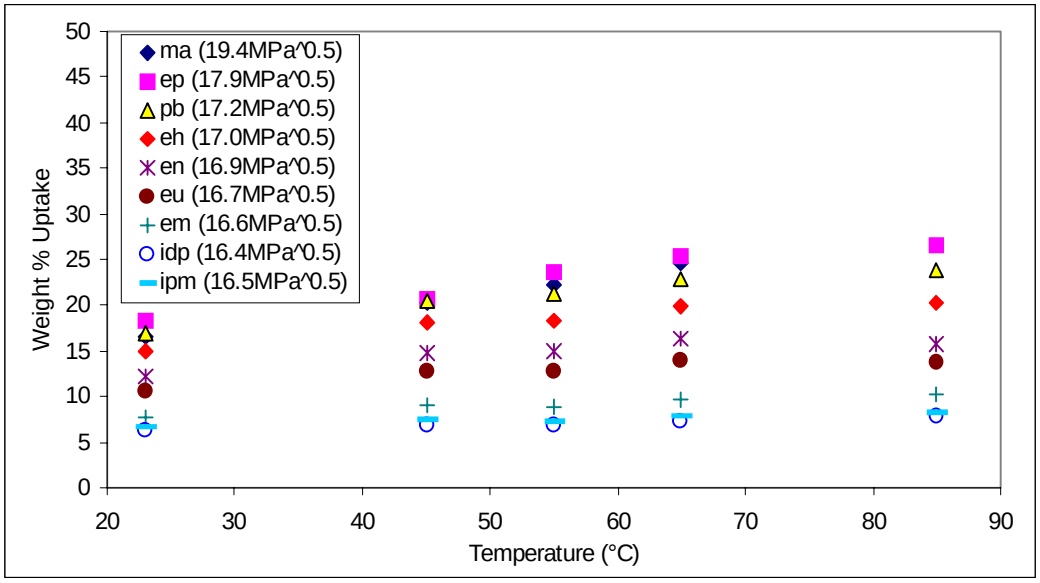

Figure 5-29. Weight percent uptake versus temperature for esters

Solubilities (S) of the esters are plotted as a function of temperature in Figure 5-29. An increase in S with temperature is observed and is more pronounced for the lower molecular weight species. This dependence is a result of a more positive heat of solution term due to the endothermic nature of the process and the thermal expansion of the matrix. In addition, the greater entropic contribution that increases with temperature aids in the solubility of the lower molecular weight esters.

Diffusion coefficients (D) of the esters were calculated from the initial slopes of linearized plots of M_t/M_∞ versus $t^{0.5}$ (Figure 5-30 through Figure 5-34), as in the case of *n*-alkanes. Linear regression of the experimental data up to 55% fractional mass uptake yielded excellent results with statistical R^2 values ranging from 0.9950 to 1.000. The values for D for all the test temperatures are listed in Table 5-20.

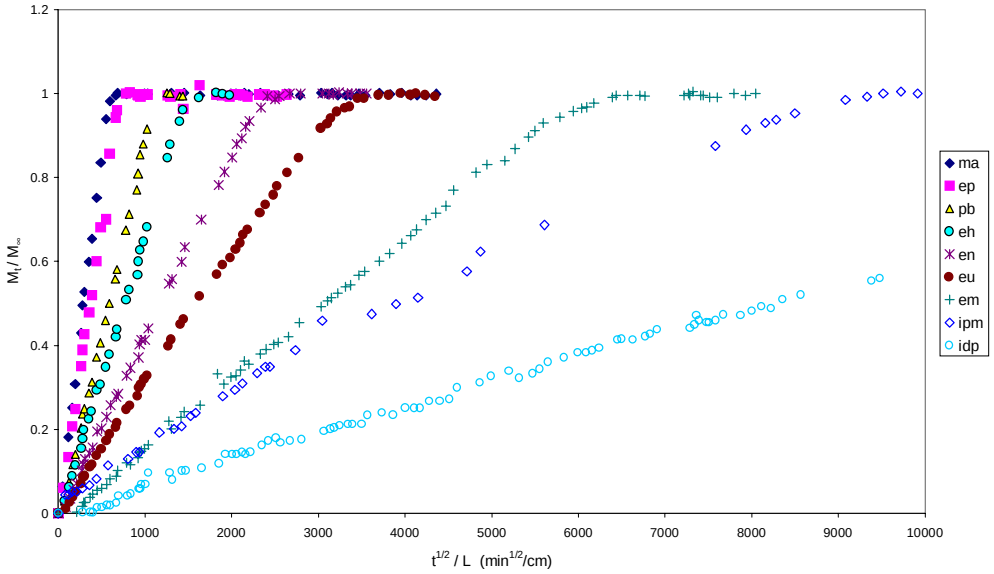

Figure 5-30. Fractional mass uptake for ester penetrants at 23°C versus square root of normalized time

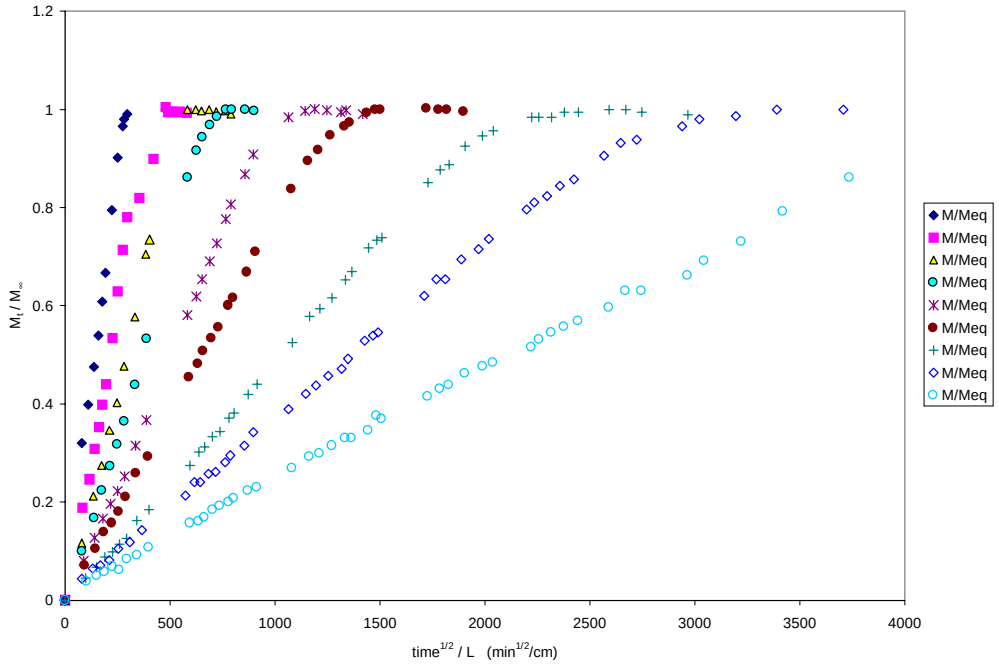

Figure 5-31. Fractional mass uptake for ester penetrants at 45°C versus square root of normalized time

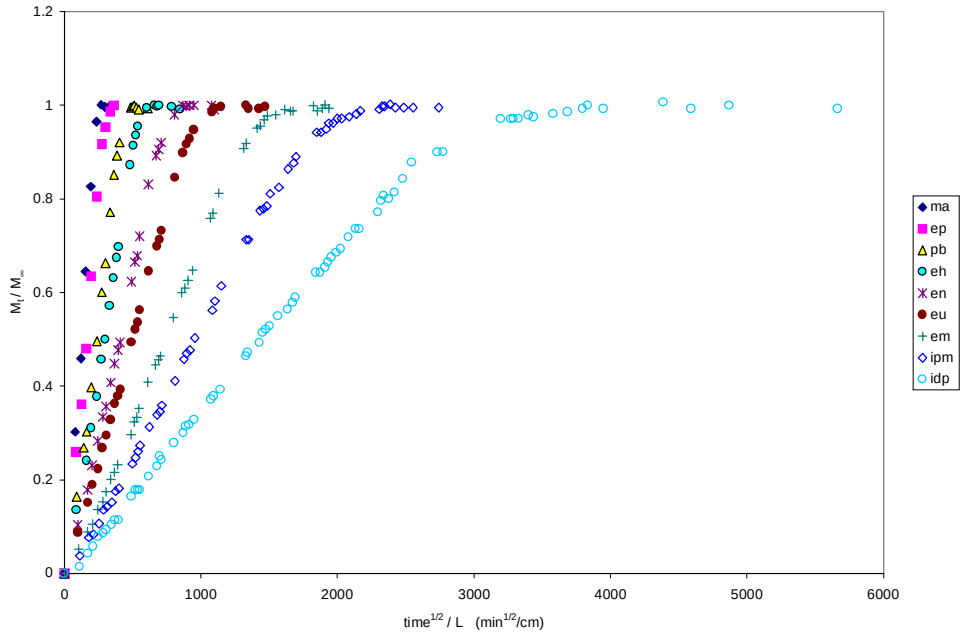

Figure 5-32. Fractional mass uptake for ester penetrants at 55°C versus square root of normalized time

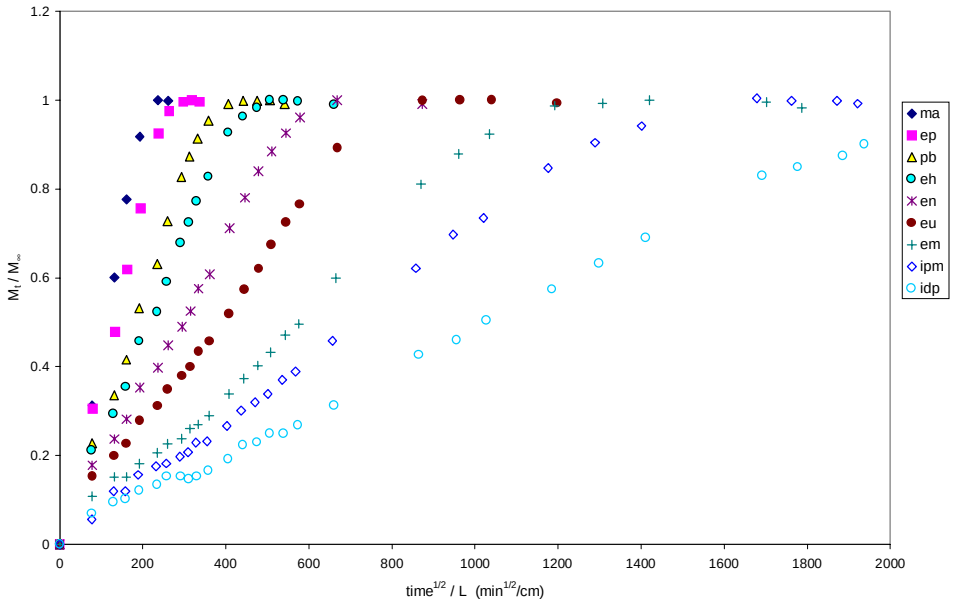

Figure 5-33. Fractional mass uptake for ester penetrants at 65°C versus square root of normalized time

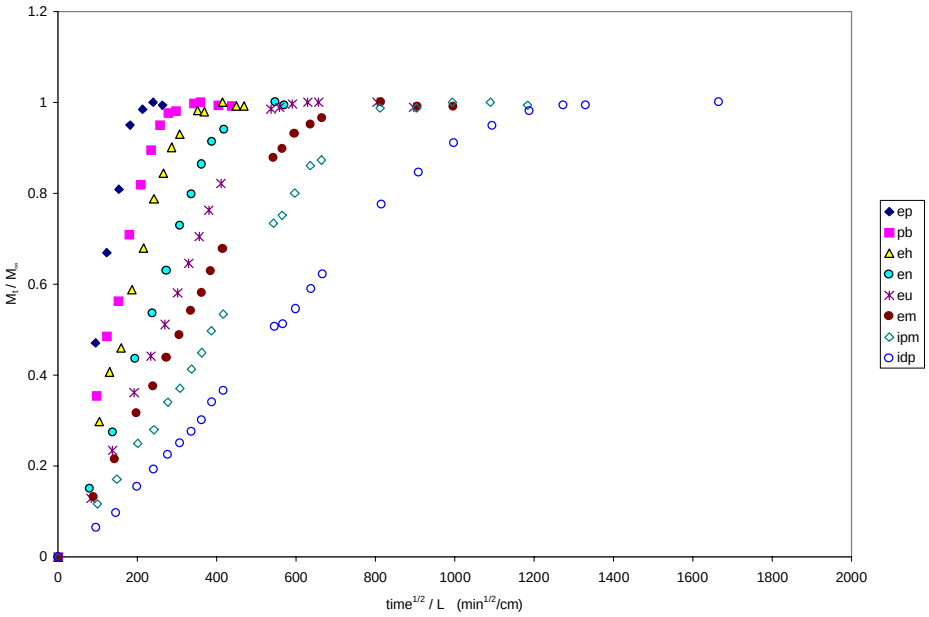

Figure 5-34. Fractional mass uptake for ester penetrants at 85°C versus square root of normalized time

Table 5-20
Diffusion coefficients (D x 10^9 cm^2/sec) for ester penetrants

	Temperature (°C)				
Penetrant	23°C	45°C	55°C	65°C	85°C
Methyl acetate	40.5	148	215	300	a
Ethyl propionate	26.0	70.1	132	182	370
Propyl Butyrate	10.3	39.4	61.7	93.9	198
Ethyl heptanoate	5.77	24.0	40.8	64.9	125
Ethyl nonanoate	2.48	12.8	21.1	33.9	68.6
Ethyl undecanoate	1.40	7.79	12.5	18.6	49.2
Ethyl myristate	.391	3.07	6.46	8.46	34.6
Isopropyl myristate	0.216	1.67	3.85	5.73	21.5
Isodecyl pelargonate	0.0516	0.496	1.71	2.76	11.6

a-*Data not obtained due to its low boiling point*

Diffusivity decreases with increasing number of carbon atoms (in the ester) and decreasing temperature. These observations are similar to those of the *n*-alkanes and may be explained based upon free volume arguments[13,20,22] discussed earlier (section 5-2).

Previous studies[16,17,18] have shown that the results such as those obtained may be used to correlate the diffusion coefficient to physical properties (such as molecular weight and molar volume) of a penetrant. This was done by means of a power law (equation (10)), whose validity for the ester series was tested as shown in Figure 5-35. The corresponding a and b coefficients are listed in Table 5-21. It is obvious from the R^2 values (in Table 5-21) that this relationship does not adequately describe the molecular weight dependence of the diffusivity of the esters studied. This is due to the inherent assumption in equation (10) of mass being the dominant factor in determining the transport process, without any regard to any shape and chemical effects. Further shortcomings of the power law for other *polar* systems have been demonstrated by Möller and Gevert[4] with phenolic penetrants.

Thus, it may be concluded that the power law expression is a good estimate of diffusivity for nonpolar systems, but fails to sufficiently account for the chemical nature of a polar species. A better description of the penetrant in terms of not only molecular weight, but also size, shape and relative interactions (with itself and with the polymer matrix) is essential.

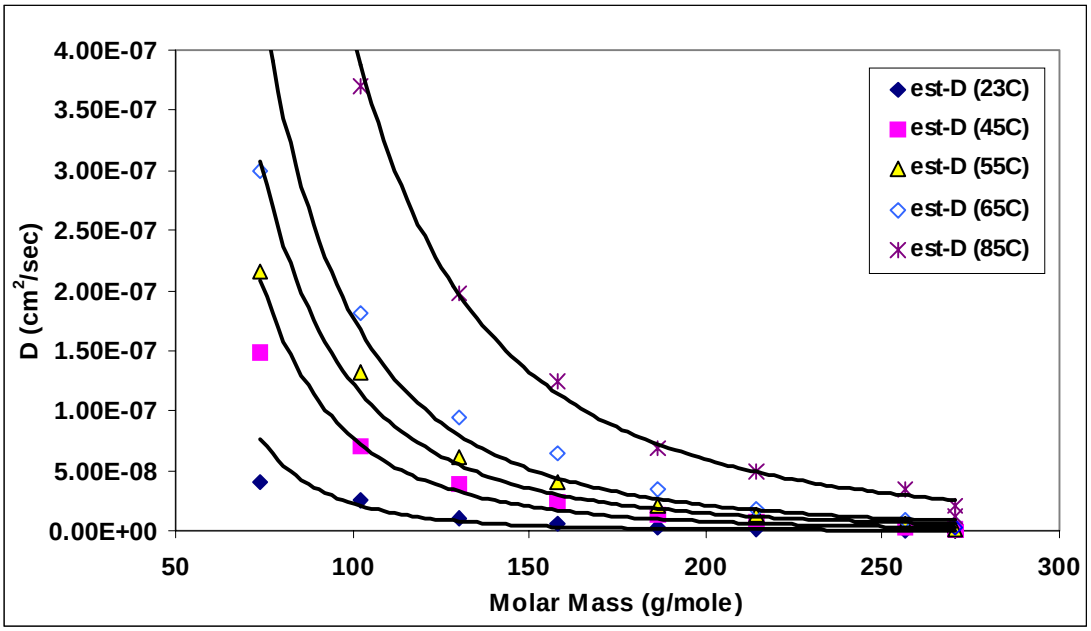

Figure 5-35 Power law fit to molecular weight of ester penetrants

Table 5-21 *b* and *n* coefficients from molar mass power law fit of ester penetrants

Temperature	b ($cm^2/sec*g/mole^{-n}$)	n	R^2
23	2.71	-4.04	0.9436
45	0.319	-3.31	0.9572
55	0.164	-3.06	0.9666
65	0.232	-3.06	0.9578
85	0.162	-2.80	0.9889

Diffusivity, D of the esters plotted as a function of V_m in Figure 5-36 yields a linear dependence for D. The mechanism of diffusion does not vary abruptly with an increase in the number of carbon atoms in the hydrophobic tail of the ester penetrants. However, a large deviation for IDP (V_m=314.56 cm^3/mole) at all the temperatures implies a significant change in mechanism in this case.

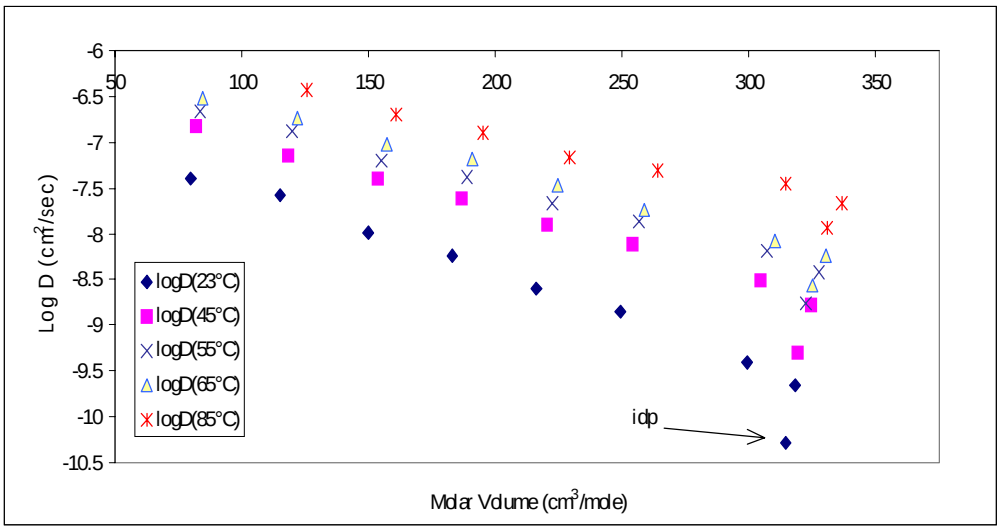

Figure 5-36. Log D versus molar volume for ester penetrants

The slopes become more positive with increasing temperature due to a greater increase in the volume of the polymer relative to that of the penetrants, thus enabling easier transport.

5.3.1 Temperature Effects and Activation Parameters

An Arrhenius model of diffusion kinetics is based upon the assumption of a constant activation energy (E_d), which is often valid for low T_g materials. Any changes in the system or mechanism due to temperature, will be evident in a large change in the E_d term. Using the Arrhenius equation of diffusion, equation (10), the values of E_d for the esters have been evaluated from the slopes of linearized plots of log D versus 1/T (Figure 5-37). No discontinuities are observed, indicating that there is no change in mechanism throughout the temperature range studied. The slopes of the lines increase with increasing molecular size due to the greater number of polymer segments that need to be involved in the diffusion process in order to accommodate a larger penetrant. The activation energies, E_d, and Arrhenius front factors, D_o, from the above analysis are listed in Table 5-22. The values of E_d for the esters are the same order of magnitude as those of the alkanes, and are typical of diffusion into a rubbery matrix.

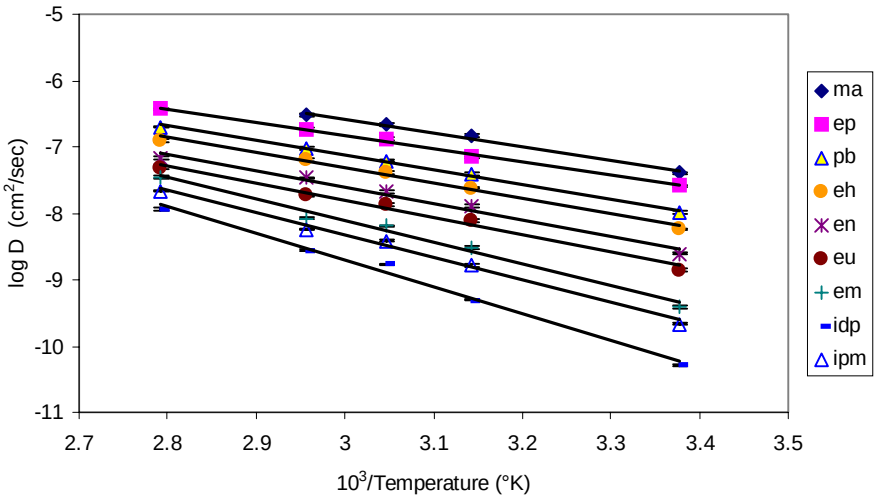

Figure 5-37. Arrhenius plots for the ester penetrants

Table 5-22. Arrhenius parameters for ester penetrants

Penetrant	Number of Carbon Atoms	E_d (kJ/mole)	Log D_o
Methyl Acetate	3	40.2	-0.278
Ethyl Propionate	5	38.3	-0.831
Propyl Butyrate	7	42.0	-0.548
Ethyl Heptanoate	9	44.2	-0.394
Ethyl Nonanoate	11	47.4	-0.178
Ethyl Undecanoate	13	49.9	0.0156
Ethyl Myristate	16	62.4	1.65
Isopropyl Myristate	17	64.8	1.82
Isodecyl Pelargonate	17	77.4	3.42

The activation energies of the esters are plotted as a function of molar volume (at 23°C) in Figure 5-38 where approximately two different slopes are observed, excluding the anomalous behavior of IDP. This is in contrast to the linear relationship observed for the *n*-alkanes (except hexane) and may be associated with a *critical* volume below which the available "hole" is large enough to allow diffusion to occur in a more simple, elemental step. Such a step involves fewer polymer segmental motions and permits diffusion of the penetrant as a single unit. Above this volume, additional energy is required to overcome the forces necessary to accommodate a larger species.

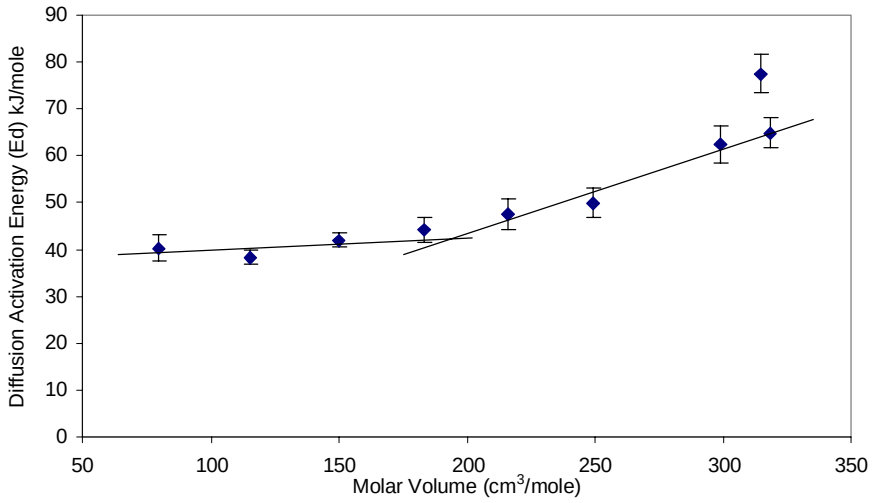

Figure 5-38. Activation energy of diffusion, E_d, versus molar volume of esters

Based on the correlations between D_o and E_d of *n*-alkanes established in section 5-2, a plot of log D_o versus E_d for the esters is shown in Figure 5-39. A linear dependence, similar to that of the alkanes is observed and may be used to predict diffusivities of similar penetrant types, by means of the general form of the Arrhenius expression (equation (10)).

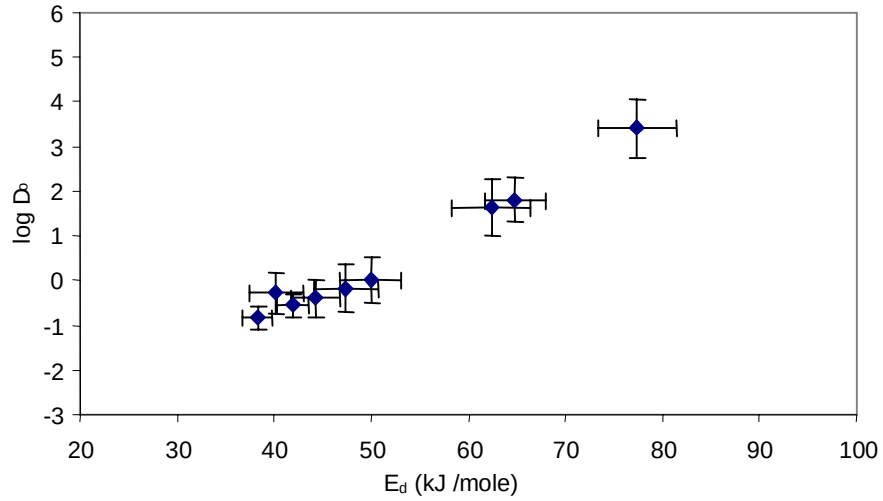

Figure 5-39. Plot of Arrhenius front factor, D_o, versus activation energy of diffusion, E_d, for ester penetrants

Permeability coefficients (P) for the ester sorption have also been calculated using the definition, P = D*S, at all the test temperatures and are listed in Table 5-23. It can be seen that the values of P decrease with increasing penetrant size, due to the decreases in both the D and S terms. This behavior is dominated by diffusivity, which changes much more dramatically than solubility. The temperature dependence of P (Table 5-23) is reflective of the increases in both D and S at higher temperatures.

Table 5-23. Permeability coefficients (P x 10^9 cm^2/sec) for ester penetrants

	Temperature				
Penetrant	23°C	45°C	55°C	65°C	85°C
Methyl Acetate	6.70	30.1	47.8	74.0	*a*
Ethyl Propionate	4.77	14.5	31.1	46.1	98.2
Propyl Butyrate	1.74	8.10	13.1	21.5	47.2
Ethyl Heptanoate	0.866	4.33	7.43	12.9	25.4
Ethyl Nonanoate	0.301	1.89	3.15	5.54	10.8
Ethyl Undecanoate	0.149	0.996	1.73	2.58	6.78
Ethyl Myristate	0.0301	0.277	0.577	0.814	3.51
Isopropyl Myristate	0.0144	0.125	0.282	0.450	1.76
Isodecyl Pelargonate	0.00324	0.0343	0.117	0.203	0.908

a-Data not obtained due to its low boiling point

The activation energies of permeation, E_p (for the esters) were evaluated based on an Arrhenius model of permeability. Plots of log P versus 1/T (Figure 5-40) yielded slopes proportional to E_p and clearly depict the temperature dependence for the esters described above.

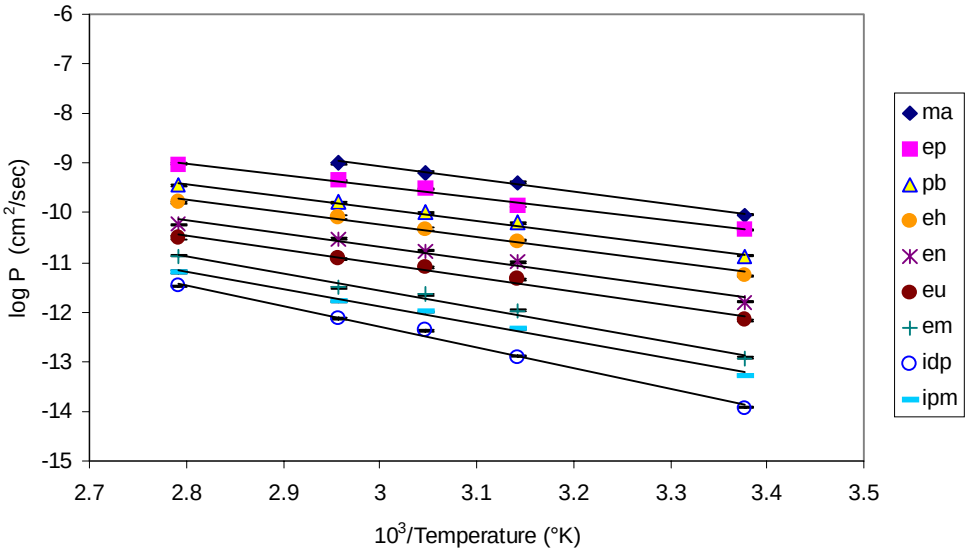

Figure 5-40. Arrhenius analysis of permeability coefficients for ester penetrants

As in the case of alkanes, the heat of solution, ΔH_s for the esters were determined from the expression, $E_p = E_d + \Delta H_s$, and are listed in Table 5-24 along with the corresponding activation parameters. An increase in ΔH_s with decreasing penetrant size is observed. The ΔH_s for the esters are more positive than those of the alkanes by about an order of magnitude and continue to suggest that an endothermic process following Henry's Law dominates the permeation mechanism.

Table 5-24. Activation parameters (E_d, E_p, and ΔH_s all in kJ/mole) for ester penetrants

Penetrant	E_p (kJ/mole)	E_d (kJ/mole)	$\Delta H_s=E_p-E_d$
Methyl Acetate	48.0	40.2	7.82
Ethyl Propionate	43.9	38.3	5.64
Propyl Butyrate	47.0	42.0	4.97
Ethyl Heptanoate	48.6	44.2	4.43
Ethyl Nonanoate	51.4	47.4	3.95
Ethyl Undecanoate	53.7	49.9	3.76
Ethyl Myristate	66.2	62.4	3.88
Isopropyl Myristate	67.7	64.8	2.85
Isodecyl Pelargonate	80.5	77.4	3.08

Based on the discussion in section 5-2, first-order kinetics have been utilized to analyze the sorption data of the ester penetrants. Further justification for this is derived from a study by Aminabhavi and Phayde[44,45], wherein the applicability of first order kinetics to elastomeric materials of high swelling ratios, has been demonstrated. The maximum swelling ratios for the systems in the current study are well within this "range of applicability". A least-squares analysis using equation (16) yielded rate constants, k′, that are listed in Table 5-26. Although the extent of swelling for the esters is greater than that of the alkanes, excellent fits with negligible deviations were obtained. K′ is found to increase with temperature and decrease with the addition of methylene units, analogous to the behavior of diffusion coefficients. This is due to the equivalence[13] of the first order kinetic equation to the "long-time approximation" for a "thin-film" Fickian diffusion process, as described earlier (section 5-2).

Additional insight into the transport mechanism can be gained by comparing the entropy of sorption values of the penetrants. A van't Hoff analysis of the solubility coefficients for each ester was performed to yield the standard enthalpy, ΔH_o, and the entropy of sorption, ΔS_o, using equation (19). These plots are shown in Figure 5-41, and their ΔH_o and ΔS_o values calculated for the esters are listed in Table 5-25. The enthalpies from this analysis agree remarkably well with those evaluated via the (E_p-E_d) method. The entropies, ΔS_o, systematically decrease with penetrant size. In order to accommodate a larger penetrant, the neighboring polymer chains "squeeze" together to a greater extent. This increases the overall order of the polymer matrix[6,9,33,35,40], and results in a more negative ΔS_o.

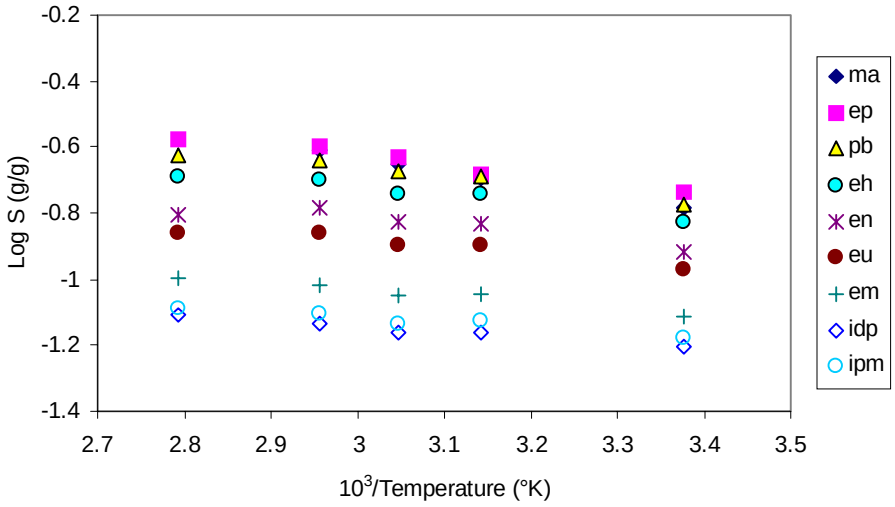

Figure 5-41. Van't Hoff analysis of ester solubility as a function of temperature

Table 5-25. Standard enthalpy (ΔH_o kJ/mole) and entropy of sorption (ΔS_o x 10^3 kJ/mole/°K)

	penetrants								
	MA	EP	PB	EH	EN	EU	EM	IPM	IDP
ΔH_o	7.82	5.64	4.97	4.53	3.95	3.77	3.88	2.85	3.08
ΔS_s	11.4	4.95	2.23	-0.270	-3.84	-5.61	-8.10	-12.6	-12.8

Table 5-26
First-order sorption kinetic parameters (k' x 10^3 min^{-1}) for the ester penetrants at 23°, 45°, 55°, 65°, and 85°C

	Temperature									
	23°C		45°C		55°C		65°C		85°C	
Penetrant	k'	R^2	k'	R^2	k'	R^2	k'	R^2	k'	R^2
MA	8.60	0.9923	28.5	0.9967	56.1	0.9880	69.7	0.9961	a	a
EP	5.10	0.9919	15.6	0.9972	34.1	0.9884	44.9	0.9894	85.5	0.9990
PB	2.10	0.9966	9.38	0.9949	15.0	0.9911	22.6	0.9860	45.1	0.9934
EH	1.20	0.9927	5.40	0.9959	8.66	0.9960	14.9	0.9936	30.4	0.9930
EN	0.50	0.9963	2.81	0.9981	4.70	0.9963	7.67	0.9931	17.8	0.9920
EU	0.26	0.9945	1.68	0.9977	3.01	0.9984	4.64	0.9948	11.4	0.9942
EM	0.07	0.9956	0.69	0.9968	1.41	0.9971	2.14	0.9976	7.12	0.9973
IPM	0.05	0.9900	0.37	0.9974	0.84	0.9977	1.40	0.9990	5.07	0.9971
IDP	0.01	0.9939	0.14	0.9914	0.33	0.9958	0.64	0.9966	2.61	0.9968

5.4 Evaluation of Polymer-Penetrant Interaction Parameter

The chemical nature of low molecular weight penetrants needs to be accounted for in order to provide a *complete* description of their transport properties. The origin of such a description dates back to the early studies by Koszinowski[28] and Eyring[46], who observed that diffusivity and activation energy of the diffusing molecules could be related to their heats of vaporization. The chemical nature of the penetrants has been described in terms of the solubility parameter (δ) (section 5-2 and 5-3) that is a material property of the pure penetrant, and is readily available from literature. δ describes the chemical nature of a material in terms of the cohesive energy density, $(\Delta U_v/V)^{1/2}$ where ΔU_v is the internal heat of vaporization and V is the molar volume. Hence, the solubility parameter is directly proportional to the extent to which a material coheres to itself upon vaporization. Based upon the familiar rule of "like-dissolves-like", the δ's of a solvent and solute are matched in order to estimate compatibility/solubility of a selected system.

Although the use of solubility parameters is very attractive in terms of ease of use, by nature of its definition, it does not describe the *extent* of specific interactions that may or may not be occurring between a given polymer-penetrant pair. Therefore, in order to obtain a better description of the chemical nature of the system, the Flory-Huggins interaction parameter[14,47] (χ) has been incorporated into this study. The parameter χ has been related to δ's of the individual species[42,48], but is only a practical means of estimating χ for nonpolar solvents. As the degree of polar character and/or specific interactions increase, so do the deviations from this method. Hence, in order to obtain interaction parameters for the current systems, the mass uptake data for both series of penetrants was utilized in the experimental determination of χ's, as described below.

5.4.1 Evaluation of Crosslink Density Using Tensile Tests

The origin of a relationship between modulus and crosslink density of a rubbery material is found in the theories of rubber elasticity[49,50]. For an elastomeric network system, the force (f) exerted by the polymer chains upon extension is given as:

(20) $$f = \left(\frac{\partial E}{\partial l}\right)_{T,V} - T\left(\frac{\partial S}{\partial l}\right)_{T,V}$$

where E = internal energy
S = entropy of system
l = length.

Assuming that the polymer behaves as an *ideal* elastomer, the change in internal energy upon elongation is negligible. Thus,

(21) $$\left(\frac{\partial E}{\partial l}\right)_{V,T} \approx 0$$

(22) $$f \approx -T\left(\frac{\partial S}{\partial l}\right)_{V,T}$$

Furthermore, it has been shown[50] that equation (22) can be rewritten as:

(23) $$f \approx -T\left(\frac{\partial S}{\partial l}\right) = \frac{\partial}{\partial l}\left[\frac{N_c kT}{2}\left\{\left(\lambda_x^2+\lambda_y^2+\lambda_z^2-3\right)-\ln\left(\lambda_x\lambda_y\lambda_z\right)\right\}\right]$$

where N_c = number of network chains in the system, and
λ = extension ratio (l/l_o).

To express force in terms of an engineering stress (σ_o), it is divided by the original cross-sectional area ($l_{ox}\, l_{oy}$). For elongation along the z-axis,

(24) $$\sigma_o = \frac{f_z}{l_{ox}l_{oy}} = \frac{N_c kT}{2l_{ox}l_{oy}} \times \frac{\partial}{\partial l_z}\left[\left(\lambda_x^2+\lambda_y^2+\lambda_z^2-3\right)-\ln\left(\lambda_x\lambda_y\lambda_z\right)\right]$$

Since $\lambda_z = \frac{l_z}{l_{oz}}$ then $d\lambda_z = \frac{dl_z}{dl_{oz}} \Rightarrow dl_z = d\lambda_z \cdot dl_{oz}$ Thus,

(25)

$$\sigma_o = \frac{f_z}{l_{ox}l_{oy}} = \frac{N_c kT}{2l_{ox}l_{oy}l_{oz}} \times \frac{\partial}{\partial \lambda_z}\left[\left(\lambda_x^2+\lambda_y^2+\lambda_z^2-3\right)-\ln\left(\lambda_x\lambda_y\lambda_z\right)\right]$$

The initial volume (V_o) may be defined as $l_{ox}l_{oy}l_{oz}$, and N_v (number of crosslinks per unit volume) as N_c/V_o. Substituting these into (25) yields,

(26) $$\sigma_o = \frac{NvkT}{2} \cdot \frac{\partial}{\partial \lambda_z}\left[\left(\lambda_x^2+\lambda_y^2+\lambda_z^2-3\right)-\ln\left(\lambda_x\lambda_y\lambda_z\right)\right]$$

For <u>affine</u> uniaxial deformation along the z-axis, ($\lambda_x\lambda_y\lambda_z$) = 1 and $\lambda_x=\lambda_y$, so the $\ln(\lambda_x\lambda_y\lambda_z)$ term $\Rightarrow$ 0. Therefore, assigning λ_z as the principal extension ratio λ yields,

$$\lambda \cdot \lambda_x^2 = \lambda \cdot \lambda_y^2 = 1 \qquad \Rightarrow \qquad \lambda_x = \lambda_y = \frac{1}{\sqrt{\lambda}}$$

Substitution for various extension ratios yields,

(27) $$\sigma_0 = \frac{N_v kT}{2} \cdot \frac{\partial}{\partial \lambda}\left[\lambda^2 + \frac{2}{\lambda} - 3\right]$$

The final expression is given as:

(28) $$\sigma_o = N_v kT\left[\lambda - \frac{1}{\lambda^2}\right]$$

In the limit of small strains, E may be defined as:

(29) $$E = \lim_{\substack{\lambda \to 1 \\ \varepsilon \to 1}} \frac{\partial \sigma_o}{\partial \lambda}$$

Differentiation of equation (29) with respect to λ yields,

(30) $$\frac{\partial \sigma_o}{\partial \lambda} = Nvk T\left(1 + \frac{2\lambda}{\lambda^4}\right)$$

Using the limit as $\lambda \to 1$,

(31) $$\frac{\partial \sigma_o}{\partial \lambda} = 3N_v kT$$

Thus,

(32) $$E = 3N_v kT = \frac{3\rho_p RT}{M_c}$$

McKenna *et al.*[51,52] have shown that M_c has a great influence on the Flory-Huggins interaction parameter, χ. Therefore, in order to insure accuracy of the M_c value evaluated, equilibrium moduli values for all the samples were calculated from the equilibrium engineering stress and strain, and substituted into equation (32) to yield values of M_c for the polymer (Table 5-27).

Table 5-27. Evaluation of crosslink density, N_v or ρ_c, and molecular weight between crosslinks, M_c, for the neat adhesive film

Sample number	Young's Modulus E (MPa)	$N_v \times 10^{-19}$ (xlinks/cm^3)
1	1.65	9.43
2	1.85	10.6
3	1.54	8.79
4	1.38	7.89
5	1.60	9.13
Ave. N_v:	9.17×10^{19} (xlinks/ cm^3)	(std.dev. 9.89×10^{18})
Ave. M_c:	6887 (g/mole of network chains)	(std.dev. 739)

Within an experimental error of 10%, an average value of M_c=6887 g/mole for the network chains was obtained from the method described above. This value of M_c is of the order of magnitude of that of many crosslinked systems such as natural rubber[51,52].

5.4.2 Evaluation of Chi Interaction Parameter

Mechanical and swelling measurements have been carried out on polymeric adhesive in order to evaluate the values of χ at different temperatures. This was based on the Frenkel-Flory-Rehner hypothesis, whose three main assumptions are:

1. $\Delta G = \Delta G_m + \Delta G_{el}$

where ΔG = the change in free energy of a swollen system
ΔG_m = change in free energy of the system due to mixing of the solvent and polymer, and
ΔG_{el} = change in free energy due to elastic deformation of the polymer network chains.

2. ΔG_m may be described by the well-known lattice model of the Flory-Huggins theory[14,47,53,54,55] which may be written as:

(33) $$\Delta G_m = RT\,[\ln(1-\phi_2) + \phi_2 + \chi_1\phi_2^2]$$

where ϕ_2 = the volume fraction of polymer, and
χ = the Flory-Huggins interaction parameter.

Equation (33) may be rewritten as[56]:

(34) $$\Delta G_m = RT\,[\ln(1-c) + c + \chi_1 c^2]$$

where c = relative concentration (dimensionless) = $w_o / \rho_p V_\infty$
w_o = initial mass of polymer
ρ_p = density of polymer, and
V_∞ = final swollen volume of polymer

3. The elastic deformation of the polymer network can be described by the "affine-deformation" model of rubber elasticity[49,56]. ΔG_{el} is described as the stored free energy in a deformed elastomeric network[57]and is given by:

(35) $$\Delta G_{el} = \frac{\rho_\rho RTV_1}{M_c}\left(c^{1/3} - c/2\right)$$

where ρ_ρ = polymer density (g/cc)
V_1 = molar volume of solvent (cc/mole)
χ_1 = Flory interaction parameter
c = relative concentration, and
M_c = average molecular weight of network chains (g/mole).

The Flory-Huggins interaction parameter, χ was determined by letting $-\Delta G_m = \Delta G_{el}$ in accordance with the Frenkel-Flory-Rehner hypothesis. Then combining equations (34) and (35) gives,

(36) $$-RT\left[\ln(1-c) + c + \chi_1 c^2\right] = \frac{\rho_\rho RTV_1}{M_c}\left(c^{1/3} - c/2\right)$$

(37) $$M_c = \frac{-\rho_\rho V_1\left(c^{1/3} - c/2\right)}{\ln(1-c) + c + \chi_1 c^2}$$

All the variables in this equation (except V_m) have been obtained experimentally. Values of V_m have been taken from the literature. Substitution of all the parameters yields the χ values for the selected polymer-penetrant system and are given in Table 5-28 (alkanes) and Table 5-29 (esters). These experimentally determined χ values are greater than what would be expected for a purely, uncrosslinked polymer and solvent. This increase may be due to the crosslinked nature of the system and/or deviations from the Flory-Rehner assumption[51,52]. Still, these values reflect the trends solubility observed from the sorption curves (i.e., smaller χ yield higher M_∞) and are indicative of poor solvents.

Table 5-28
Evaluated χ parameters for *n*-alkanes as a function of temperature

	Temperature				
Penetrant	23°C	45°C	55°C	65°C	85°C
Hexane	1.51	1.50	1.49	1.48	a
Heptane	1.61	1.60	1.59	1.58	1.58
Nonane	1.76	1.70	1.69	1.69	1.70
Decane	1.81	1.76	1.75	1.75	1.77
Undecane	1.87	1.84	1.82	1.82	1.82
Tridecane	1.99	1.99	1.98	1.97	1.97
Pentadecane	2.17	2.15	2.13	2.12	2.10
Hexadecane	2.27	2.24	2.20	2.21	2.22
Heptadecane	2.31	2.31	2.25	2.29	2.28

a-Data not obtained due to low boiling temperature

Table 5-29
Evaluated χ parameters for ester penetrants as a function of temperature

	Temperature				
Penetrant	23°C	45°C	55°C	65°C	85°C
Methyl acetate	1.37	1.25	1.21	1.15	a
Ethyl propionate	1.29	1.21	1.15	1.12	1.09
Propyl butyrate	1.31	1.22	1.20	1.16	1.13
Ethyl heptanoate	1.38	1.27	1.27	1.22	1.20
Ethyl nonanoate	1.49	1.38	1.37	1.32	1.33
Ethyl undecanoate	1.57	1.45	1.45	1.40	1.40
Ethyl myristate	1.77	1.66	1.67	1.62	1.58
Isopropyl myristate	1.86	1.78	1.79	1.74	1.71
Isodecyl pelargonate	1.91	1.84	1.85	1.80	1.75

a- Data not obtained due to low boiling point

5.5 Discussion

The diffusion characteristics of the *n*-alkane and ester series of penetrants have been discussed individually in the previous sections. A comparison of the two, in an effort to develop fundamental relationships regarding transport phenomenon, is given below. The majority of diffusion theories are based upon the concept of molecular size. Although size is very important, other factors such as shape of a penetrant in a particular polymer environment need to be considered. Moreover, from a fundamental viewpoint, an understanding of the specific interactions between the penetrant and the polymer matrix, and their role in the diffusion process, should be taken into account.

In the current study, the linear alkane penetrants have been chosen to investigate the isolated effects of molecular size and shape, while the esters enable a means of studying the chemical effects. This is possible since the ratio of polar to nonpolar character of the esters may be varied by the addition of CH_2 units. Together, the two series provide further insight into the contribution of factors such as size, shape, and chemical nature of the penetrant molecule to the observed transport behavior of the polymer.

5.5.1 Molecular Size Considerations

The dependence of diffusivity (D) upon molecular mass (M) has been described using the power law relationship (equation (9)). Excellent results were obtained for the *n*-alkanes, while the esters exhibited large deviations over an analogous molecular weight range. Linearized plots of log D versus log M for the esters and alkanes are shown Figure 5-42. To aid in the comparison, only the data at 23°C and 65°C are shown in Figure 5-43. The alkanes follow a linear dependence over the broad molecular weight range studied, with any deviations being negligible. However, the esters possess a large curvature with the extremes (methyl acetate and IDP) approaching the behavior of *n*-alkanes, for all the temperatures. However, the "radii of curvature" for the ester curves decrease with temperature, as the effects of the polar group become less significant.

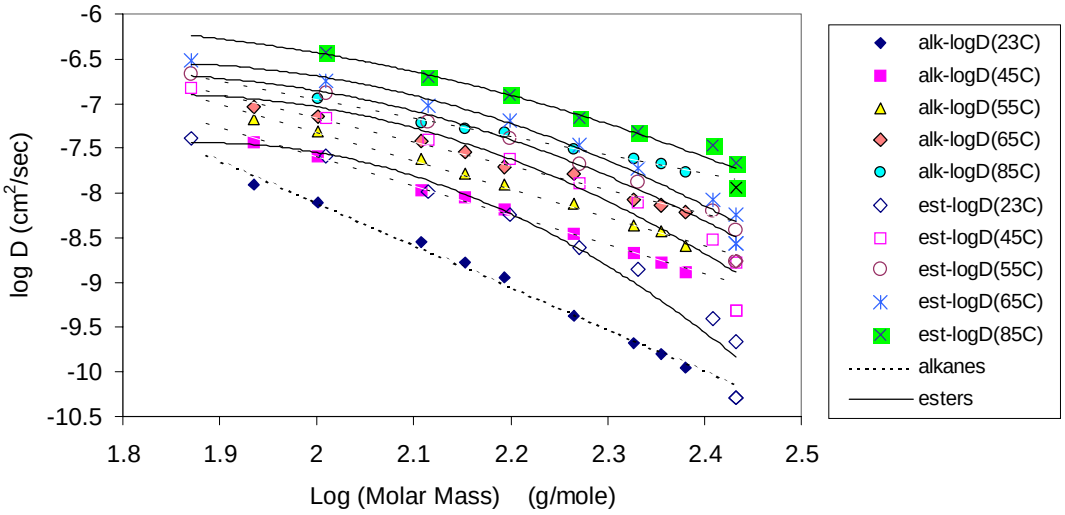

Figure 5-42. Log-Log plot of D and molecular weight for alkanes and esters

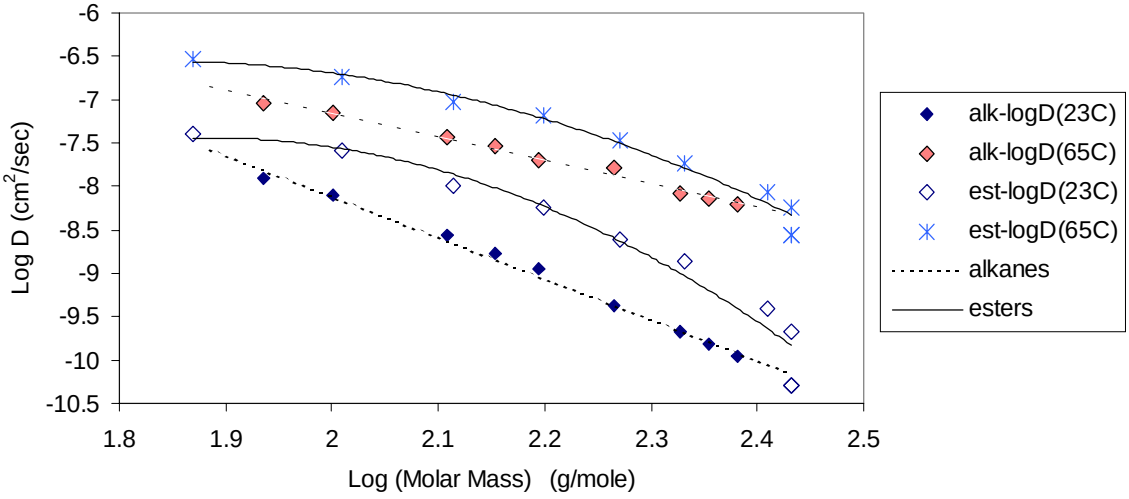

Figure 5-43. Simplified view of Log-Log plot of Figure 5-42 showing 23° and 65°C data

Plots of log D versus molar volume for the esters and alkanes are shown in Figure 5-44. The slopes for the alkanes are much higher than those esters, and decrease with increasing temperature. This is due to the additional free volume of the expanding polymer matrix and the increasing chain segmental mobility at higher temperatures. For the esters, however, the slopes do not change as rapidly as those of the alkanes, signifying a weaker temperature-volume dependence. The behavior of the larger esters approaches that of the corresponding alkanes, indicative of weaker specific interactions between the polymer and the larger esters. These observations are consistent with those of Sfirakis and Rogers[58] for linear alcohols in poly(methyl methacrylate).

The activation energies of diffusion, E_d for the two types of penetrants are compared in Figure 5-45. E_d values for the lowest molecular weight penetrants of the esters and alkanes coincide with each other. The remaining esters possess E_d's that are generally lower than those of the alkanes and approach the alkane values as the number of carbon atoms increases.

Due to the fact that the esters possess an inherently lower volume than the corresponding alkanes, it is beneficial to study the dependence of E_d on molar volume (V_m) as shown in Figure 5-46. A behavior similar to that of molar mass is observed. The fact that the lowest molecular weights of the two series coincide may be due to the inherent nature of the polymer. Any differences in chemical nature are negligible, while only the size of the penetrant is important in this region. Furthermore, the change in slope towards zero implies that there exists a critical volume, below which the polymer matrix can more easily and rapidly accommodate the diffusing species. In this "lower limit", E_d becomes independent of chemical type since normal, segmental motions resulting from thermal energy are sufficient to allow the penetrant molecules to diffuse in a simple "step." Above this region, the E_d values of both series increase with the alkanes exhibiting a sharper variation. Thus, it can be seen that there are obvious effects due to the presence of the polar ester group. The role of penetrant *shape* in the differences between the transport properties of the alkanes and esters will be discussed in the following section.

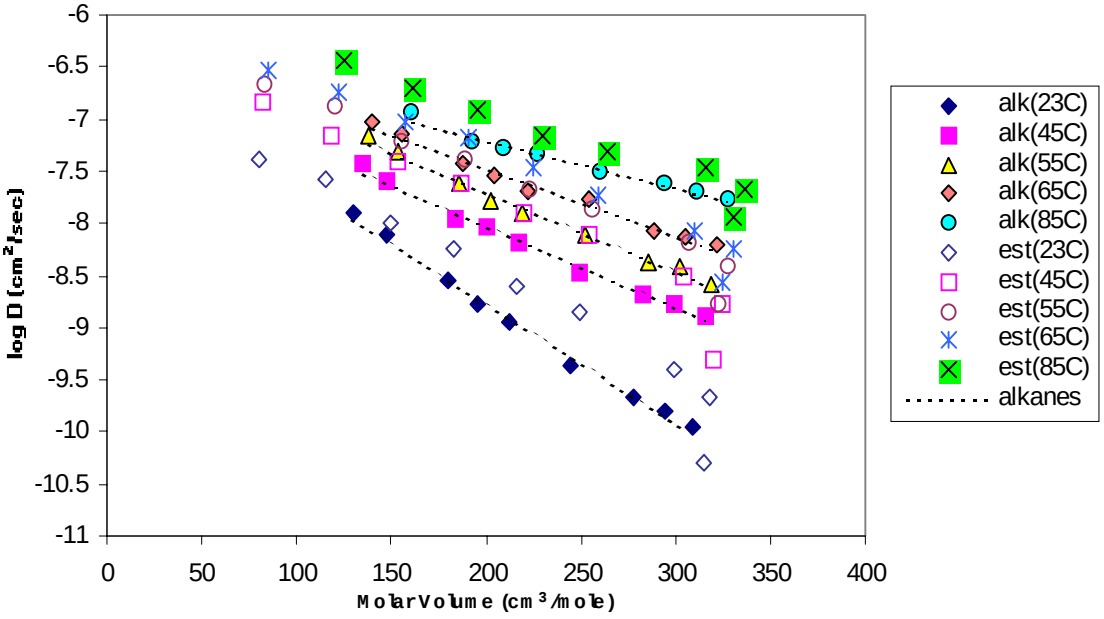

Figure 5-44. Composite graph showing the penetrant size effects for both penetrant series. A plot of log diffusivity (cm^2/sec) versus the molar volume of each penetrant at each test temperature.

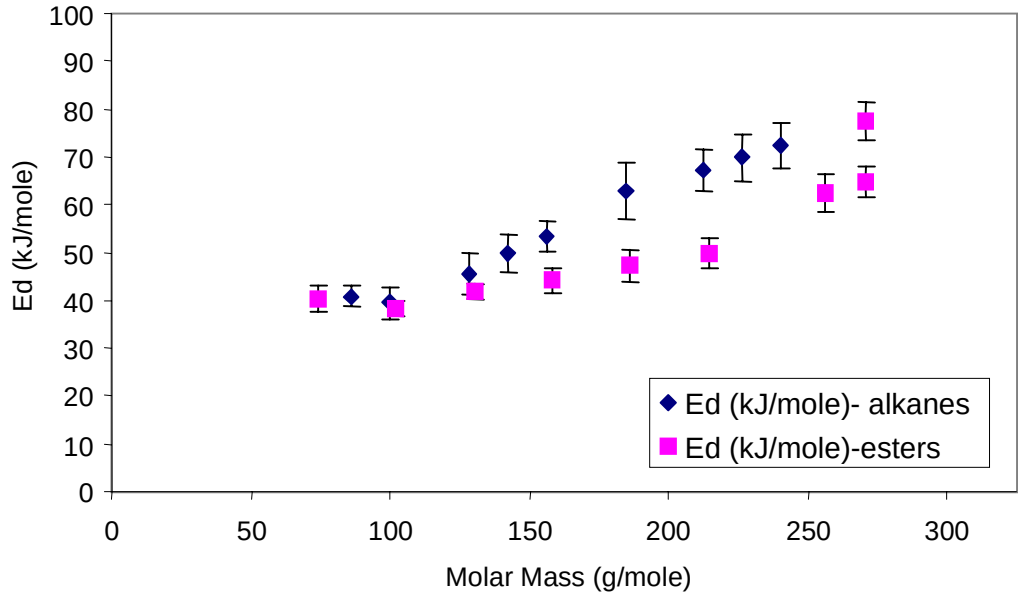

Figure 5-45. Comparison between the molecular weight dependence of activation energies for diffusion for the *n*-alkane and ester penetrants

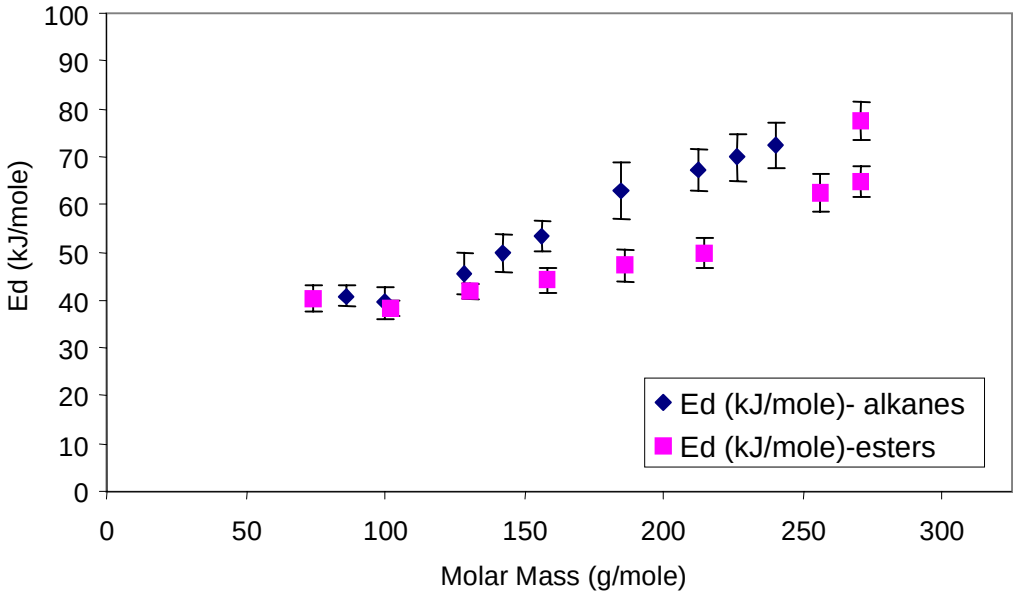

Figure 5-46. Comparison between the molar volume dependence of the activation energy for diffusion of the *n*-alkane and ester series of penetrants

5.5.2 Shape Considerations

The diffusion of a "small" molecule such as simple gases or organic vapors is presumed to take place via long-range polymer chain segmental motions. These "small" molecules are usually described in terms of a spherical geometry. Although these segmental motions exist in the case of a "large" penetrant, additional concerns regarding the greater redistribution of free volume necessary to accommodate the molecule in the polymer structure must be addressed. As a result, particular attention should be paid to the specific *shape* a penetrant molecule may assume in order to alleviate some of the space requirements. The average shape of the penetrant is determined by the minimum energy conformations that are available to it within the chemical environment of the polymer.

Studies[7,16,17] on the transport of aliphatic hydrocarbons suggest that diffusion may occur along the long axis of the penetrant. The limiting step is the creation of a vacancy large enough to accommodate the penetrant. An extended geometry of the penetrant is favored since it results in less perturbation of the polymer chain configurations to form this vacant site.

The linear dependence of diffusivity upon molecular size of the penetrant is depicted in the plots of log D versus the number of carbon atoms for the alkanes and esters with the exception of IDP (Figure 5-47 and Figure 5-48). In view of the classical free-volume interpretation of log D being directly proportional to the free volume required for a penetrant jump[59], this linearity implies that diffusion occurs along the direction of long axis of the solvent molecules. Therefore, increasing the number of methylene units only lengthens the molecule without significantly altering its diameter. The same behavior was observed by Storey *et al.*[8] with poly(vinyl chloride) as the length of *n*-alkyl phthalate plasticizers was increased. Further support can be drawn from Moisan[60] who investigated the diffusion of linear methylesters in LDPE, and Dubinin *et al.*[61] from their studies on a series of esters and benzophenones in *i*-polypropylene.

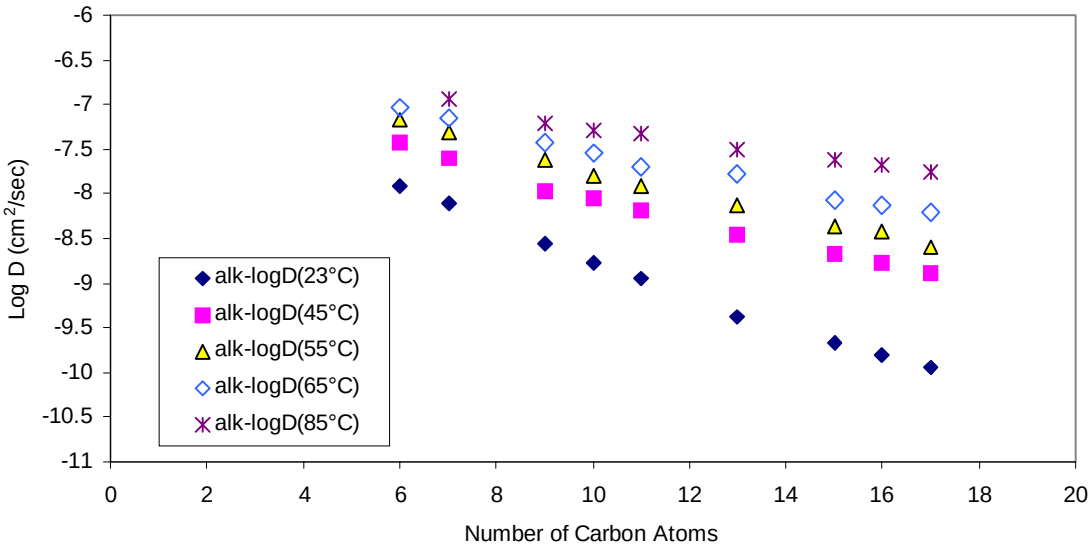

Figure 5-47. Plot of log D (cm^2/sec) versus the number of carbon atoms for *n*-alkanes

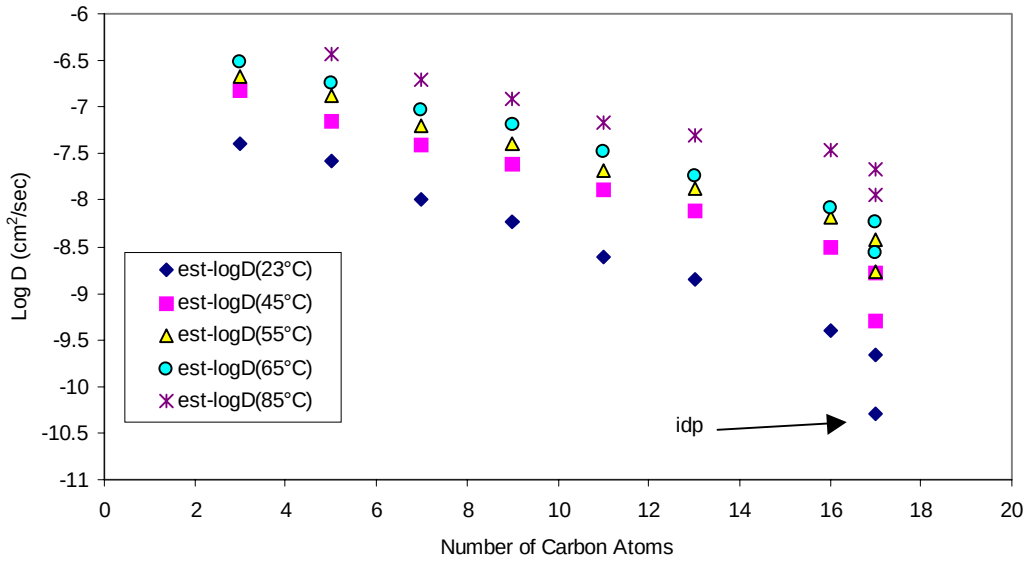

Figure 5-48. Plot of log D (cm^2/sec) versus number of carbon atoms for ester penetrants

Another means of analyzing shape involves the comparison of the diffusion activation energies of each penetrant, E_d, per addition of a methylene (-CH_2-) unit. Values of E_d per methylene unit for both series are given in Table 5-30. Those in the lower molecular weight region where E_d values are relatively constant have not been shown. Möller and Gevert[4] have estimated E_d values per methylene group to be ~ 3.5 kJ/mole for linear alkanes and ~ 1.0 kJ/mole for esters, on systems known to diffuse linearly along their long-axes. The values of E_d/CH_2-unit obtained for both the *n*-alkanes and esters in this study are remarkably close to these literature values, implying that they diffuse in a similar manner. However, the much larger value for IDP implies that this penetrant does not diffuse along its long axis.

Table 5-30. Activation energy per addition of a methylene (CH_2) unit (kJ/mole/CH_2) for both the *n*-alkane and ester penetrants.

Alkanes		Esters	
Number of Carbons	E_d / CH_2-unit	Number of Carbons	E_d / CH_2-unit
9	3.11	7	1.85
10	4.12	9	1.11
11	3.54	11	1.59
13	4.78	13	1.27
15	2.28	16	4.14
16	2.46	17	2.45
17	2.43	*17	15.08

* Isodecyl Pelargonate (IDP)

The specific interactions between a polymer and penetrant vary from one system to the other and may have an effect on the preferred conformations of the penetrant within a selected polymer matrix. A series of Monte-Carlo molecular simulations were performed on a few selected penetrants from each series using Macromodel® 5.0. The selection process was necessary to minimize computational time. Details pertaining to the model and software application itself are given in Appendix J.

Each experiment was designed to determine the most probable energy conformations of a penetrant within a chemical environment whose energetics were similar to those of water ($\varepsilon = 78.3$). This environment was chosen due to the polar nature and hydrogen bonding capability of the polyamide matrix and the fact that specific interactions between the polymer and ester penetrants are known to exist from previous results (section 4-11). The number of iterations necessary depended upon the number of atoms and possible bond angles and rotations. In this case, the term "iterations" refers to the number of random structures generated to be minimized. The solvents selected and the number of iterations are given below:

Table 5-31. Number of iterations for the penetrants selected in Monte-Carlo analysis

Alkane penetrant	# of iterations	Ester penetrant	# of iterations
Hexane	1000	Ethyl propionate	1000
Nonane	1000	Ethyl heptanoate	1000
Decane	2000	Ethyl Nonanoate	1000
Tridecane	8000	Ethyl Myristate	1000
Pentadecane	8000	Isopropyl Myristate	5000
Hexadecane	10,000	Isodecyl Pelargonate	5000
Heptadecane	10,000		

The energy of each minimized conformation is used to interpret the plausibility of its existence and to obtain an idea of the range of energies necessary to produce these conformations. Furthermore, atomic distances were evaluated and, along with steric volume calculations, average descriptions of geometry in terms of an aspect ratio have been given. This ratio describes the degree of linearity / non-linearity possessed by a certain penetrant. The twenty lowest energy conformations from each Monte-Carlo simulation have been utilized in the analysis and discussion and proved adequate due to the small energy differences amongst all the minimum conformations and the similarity in their shapes. *CPK* images for the *n*-alkanes are shown in Figure 5-50 through Figure 5-56, and for the esters in Figure 5-57 through Figure 5-62.

A penetrant within a polymer matrix may exist in a virtual cylindrical "tube", as in the study of Mauritz *et al.*[18]. Assuming this type of geometry, the dimensions of length and radius and aspect ratios (defined as length/diameter) have been evaluated to approximate the average shape of the molecules within the selected chemical environment. "Average" aspect ratios and additional geometrical information are given in Table 5-32. A complete listing of all simulation results is given in Appendix E.

Table 5-32. Geometrical parameters obtained from Monte-Carlo simulations of *n*-alkane and ester penetrants (length/diameter = L/2r)

Penetrant	Volume ($Å^3$)	Ave. radius (Å)	Ave.cross-section. Area ($Å^3$)	Ave. Aspect Ratio (L/2r)
Hexane	113.6	2.354	17.46	1.409
Nonane	167.5	2.292	16.53	2.238
Decane	186.0	2.296	16.60	2.478
Tridecane	239.5	2.390	18.14	2.948
Pentadecane	270.5	2.450	19.16	3.163
Hexadecane	291.0	2.639	22.20	2.750
Heptadecane	308.5	2.708	23.48	2.780
Ethyl Propionate	109.0	2.198	15.19	1.636
Ethyl Heptanoate	179.0	2.459	19.21	2.050
Ethyl Nonanoate	213.5	2.482	19.61	2.399
Ethyl Myristate	299.5	2.598	21.69	3.069
Isopropyl Myristate	318.0	2.696	23.27	2.889
Isodecyl Pelargonate	318.0	3.270	33.66	1.467

The aspect ratios (L/2r = L/D) for the esters and alkanes are plotted as a function of the number of carbon atoms (C), in Figure 5-49. The L/2r values for both the series increase with the addition of carbon units, indicative of a greater tendency towards a linear geometry. However, a small decrease is observed for the penetrants with C > 15, reflective of the greater ability of the longer chains to fold back upon themselves, while still being linear. This behavior is justified by the high degree of flexibility possessed by the methylene moieties that comprise the long hydrophobic tail.

The *n*-alkanes and esters behave similarly with respect to the shape of the molecules. This is due to the fact that the hydrophobic tail of the esters acts essentially independent of the ester group with respect to geometry. This in turn is a result of the ester functionality being located near the end of the molecule, thus allowing the ester to behave more like the alkanes.

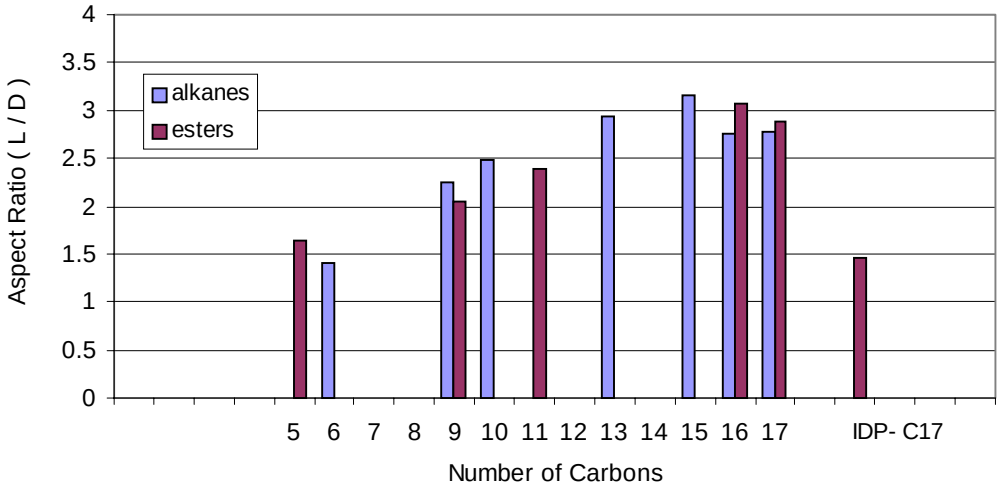

Figure 5-49. Plot of aspect ratios calculated for select *n*-alkanes and esters from the geometric dimensions provided by Monte-Carlo simulations

The lowest molecular weights of both series exhibit aspect ratios approaching those of one, although they are linear. This is due to the shorter lengths of the molecules with respect to their lateral dimensions. Thus, hexane (HX) and ethyl propionate (EP) possess similar aspect ratios and cross-sectional areas, in addition to similar mass and length. This could be the reason why the activation energies of diffusion for these smaller molecules tend to coincide with each other. Therefore, the concept of a "jump length" for penetrant diffusion may be applied to the smaller molecules that are able to translate as a whole, regardless of chemical nature.

The effects of methyl *branches* on the shape and transport of a small molecule have been clearly demonstrated by Aitken and Barrer[62] and by Peters *et al.*[63]. Although the IPM molecule in the current study has an additional terminal methyl branch, its effects are not significant. This is due to the fact that a much longer alkyl chain attached to the other side of the ester group dominates the overall size and shape of the molecule. The similarities in the behavior of IPM with those of the analogous *n*-alkane reflect these ideas.

Isodecyl pelargonate (IDP) also contains methyl branches located at the ends of the molecule. However, in this case, the effects of branching and branch location play a minor role compared to that of the *placement* of the ester functionality. The ester group is located in the *middle* of this molecule as opposed to the rest of the series, wherein the ester group is positioned near the end. It can be seen from Figure 5-49 and Figure 5-62 that the shape of IDP approaches that of a sphere. Bond angles about the ester group induce the aliphatic tails to coil upon themselves giving rise to a more spherical geometry. This analysis in conjunction with the E_d/CH_2 values described earlier, explain why the transport properties of IDP are highly unlike those of the "linear" esters. The most obvious reason is the large increase in cross-sectional area that accompanies the

spherical geometry, making it more difficult for the polymer matrix to accommodate its size. Also, the ester group becomes more "shielded", virtually eliminating any favorable interactions that may have occurred. This type of "shielding" behavior has been observed in phenolic alcohols[43] as a result of the presence of an aliphatic branch adjacent to the OH group.

Thus, the differences in observed diffusion properties between the alkanes and esters are not a result of differences in shape, with exception of the anomalous IDP. So far, size and shape of the molecules have been investigated in interpreting the diffusion behavior. In order to gain further insight into the transport phenomenon, the effects of chemical nature of the penetrants need to be considered.

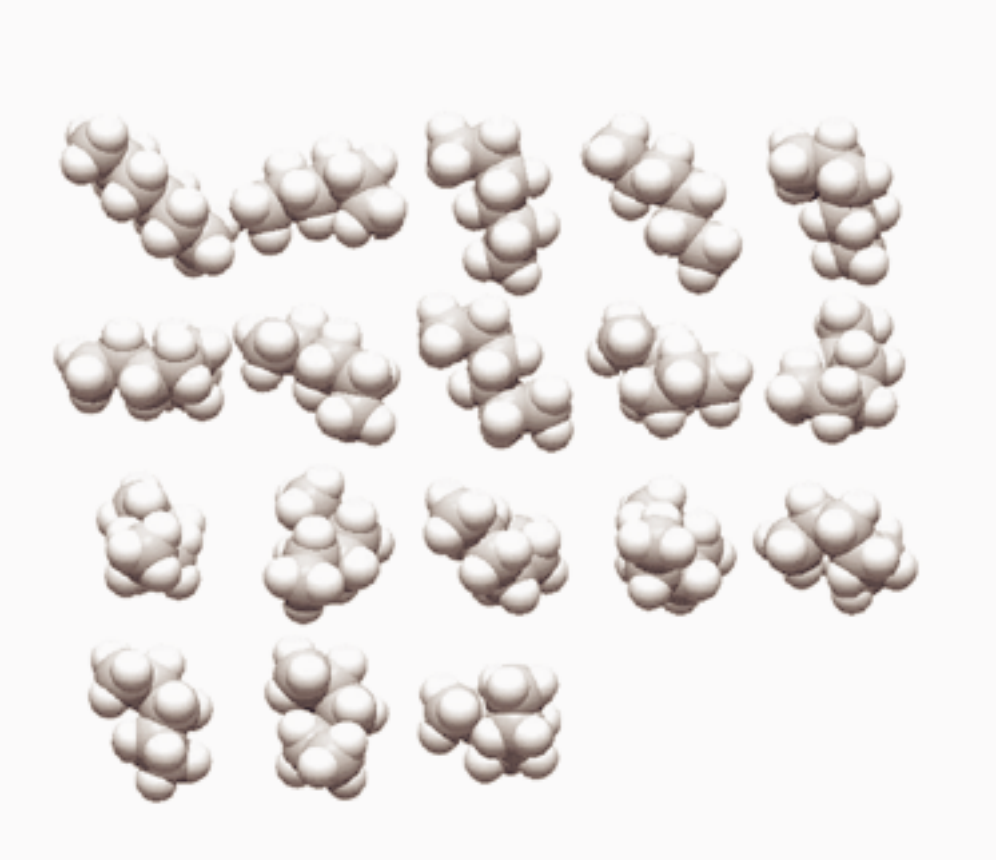

Figure 5-50. CPK images from Monte-Carlo simulations of hexane

Figure 5-51. CPK images from Monte-Carlo simulations of *nonane*

Figure 5-52. CPK images from Monte-Carlo simulations for *decane*

Figure 5-53. CPK images from Monte-Carlo simulations for *tridecane*

Figure 5-54. CPK images from Monte-Carlo simulations for *pentadecane*

Figure 5-55. CPK images from Monte-Carlo simulations for *hexadecane*

Figure 5-56. CPK images from Monte-Carlo simulations for *heptadecane*

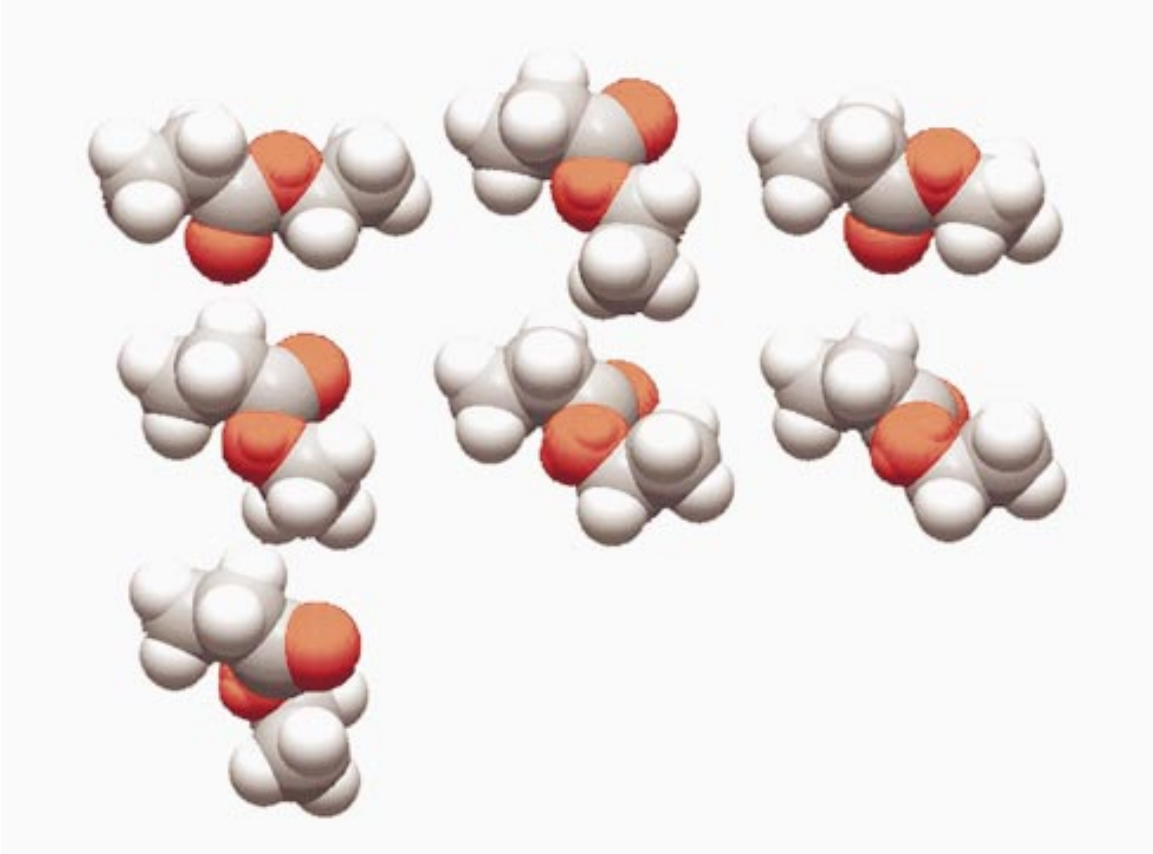

Figure 5-57. CPK images from Monte-Carlo simulations for *ethyl propionate*

Figure 5-58. CPK images from Monte-Carlo simulations for *ethyl heptanoate*

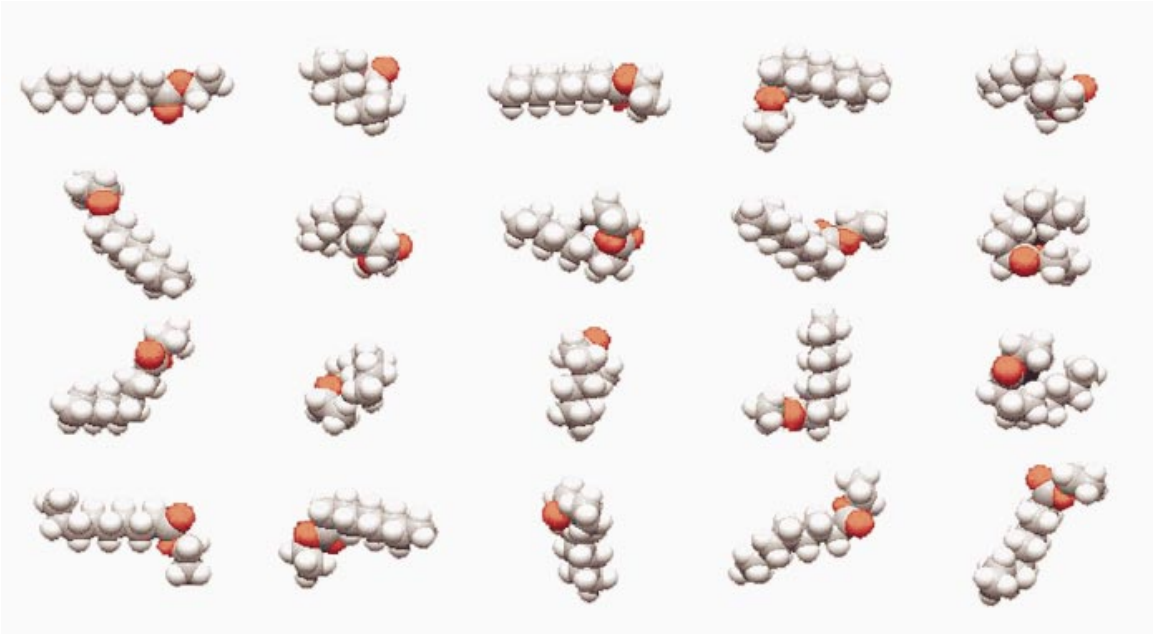

Figure 5-59. CPK images from Monte-Carlo simulations for *ethyl nonanoate*

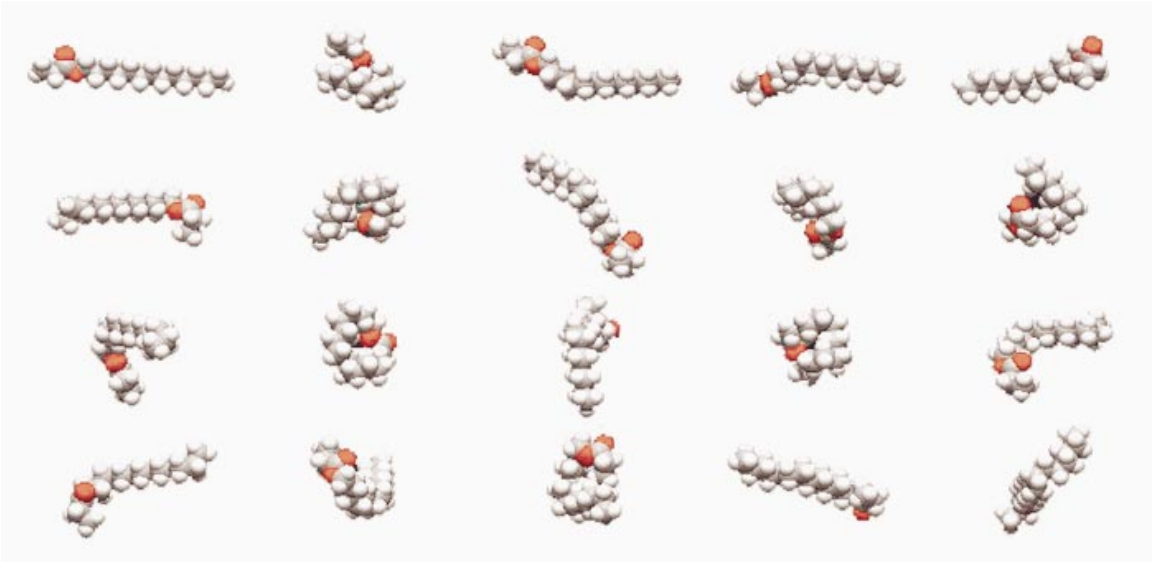

Figure 5-60. CPK images from Monte-Carlo simulations for *ethyl myristate*

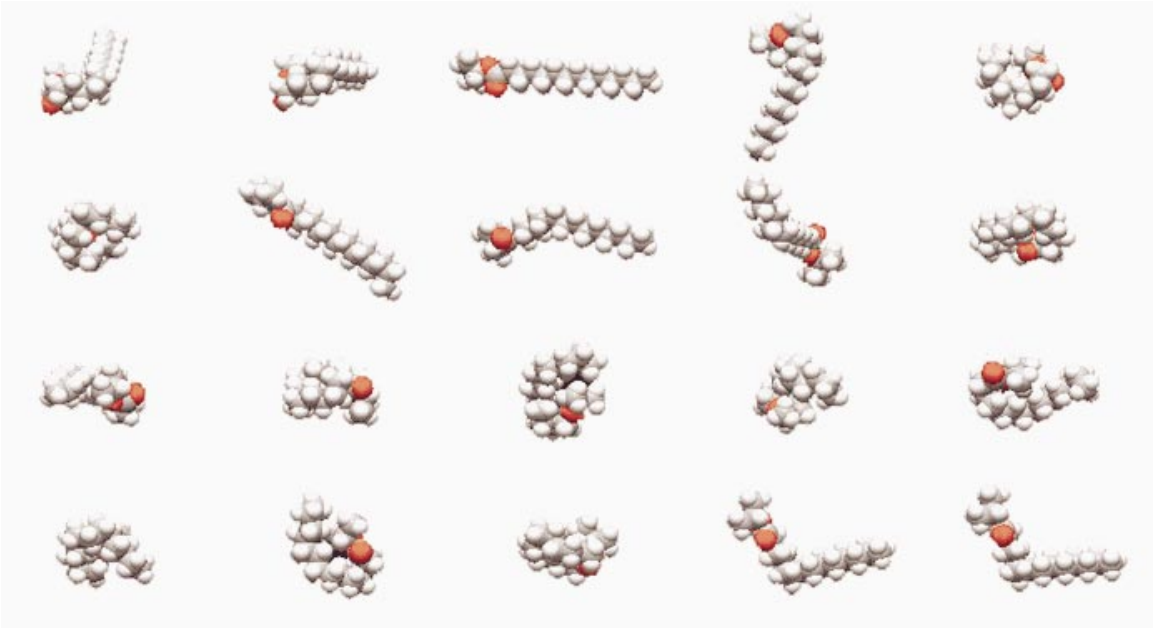

Figure 5-61. CPK images from Monte-Carlo simulations for *isopropyl myristate*

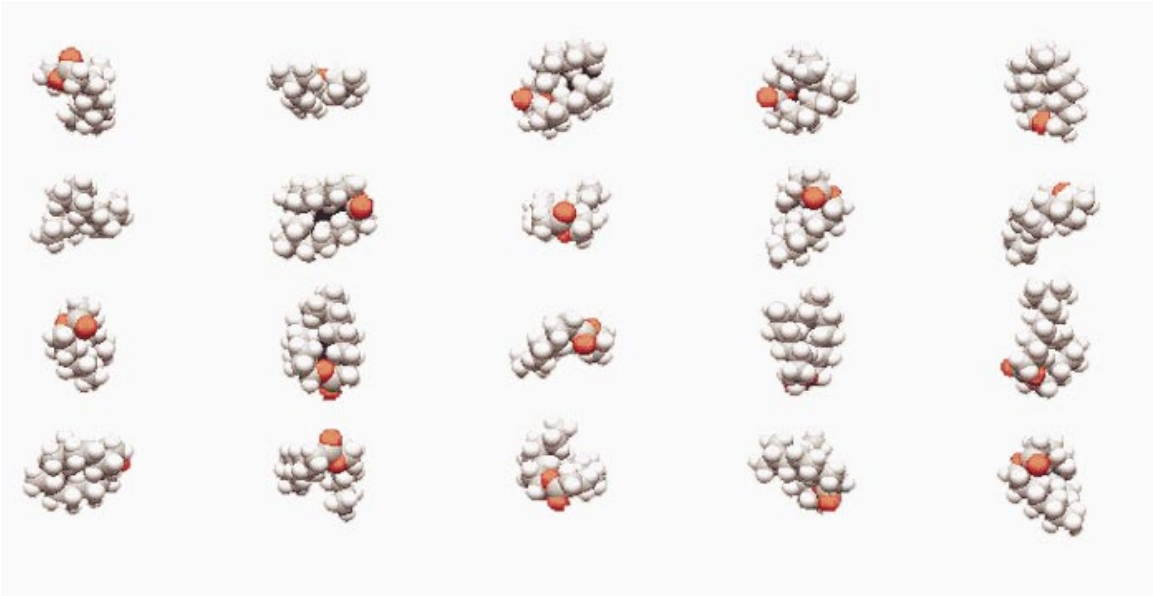

Figure 5-62. CPK images from Monte-Carlo simulations for *isodecyl pelargonate*

5.5.3 Chemical Considerations

The necessity for a description of the chemical nature of the low molecular weight penetrants is evident from the discussions regarding molecular size and shape given in the previous section. Utilization of solubility parameters as a means of comparison of the two series of penetrant was attempted. However, this method proved unsuccessful in predicting a qualitative relationship for the effects of chemical contributions on the diffusion process. Thus, the Flory-Huggins interaction parameter (χ) has been used to describe the transport process more accurately.

Chi (χ) is a dimensionless value that was originally incorporated into the calculation of the entropy of mixing term in the thermodynamic description of polymer solutions by P.J. Flory[14] and M. L. Huggins[47]. It accounts for the specific interactions between polymer segments and solvent molecules. Previous studies[14,53,54] have shown that this parameter is dependent upon concentration and temperature. In this study, the temperature dependence of χ has been described in detail.

The temperature dependence of the interaction parameter χ for the penetrants has been investigated as shown in the plots of χ versus temperature (Figure 5-63 and Figure 5-64). The alkanes exhibit virtually no dependence upon temperature, indicative of low heats of solution. The esters, on the other hand, systematically decrease with increasing temperature, reflective of an increase in the "energy" change associated with their sorption. This behavior supports the earlier discussion regarding the endothermic nature of the solution process for the esters. The experimentally determined χ values are consistent with the equilibrium sorption values obtained earlier, as can be seen in Figure 5-65 and Figure 5-66.

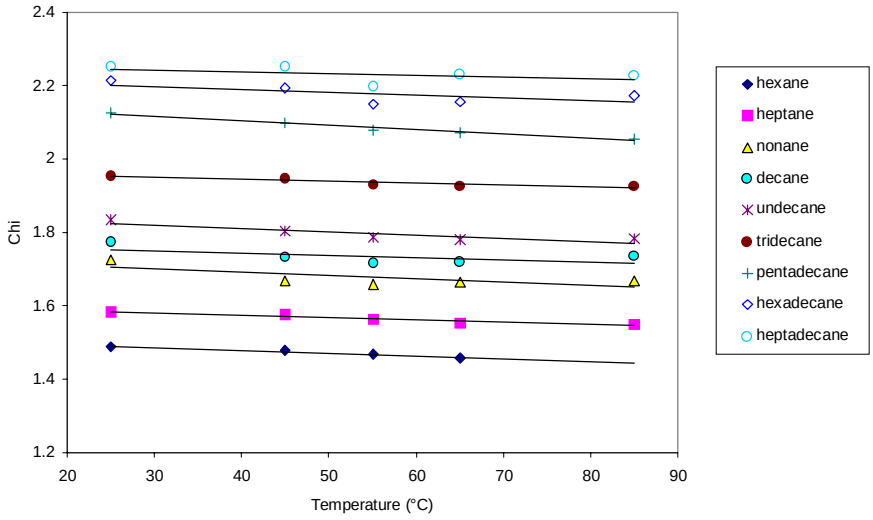

Figure 5-63. Temperature dependence of Flory-Huggins interaction parameter χ for *n*-alkanes

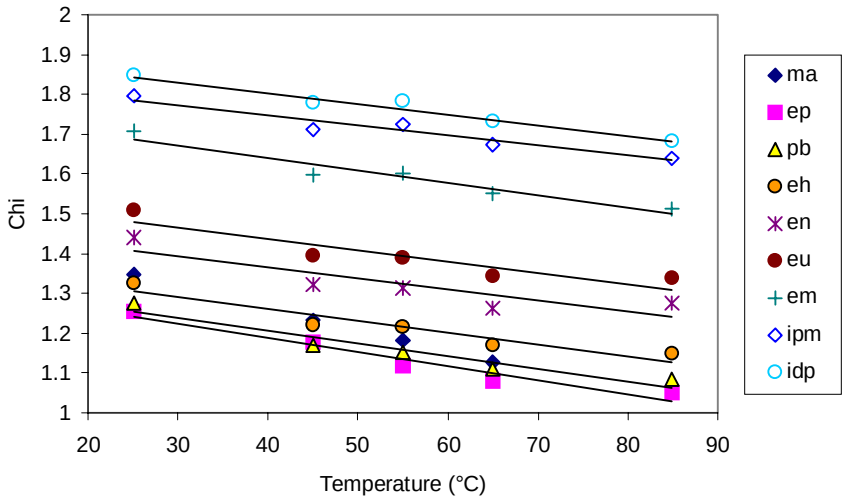

Figure 5-64. Temperature dependence of Flory-Huggins interaction parameter for esters

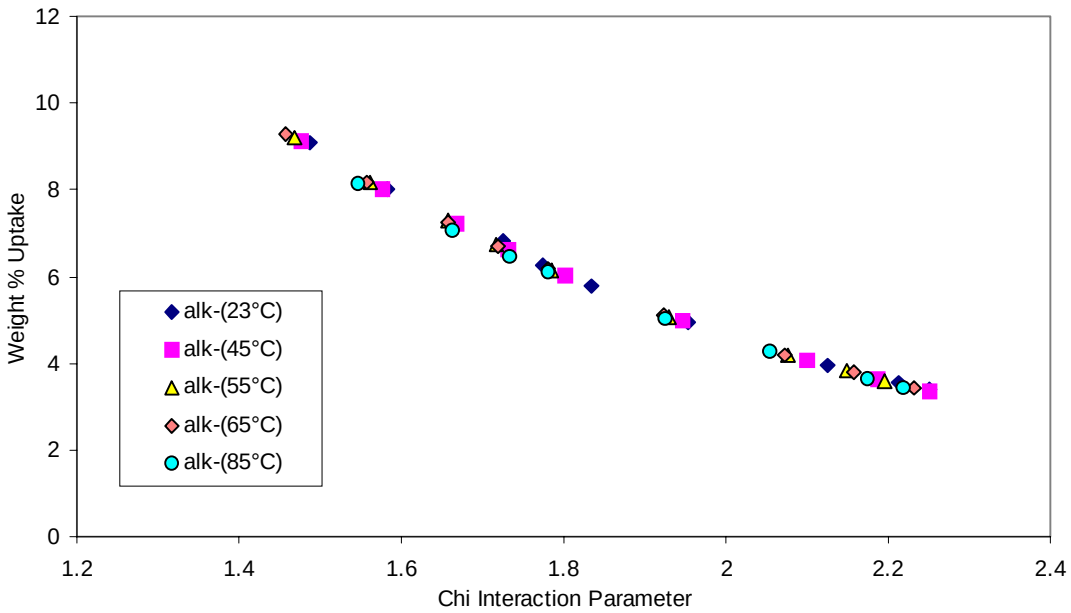

Figure 5-65. Equilibrium sorption versus Flory-Huggins interaction parameter for *n*-alkanes

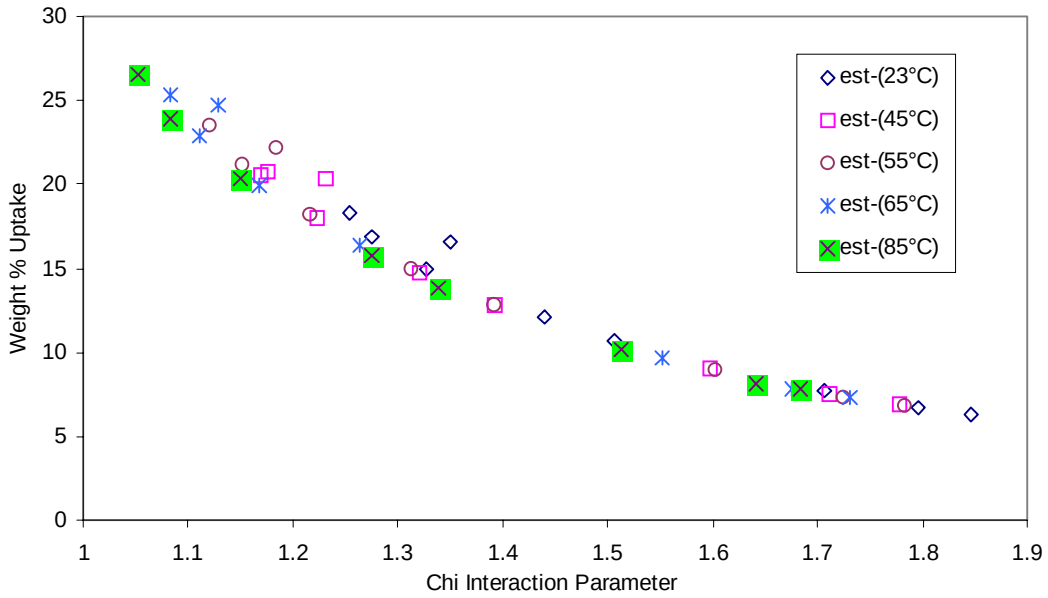

Figure 5-66. Equilibrium sorption versus Flory-Huggins interaction parameter for ester penetrants

The interaction parameter (χ) has been used as a means of comparison of the behavior of penetrant in order to isolate the chemical effects involved in the diffusion process. The activation energies of diffusion, E_d, for the esters and alkanes are plotted as a function of χ in Figure 5-67. A general trend of increasing E_d with increasing χ is observed for both. Yet, for a selected χ the corresponding E_d is greater for the ester than that of the corresponding alkane. This due to the fact that for a given χ, the size of the penetrant is much larger for the esters. Additional parameters regarding the physical nature of the penetrant were necessary to provide a universal relationship between E_d and χ that could explain this behavior.

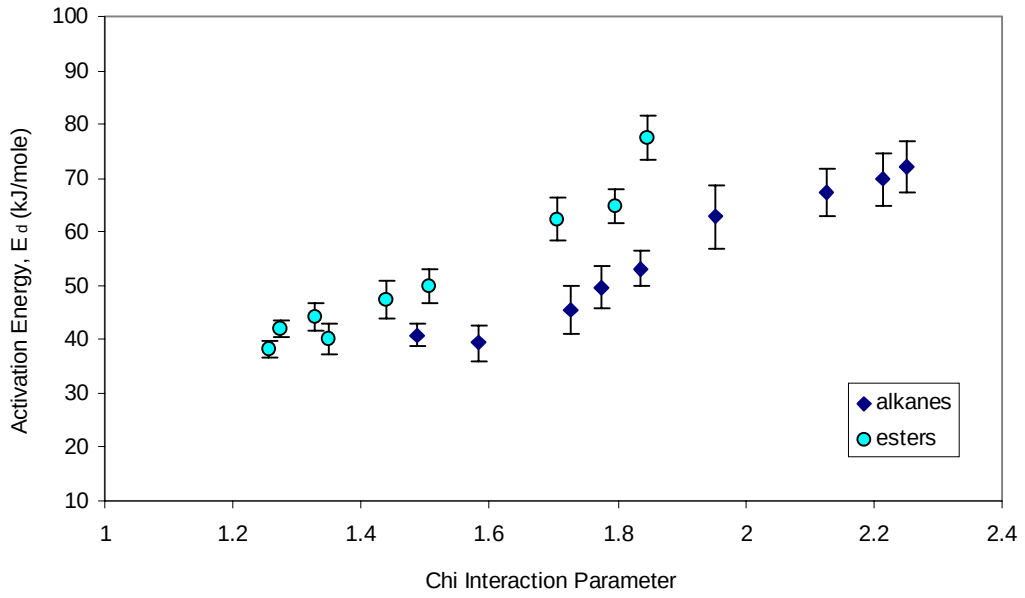

Figure 5-67. Activation energy of diffusion for the *n*-alkane and ester penetrants versus the Flory-Huggins interaction parameter

The diffusion coefficients, D for the alkanes show a linear dependence with χ as shown in Figure 5-68. The slopes of these lines decrease with increasing temperature. This trend is analogous to that obtained for diffusivity as a function of mass of the penetrant (Figure 5-69). These results imply that the linearity seen in Figure 5-68 is simply a manifestation of the effects of mass.

The variation in D as a function of χ for the esters is shown in Figure 5-70. A linear dependence similar to that of the alkanes is observed with the exception of IDP and the lowest molecular weight esters (MA and EP). The values of χ for methyl acetate (MA) are larger than those of ethyl propionate (EP). Yet, its diffusivity is greater that that of EP indicating the dominance of size effects in this case.

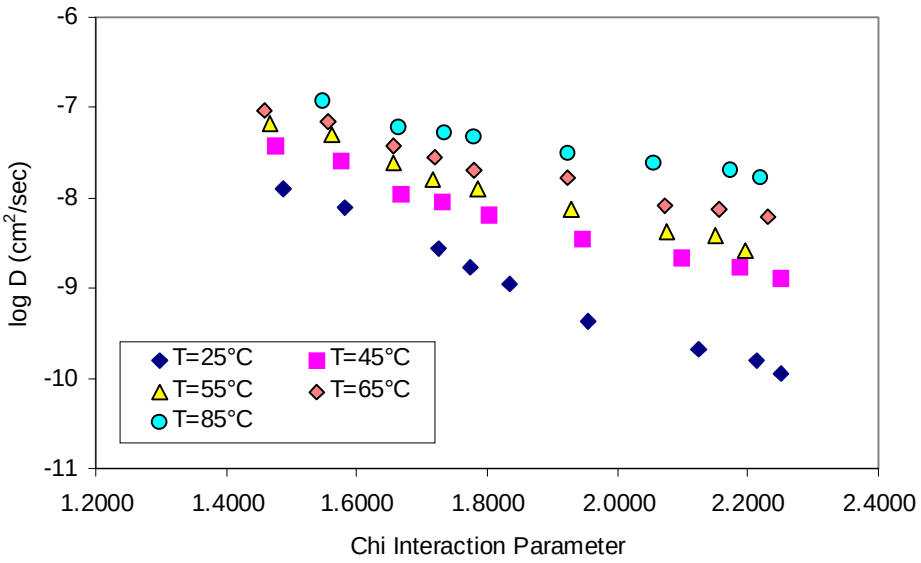

Figure 5-68. Log Diffusivity (cm^2/sec) versus Flory-Huggins interaction parameter for *n*-alkane penetrants

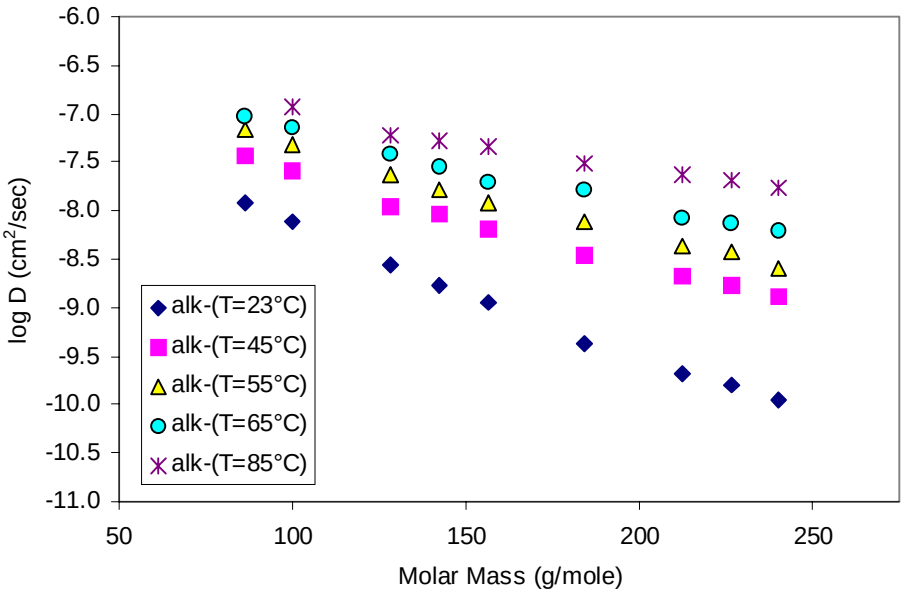

Figure 5-69. Log Diffusivity (cm^2/sec) versus molecular weight for *n*-alkane penetrants

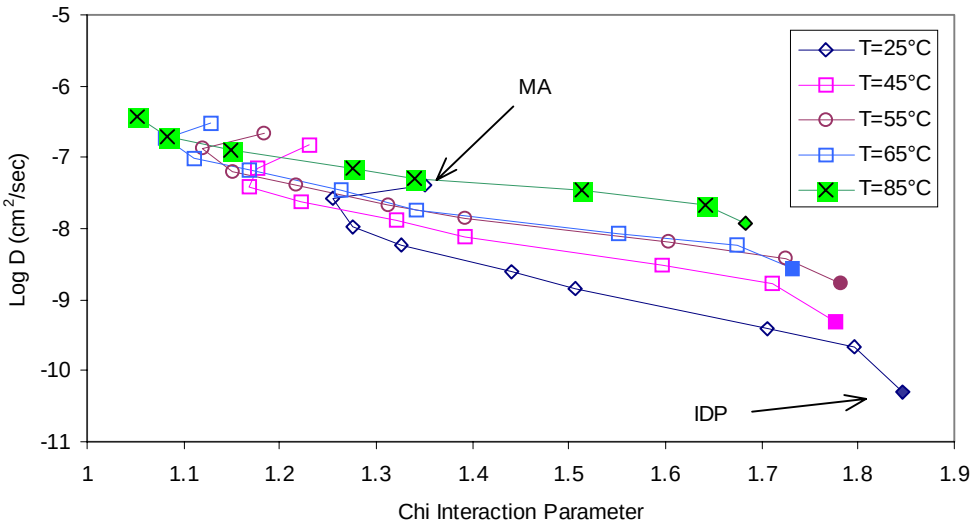

Figure 5-70. Log Diffusivity (cm^2/sec) versus Flory-Huggins interaction parameter for ester penetrants

A comparison of the above plots for both series of penetrants at 23°C is given in Figure 5-71. It can be seen that for an interaction parameter (χ), diffusion of the ester is slower than that of the alkane. This is explained by connecting the alkanes and esters of similar molecular weight by a straight line. For a selected molecular weight, the χ values of the esters are much lower (more soluble), and their diffusion coefficients higher than those of the alkanes. This is reflective of the favorable chemical effects due to the increased polarity of the esters. The upward curvature for the lower molecular weight esters towards faster diffusion coefficients shows the effects of *two* favorable factors in this region – the increase in *polarity* and the decrease in molecular *size*, to the point where the size completely dominates the diffusion behavior.

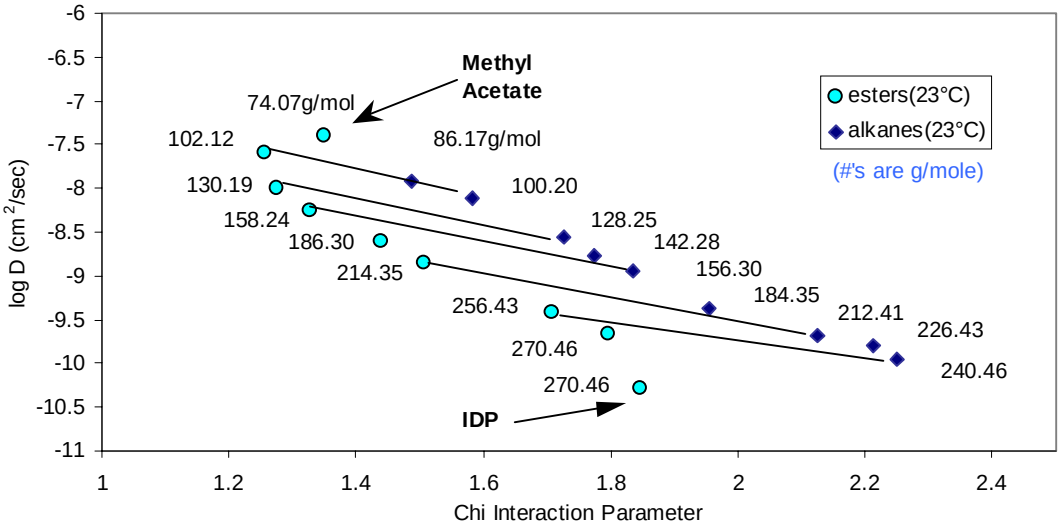

Figure 5-71. Log Diffusivity (cm^2/sec) versus Flory-Huggins interaction parameter for *n*-alkanes and esters at 23°C

It can be concluded from the above discussion, that the diffusion properties of these systems are influenced by a combination of two factors - *size* and *chemical nature*. It has been shown that diffusivity increases with decreasing molecular size and increasing extent of specific interactions (lower χ). These results are combined to yield a basic relationship,

(38) $D \propto 1/(\text{Mass} * \chi)$

Equation (38) may be rewritten in terms of molar volume (V_m) as,

(39) $D \propto 1/(\text{molar volume} * \chi)$.

In order to test the validity of this proportionality, plots of log D versus $1/(\chi * V_m)$ for the esters and alkanes at all test temperatures were made and are shown in Figure 5-72. The diffusion behaviors of all the penetrants closely follow the relationship proposed in equation (39). Thus, equations (38) and (39) qualitatively describe the effects of *size and chemistry of the penetrants* on their transport process. However, in order for all the isotherms of the two series to be superimposable, it is necessary to introduce a temperature-dependent parameter that describes the changing *state* of the polymer with temperature.

The activation energy, E_d describes the "*temperature dependence*" of the diffusion coefficient (D) for a selected polymer-penetrant system. It has also been shown[26,27,64,65] to be dependent upon the "*state*" of a polymer (i.e. cohesive energy density, fractional free volume, etc…). So, it was possible to study the effect of introducing the (above mentioned) temperature-dependent parameter, via the utilization of E_d. A plot of E_d versus (χ*V_m) for all the penetrants (except IDP) is shown in Figure 5-73. All the isotherms (a total of ***85 data points***) are represented by a single function, indicating that the incorporation of a parameter that accounts for temperature (such as E_d) ***markedly*** improves the description of the diffusion behavior of the system. Presently, there is no known literature on such a parameter. However, the introduction of one would lead to the concept of a multi-parameter model that accurately describes the transport properties of penetrant-polymer systems similar to the ones studied.

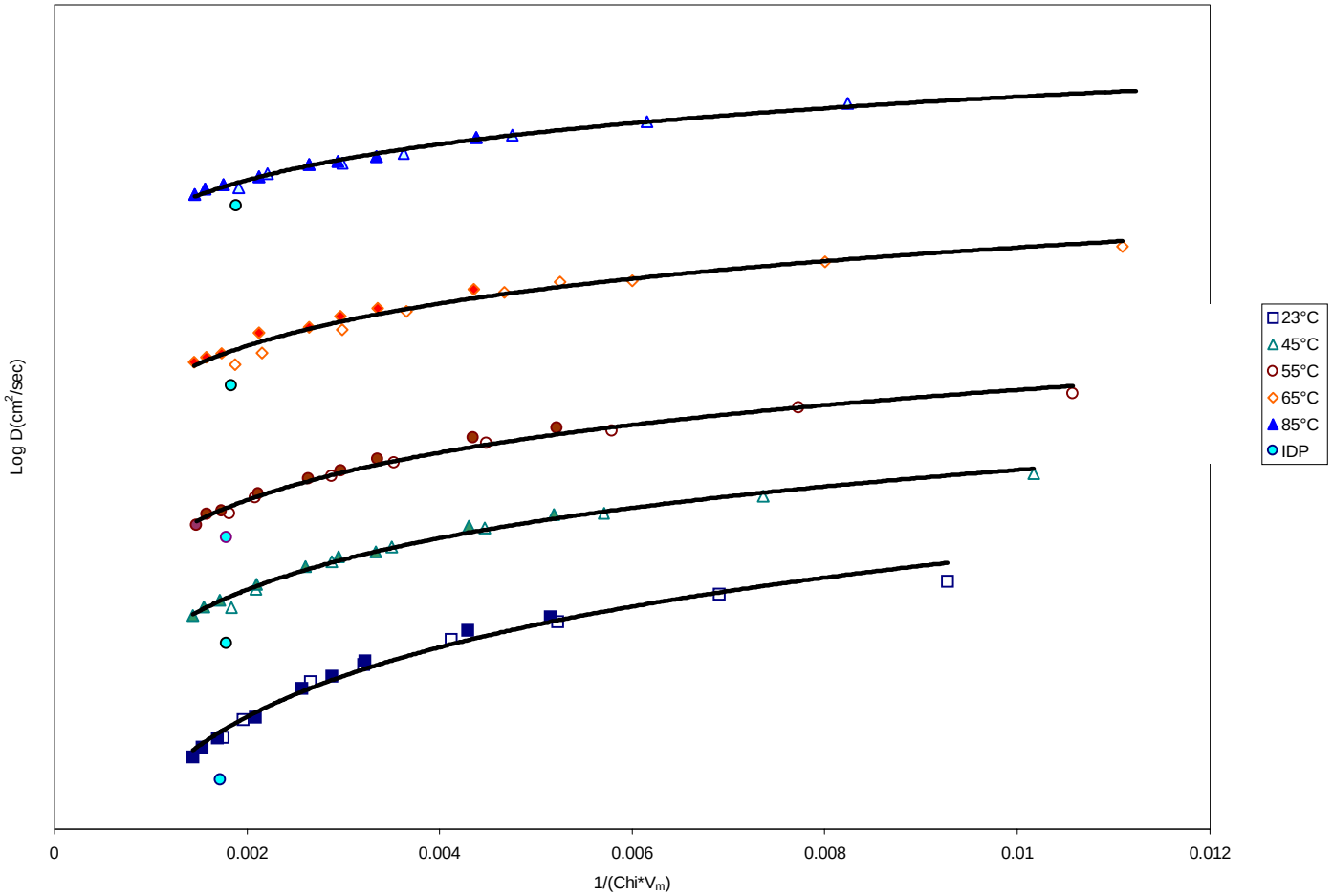

Figure 5-72. Plot of log D (cm^2/sec) versus $(chi*V_m)^{-1}$ for esters and alkanes. Esters are designated with open symbols. Data have been shifted along the y-axis for the sake of clarity.

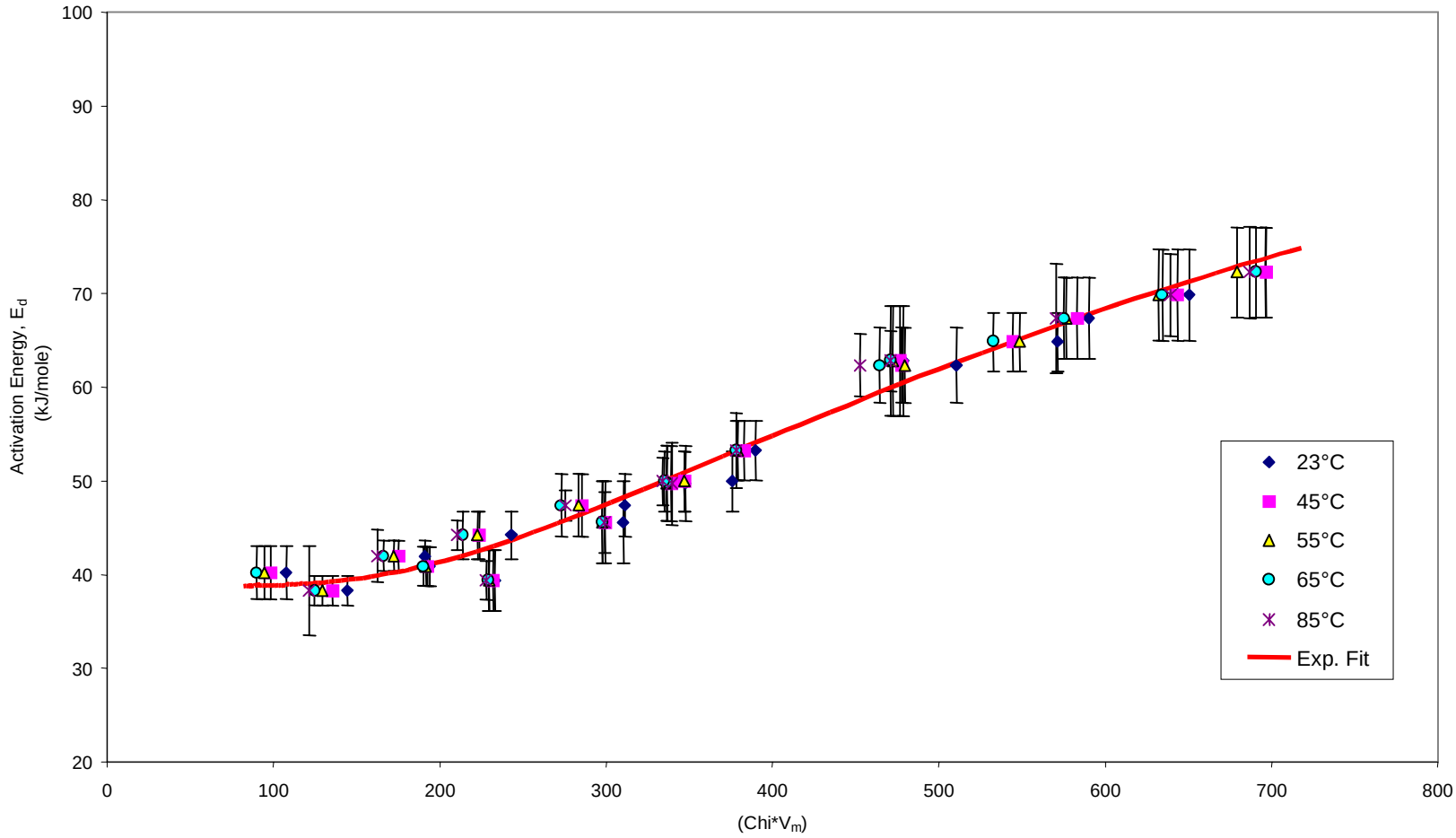

Figure 5-73. Activation energy of diffusion (E_d, kJ/mole) for both *n-alkanes* and *esters* versus (Chi*V_m). A first-order exponential has been shown since it can adequately describe the "plateau" region at lower activation energies.

5.6 Summary

The diffusion properties of linear *n*-alkanes and esters in a polyamide-based polymeric adhesive have been investigated. These penetrants were chosen in order to be able to study the isolated effects of size, shape, and chemical nature of the molecules on the transport process.

Systematic differences between the sorption curves of the two series were explained on the basis of their variations in size and chemical nature. Detailed analysis of the data showed that a vacant site was created prior to dissolution of a penetrant into that site, indicative of a Henry's Law type of sorption. Further support for this conclusion was derived from the heats and entropies of solution evaluated for these systems.

Gross deviations from the expected molecular weight dependence were observed and implied that additional factors influenced the transport. Possible geometric *shape* differences were investigated, and it was found that the diffusion of these penetrants occurred in the direction of their long-axes. The general shape of both the esters and alkanes were similar and did not change as the number of penetrant carbon atoms increased. Hence, differences in the diffusion behavior of the two series were not attributed to differences in their shapes except for the anomalous IDP. Molecular modeling was utilized to support this interpretation through evaluations of minimum energy conformations and "average" aspect ratios for each species. The "anomalous" behavior of the IDP penetrant was also explained from this shape analysis. Placement of the ester functionality in the middle of this molecule induced a spherical geometry and a larger cross-sectional area. These factors, in addition to the increased shielding of the ester moiety resulted in a diffusion mechanism that was different from that of the remaining penetrants.

The concept of molecular volume was used to give an approximate description of the "space-filling" requirements of a penetrant within a polymer matrix. Differences in diffusion properties between the two series were interpreted in terms of free volume arguments.

Differences in specific interactions between the polymer and penetrant molecules were characterized using the Flory-Huggins interaction parameter, χ. Although these analyses clearly pointed out the favorable contributions of the ester functionality, the χ parameter (by itself) did not accurately describe the behavior of both series. Relationships involving the interaction parameter (χ) and the molar volume (V_m) were proposed. They accounted for both the size and chemical effects simultaneously, thereby providing a better description of the transport behaviors of these systems. These relationships were successfully applied to both the series, due to the fact that their *shapes* and *mechanisms* were very similar.

Thus, the transport properties of two series of esters and *n*-alkanes were *thoroughly* investigated and the contributions of various influencing factors including *shape, size,* and *chemistry of the penetrants* were accounted for.

Endnotes

[1] D.T. Turner and A.K. Abell, *Polymer*, 28, 297, (1987).
[2] C.Y. Hui, K.C. Wu, R.C. Lasky, and E.J. Kramer, *Journal of Applied Physics*, 61, 5129 (1987).
[3] J.K. Vrtis and R.J. Farris, *Journal of Applied Polymer Science*, 59, 1849-1855 (1996).
[4] K.Möller and T. Gevert, *Journal of Applied Polymer Science*, 51, 895-903 (1994).
[5] U.S. Aithal and T.M. Aminabhavi, *Journal of Chemical Education*, 67, 82 (1990).
[6] S.B. Harogoppad and T.M. Aminabhavi, *Macromolecules*, 24, 2598- (1991).
[7] M.G. Kulkarni and R.A. Mashelkar, *Polymer*, 22, 1665-1672 (1981).
[8] R.F. Storey and K.A. Mauritz, and B.D. Cox, *Macromolecules*, 22, 289-294 (1989).
[9] L.Y. Shieh and N.A. Peppas, *Journal of Applied Polymer Science*, 42, 1579 (1991).
[10] L.M. Lucht and N.A. Peppas, *Journal of Applied Polymer Science*, 33, 1557 (1987).
[11] T.J. Aminabhavi and R.S. Munnoli, *Canadian Journal of Chemical Engineering*, 72, 1047-1054 (1994).
[12] T.J. Aminbhavi, H.T.S. Phayde, J.D. Ortego, and W.M. Stahl, *Journal of Applied Polymer Science*, 63, 1223-1235 (1997).
[13] T.J. Aminabhavi and R.S. Khinnavar, *Polymer*, 34, 5, 1006-1018 (1993).
[14] P.J. Flory, Principles of Polymer Chemistry, Cornell University Press, Ithaca, NY. 1953.

[15] C.M. Balik, *Macromolecules*, 29, 3025-3029 (1996).
[16] S.P. Chen and J.A.D. Edin, *Polymer Engineering and Science*, 20, 1, 40-50 (1980).
[17] M.G. Kulkarni and R.A. Mashelkar, *Polymers*, 22, 1665-1672 (1981).
[18] K.A. Mauritz, R.F. Storey, and Scott George, *Macromolecules*, 23, 2, 441-450 (1990).
[19] A. Einstein, Investigations of the Theory of the Brownian Movement, ed. R. Fürth, Dover, New York, 1956.
[20] H.Fujita, *Advances in Polymer Science*, 3, 19 (1961).
[21] H.Fujita and A. Kishimoto, *Journal of Polymer Science*, 25, 547 (1958).
[22] A.C. Newns and G.S. Park, *Journal of Paint Technology*, 42, 16 (1970).
[23] R.J. Roe, H.E. Bair, and C.J. Gieniewski, *Journal of Applied Polymer Science*, 12, 843 (1974).
[24] T.P. Gall, R.C. Lasky, and E.J. Kramer, *Polymer*, 31, 1491-1499 (1990).
[25] M.J. Hayer and G.S. Park, *Transactions of theFaradaySociety*, 51, 1134 (1955).
[26] J.L. Duda, J.S. Vrentas, S.T. Ju, and H.T. Liu, *AICHe*, 28, 2, 279-285 (1982).
[27] P. Meares, Polymers: Structure and Bulk Properties, Van Nostrand, London. (1965).
[28] J. Koszinowski, *Journal of Applied Polymer Science*, 32, 4765-4786 (1986).
[29] J.Crank and G.S. Park, Diffusion in Polymers, Academic Press, London. (1968).
[30] A.W. Lawson, *Journal of Chemical Physics*, 19, 131 (1960).
[31] W.J.Koros, Barrier Polymers and Structures, ACS, Washington, DC. (1990).
[32] D.W. van Krevelen and P.J. Hoftyzer, Properties of Polymers, Their Estimation and Correlation with Chemical Structure, Elsevier Scientific Publishing Co., Amsterdam, 1976.
[33] V.T. Stannet, H.B. Hopfenberg, J.H. Petropoulus, *International Review of Science: Physical Chemistry Series*, 8, 329 (1972).
[34] T.M. Aminabhavi, U.S. Aithal, and S.S. Shukla, *Journal of Macromolecular Science, Reviews in MacromolecularChemical Physics*, C28, 421 (1988).
[35] S.B. Harogoppad and T.M. Aminabhavi, *Polymer*, 32, 5 (1991).
[36] E. Southern and A.G. Thomas, *Journal of Polymer Science (A)*, 3, 641- (1965).
[37] E. Southern and A.G. Thomas, *Transactions of the Faraday Society*, 63, 1913 (1967).
[38] I.C. Poinescu, C. Beldi, and C. Vlad, *Journal of Applied Polymer Science*, 29, 23 (1984).
[39] P.M. Smith and M.M. Fisher, *Polymer*, 25, 84 (1984).
[40] L.Y. Shieh and N.A.Peppas, *Journal of Applied Polymer Science*, 42, 1579-15897 (1991).
[41] J.M.G. Cowie, Polymers: Chemistry and Physics of Modern Materials, 2nd ed., Blackie Academic and Professional Press, London. 1991.
[42] Handbook of Polymer Science, ed. J. Brandrup and E.H. Immergut, Wiley-Interscience, New York. 1989.
[43] J. Koszinowski, *Journal of Applied Polymer Science*, 31, 2711-2720 (1986).

[44] T.H. Aminabhavi and H.T.S. Phayde, *Polymer*, 36, 5, 1023-1033 (1986).

[45] T.M. Aminabhavi and H.T.S. Phayde, *Journal of Applied Polymer Science*, 55, 1335-1352 (1995).
[46] W.E. Roseveare, R.E. Powell, and H. Eyring, *Journal of Applied Physics*, 12, 669 (1941).
[47] M.L. Huggins, *Journal of Physical Chemistry*, 46, 151 (1942).

[48] CRC Handbook of Solubility Parameters and Other Cohesion Parameters, 2nd ed., ed. A.F.M. Barton, CRC Press, Boca Raton. 1991.
[49] L.R.G. Treloar, The Physics of Rubber Elasticity, 3rd ed., Clarendon Press, Oxford. 1975.

[50] G.L. Wilkes, private communication
[51] G.B. McKenna, K.M. Flynn, and Y. Chen, *Polymer Communications*, 29, 272-275 (1988).
[52] G.B. McKenna, K.M. Flynn, and Y. Chen, *Polymer*, 31, 1937-1945 (1990).
[53] P.C. Hiemenz, Polymer Chemistry, The Basic Concepts, Marcel Dekker, Inc., New York, 1984.
[54] H. Marand, private communications
[55] M. Gottlieb, "Swelling of Polymer Networks," Chapt. 27
[56] T.C. Ward, private communications
[57] A.R. Schultz, Characterization of Macromolecular Structure, Ed. D. McIntyre, National Academy of Sciences Publication # 1573, 389-405 (1968).
[58] A. Sfirakis and C.E. Rogers, *Polymer Engineering and Science*, 21, 9, 542-547 (1981).
[59] M.H. Cohen and D. Turnbull, *Journal of Chemical Physics*, 31, 1164-1171 (1959).
[60] J.Y. Moisan, *European Polymer Journal*, 17, 857 (1981).
[61] M. Dubini, O. Cicchetti, G.P. Vicario, and E. Bua, *European Polymer Journal*, 3, 472 (1967).
[62] A. Aitken and R.M. Barrer, *Transactions of the Faraday Society*, 51, 116 (1955).
[63] H. Peters, P. Vanderstractem, and L. Verhoeye, *Journal of Chemical Technology and Biotechnology*, 29, 581 (1979).
[64] R.J. Pace and A. Daytner, *Journal of Polymer Science: Polymer Physics Edition*, 17, 437-451 (1979).
[65] S.T. Ju, J.L. Duda, and J.S. Vrentas, *I & EC Product Research and Development*, 20, 330-335 (1981).